2012

Carbon-carbon bond forming reactions for bio-oil upgrading: heterogeneous catalyst and model compound studies

Ryan William Snell
Iowa State University

Carbon-carbon bond forming reactions for bio-oil upgrading: heterogeneous catalyst and model compound studies

by

Ryan William Snell

A dissertation submitted to the graduate faculty

in partial fulfillment of the requirements for the degree of

DOCTOR OF PHILOSOPHY

Major: Chemical Engineering

Program of Study Committee:
Brent H. Shanks, Major Professor
Dennis R. Vigil
Robert C. Brown
Keith L. Woo
Andrew C. Hillier

Iowa State University

Ames, IA

2012

To my wife Sarah and our newborn son Soren…

Table of contents

Acknowledgements

This thesis would not be possible without the encouragement, leadership, and support of my major professor Brent Shanks. I am particularly grateful of his continuous focus on the big picture even while examining the fundamental science of a project and of his mentoring style which allows for the development of independent thinkers and researchers. I would also like to thank all members-current and past-of the Shanks' research group for helpful discussions and encouragement. In particular I would like to acknowledge Karl Albrecht, Shaojun Miao, and Sikander Hakim for their guidance during the beginnings of graduate school as well as Keenan Deutsch and Tianfu Wang for their support as I am finishing up. Undergraduate researchers Elliot Combs, Linda Lippold, Dan Weis, and Rawini D-Mudiyanselage who all contributed to this work should be recognized for their efforts as well.

Performing the research and class work needed to finish this thesis and graduate school in general has consumed a significant amount of my time and efforts for the past 4-5 years. With this in mind, I'm indebted to my parents and brother; Carol, Mick, and Jared Snell for their encouragement. Most of all, I must thank my wife, Sarah Snell, who put up with my late nights and weekends needed to complete this work. For her encouragement and efforts to keep me focused on what is truly important, I will be forever grateful.

Abstract

Development of a renewable liquid transportation fuel is likely to be one of the most important challenges faced by scientists during the 21st century. As biomass provides a renewable source of carbon it is ideally situated to supply this alternative to the traditional petroleum derived feedstocks. While there have been a number of different techniques used to convert biomass to liquid fuels, fast pyrolysis is particularly promising as it can quite efficiently break down biomass directly into a liquid. This resulting liquid, called bio-oil, is a very complex mixture containing a large number of oxygen functionalized compounds. Unfortunately, this oil has a number of issues that must be resolved before it can be effectively utilized as a liquid transportation fuel including acidity, reactivity, and low energy density. With this in mind, heterogeneously catalyzed C-C bond forming reactions potentially valuable for the upgrading of bio-oil were investigated.

The aldol condensation is a well known reaction in organic chemistry usually promoted through the use of strong acid or bases. However, uses of these types of catalysts will likely cause undesirable side reactions. Ideally cooperative catalysis allows for weaker acids and bases to work in tandem to promote the reaction. Use of aluminum phosphate catalysts allowed for the tuning of the acidity and basicity of the materials through a nitridation process and hence probing of this cooperative catalysis. Through performing aldol condensations using model bio-oil compounds acetaldehyde, acetone, and MEK, it was found that acid and base sites were both needed to efficiently promote the cross condensation of the aldehyde and ketone. After reaction testing, a mechanism was proposed demonstrating the benefits of using heterogeneous catalysts as it allows for the coexistence of both acid and base sites.

Ketonization of carboxylic acids is also an ideal reaction for bio-oil upgrading as it removes acidity and oxygen as well as creates C-C bonds. However, this reaction is almost always performed in the vapor phase due to the high temperatures necessary to achieve significant conversions. In order to try to engineer a more active catalyst able to perform the reaction at lower temperatures, more must be understood about ketonization. Condensed phase ketonization was examined using ceria catalysts calcined at different temperatures. It was found that the reaction proceeded either through the formation of carboxylates in the bulk or on the surface of the catalyst depending on the temperature of calcination. Moreover, through in-situ XRD, this trend was found to be true in the vapor phase as well. Kinetic studies found that the mechanism for both these routes was likely the same.

As ketonization had been claimed to be sensitive to the surface structure of the ceria catalyst, shape selective ceria nanocrystals were synthesized and examined in acetic acid ketonization both in the vapor and condensed phases. It was found that in the condensed phase the catalysts underwent carboxylate formation in the bulk thus changing the crystal structure of the materials. However, in the vapor phase this did not occur but a clear trend with surface structure was not determined. Thus it is likely the surface structure of the ceria catalysts isn’t of large influence in realistic ketonization conditions. Reaction condition influences were probed as well. It was found that the temperature of ketonization greatly influenced the reaction pathway with intermediate temperature reactions resulting in metal carboxylate formation in the bulk and high temperatures promoting the reaction on the surface. Discussion of these temperature regimes and a more detailed proposed mechanism are delivered.

Lastly, ketonization using mixed metal oxides was studied. It was found that mixing of ceria with another oxide greatly changed the catalyst properties. Coupled with reaction testing, experiments determined that metal carboxylate formation and decomposition are of supreme importance for ketonization and are influenced by mixing of oxides. Along with the work using pure ceria catalysts, this research into ketonization is a significant step forward into understanding of the reaction and how it can be applied to the upgrading of fast pyrolysis bio-oil.

Chapter 1

General introduction and project goals

1.1 Introduction

As the world's consumption of petroleum based energy increases, in large part due to growth of developing economies like China and India, it is imperative that cheap, clean, safe, and renewable alternatives are created. This need has been highlighted in light of recent events such as the BP gulf oil spill and the rapid escalation in pump costs of gasoline. The United States has been particularly dependent on liquid fuels with expected consumption to slowly increase from the 20 million barrels consumed per day in 2008 to 22 million barrels per day by 2035.[1] Transportation has been largely to blame, as it accounts for 25% of the U.S. overall energy consumption.[2] Further exacerbating the United States' energy struggles is the fact that large fractions of these fuels are imported from countries with volatile political environments. The breakdown of the largest exporters of oil to the U.S. are given in Table 1.[3] Despite scientific gains in alternative energies like hydrogen fuel cells, solar, and wind energy, the historical and current dependence on liquids for transportation and other uses has led to an infrastructure that will be difficult to change. Therefore production of a clean renewable liquid fuel is imperative, particularly for the near future. Biomass is unique as it provides for a readily available renewable source of liquid carbon based fuels that could potentially fit into the current infrastructure. Unfortunately, there has not been development of a method that doesn't require significant infrastructure changes and can easily convert a variety of biomass types to drop-in liquid fuels.

1.2 Biomass conversion processes

There have been a number of different processes developed during exploration of biomass to fuel conversions. These techniques consist primarily of biochemical and thermochemical methods. Common thermochemical processes are liquefaction, combustion, gasification, and pyrolysis while typical biochemical processes are digestion and fermentation.[4] While combustion and digestion are used more for electricity and methane production, there are still some of these processes that allow for production of desirable liquid fuels. As an example, gasification creates a syngas mixture that could be subsequently upgraded via Fisher-Tropsch synthesis to make transportation-length hydrocarbons.[5] Liquefaction can also create liquid fuels, but is largely ignored as an option due to its high costs.[4] Fermentation is primarily used for the production of ethanol, but is not likely a good option in development of a widely transportable and inexpensive drop-in fuel due to limitations on feedstock as well as its different chemical properties in comparison to more common hydrocarbons. However, the pyrolysis process is especially well designed for the creation of liquid drop-in fuels. This is due to reasons such as its low costs, simple process, and feedstock flexibility. To maximize the liquid product of pyrolysis, a technique termed fast pyrolysis is performed.[6] This process involves the rapid heating of biomass in an inert atmosphere at temperatures around 425-500 °C.[6] Gases, char, and a liquid product called bio-oil are the resulting products. The conditions of the process can be manipulated in order to maximize the oil produced at yields up to 78%.[2]

1.3 Bio-oil composition

The oil derived from the fast pyrolysis of biomass is an extremely complex mixture of oxygenated compounds that fluctuates widely based on the type of biomass used as well as process variables. Examination of molecular structures of the main components of biomass—

hemicellulose, cellulose, and lignin—makes it obvious that decomposition of the different materials will result in different products. Pyrolysis of the lignin fraction of biomass gives a high content of phenolic compounds while the breakdown of the cellulose and hemicellulose components results in smaller oxygenated molecules. As may be expected due to the complexity of the feedstock, the resulting bio-oil has a diverse range of chemical species. In fact, bio-oil characterization has found over 300 different compounds.[7] Organics such as esters, ketones, sugars, phenols, guaiacols, syringols, furans, acids, alcohols, aldehydes, along with other molecules containing multiple functional groups are prevalent in the oil.[8] However, water is the most common molecule of all, comprising 15-30 wt%.[7] As the research presented in the following chapters deals primarily with the aldehydes, ketones, and carboxylic acids found in the oil, Table 2, Table 3, and Table 4 show the varying types of molecules falling into these respective categories. As can be seen from the tables, many of these compounds are fairly volatile and of low molecular weight.

1.4 Difficulties associated with bio-oil

As may be expected from a rapid process like fast pyrolysis, the resulting products are not at thermodynamic equilibrium. Storage of the crude bio-oil is therefore difficult as it undergoes reactions resulting in increased viscosity and phase separations over time.[8] Common reactions occurring in the oil include esterification, homopolymerization, transesterification, hydration, hemiacetal formation, acetalization, and oxidation.[8] Acids present in the oil could clearly catalyze some of these reactions. Carboxylic acids also lower the pH of the oil to 2-3, resulting in significant corrosion issues during storage and transport.[7] Energy density of the bio-oil is low due to the prevalence of oxygenated

compounds. In fact, oxygen makes up 35-40 wt% of the oil resulting in an energy density of less than 50 % of fuel oils.[7]

1.5 Potential solutions

There are a couple of different processes that can help alleviate some of the aforementioned struggles in the use of pyrolysis to make hydrocarbon type liquids. These operations consist of both pre-pyrolysis treatments of the biomass as well as post pyrolysis catalytic conversions. Patwardhan et al. has explored the effects that inorganic species present in biomass can play during the pyrolysis process.[9] It was found that the existence of inorganic salts promoted the decomposition of cellulose to smaller molecules.[9] Thus pretreatments that remove or add these types of species would allow for some control over the final bio-oil composition. The treatments could then be tailored to create an oil product modified for particular applications. Post-pyrolysis catalytic treatments have been found to be extremely beneficial to upgrading of bio-oil to fuel. One common technique is to perform hydrodeoxygenation (HDO) of the oil. It is easy to see how this would create a better fuel as oxygen is removed, ridding the oil of carboxylic acids as well as other reactive molecules, while increasing energy density. This method has been the topic of a number of recent publications.[10-12] However, with the large amount of oxygen contained in the oil, massive quantities of hydrogen will be needed for this process to be successful. Another downside to HDO is that the many low molecular weight molecules in the bio-oil will be unusable as liquid fuel sources after hydrogenation. This will result in the loss of significant amounts of renewable carbon that could have been used for our desired applications. Therefore hydrodeoxygenation as the primary upgrading step is not preferred.

Another upgrading option would be to perform catalytically controlled reactions that could remove oxygen and carboxylic acids as well as increase carbon chain lengths of the small molecules before a final hydrodeoxygenation step. There are a number of locations during the pyrolysis process that this catalytic upgrading could occur. The options could be broadly grouped into categories of either before or after condensation of the oil. Upgrading before condensation of the oil has a number of potential drawbacks. One difficulty is potential exposure of the catalysts to inorganic species that could act as poisons. These inorganic species could be removed before condensation of the oil. Another problem with the vapor phase upgrading is the presence of coking species like lignin derived phenolics that could also be removed by fractionation during condensation. Vaporizing the bio-oil after condensation is not practical either as the oil contains a number of thermally unstable compounds. Therefore condensed phase upgrading of the bio-oil is the preferred path. A potential upgrading scheme similar to that proposed by Deng et al. can be observed in Figure 1.[13] Here, the low molecular weight organic acids first undergo decarboxylative coupling to form small ketones. These ketones are then reacted with the prevalent low molecular weight aldehydes present in the oil using the aldol condensation. Ketonization and aldol condensation reactions are ideal for the bio-oil upgrading process as they can efficiently create carbon-carbon bonds between the low molecular weight acids, ketones, and aldehydes so that they are not eliminated as potential liquid fuels during hydrodeoxygenation. The two reactions are also beneficial in that they remove oxygen in the form of water and CO_2 as well as ridding the oil of the acidic carboxyl groups. Discussion and research will focus on these two reactions and their potential use in the bio-oil upgrading process for the remainder of this document.

1.6 Aldol condensations

1.6.1 General chemistry and mechanisms

Aldol condensations of ketones and aldehydes are a well known group of reactions in the organic chemistry field. Reactions can involve the cross condensation of an aldehyde with a ketone or a self condensation of either the aldehyde or ketone. Generally, aldehydes can self-condense much more readily than can ketones. This occurs as the ketone's carbonyl is more hindered than and not as electrophilic as that of an aldehyde.[14] However, the self-condensation of a ketone can proceed to significant yields if the product is continuously removed from the catalyst so that the retro-aldol reaction does not occur.[14]

Aldol condensations have been known to be catalyzed by both acids and bases. Mechanisms differ depending on the catalyst used. Typical base and acid catalyzed mechanisms can be seen in Figure 2 and Figure 3. In the figures, dehydration is shown following the condensation. This is common for aldol condensations as it forms a more stable conjugated structure.[14] As is shown, the base catalyzed mechanism begins with a deprotonation of the α-carbon of one of the reactants to form an enolate anion. This enolate anion then acts as the nucleophile in an attack on the carbonyl of the other molecule involved to form an alkoxide anion. Protonation of this alkoxide generates the product and reforms the catalyst. Acid catalysis begins by carbonyl protonation followed by deprotonation of the α-carbon to form an enol. This enol acts as the nucleophile, and attacks an activated electrophile. In a mixture of aliphatic aldehydes and ketones, the base catalyzed product is primarily the cross condensation in which the ketone acts as the nucleophile and the aldehyde as the electrophile.[15] With ketones containing both methyl and methylene carbons, acids and bases can promote condensation at different locations. Acid catalysts have been found to

promote condensation occurring at the methylene carbon while base catalysts can catalyze the condensation at both the methyl and methylene carbons depending on reaction conditions.[16] The differences between these catalysts is in large part due to the different rates of formation and stabilities of the intermediate enols and enolate anions.[16]

There are a couple of options for which step in the mechanism is rate determining. For base catalysis, this step is typically either deprotonation or condensation, often depending on the concentration of reactant.[16] If the electrophile is an aliphatic aldehyde normally the first deprotonation step is rate controlling.[17] However, for low concentrations, the condensation can become rate limiting causing the reaction to become second order with respect to the aldehyde.[16] For a number of aldol-condensations involving ketones, the condensation step is rate limiting.[16] Acid catalysis results in a situation where the condensation is the rate limiting step as well.[16] Achieving good selectivities with the aldol reaction is a struggle for chemists as the product can often continue to undergo condensations. However, for applications to fuels, where a range of molecule sizes is desired, this is not as much of a concern. Ideally for bio-oil upgrading, condensation becomes more difficult as the chain length of the compound increases.[16] Therefore, reaction conditions as well as catalytic properties could be tailored to achieve carbon chains of the appropriate length for the desired type of fuel. As the products of the aldol condensation can be quite difficult to analyze due to multiple condensations and dehydrations, most work in literature has explored the reaction using an enolizable aldehyde along with an aldehyde containing no α-hydrogen such as benzaldehyde. This constraint prevents multiple condensation reactions from occurring, thus allowing reaction analysis to be more easily performed. Work done with the small compounds typically found in bio-oil has been primarily done in the gas phase due

to the volatility of the low molecular weight aldehydes and ketones. Unfortunately these typically researched conditions and molecules are not particularly pertinent to our desired application.

1.6.2 Heterogeneous catalysts

Although historically catalyzed with homogeneous strong acids and bases, recent research—for both economic and environmental reasons—has begun to focus on the development of effective heterogeneous catalysts. Common heterogeneous catalysts investigated for aldol applications include aluminophosphates and nitrides [18, 19], Mg-Al mixed oxides[20], hydrotalcites[21, 22], titania[23], functionalized MCM-41[24], zeolites[25], molybdenum nitride[26], MgO[27], functionalized SBA-15[28, 29], and anion exchange resins[30]. There is also work involved with development of catalysts containing both the acid/base moieties necessary for the aldol condensation along with hydrogenation sites.[31, 32] Hydrogenation abilities of these materials allows for bypassing thermodynamic limitations on more reversible condensation reactions. This transpires as the α-β pi bond becomes saturated and prevents the retro-aldol reaction from occurring. Another advantage to these types of catalysts would be potential one-pot synthesis of saturated compounds. It is easy to see from Figure 1, how this could be beneficial for bio-oil upgrading applications.

As described in section 1.4, due to the various functionalities in the pyrolysis oil, a number of different undesirable chemical reactions can proceed during storage. Obviously, the addition of a strong acid or base to catalyze the aldol condensation would promote a number of deleterious side reactions in the complex mixture. Therefore the development and understanding of a weak acid or base heterogeneous catalyst able to selectively catalyze the aldol condensation would be of particular value. Recently, synthesis of bifunctional catalysts

that contain both weak acids and bases has demonstrated that cooperative acid-base catalysis can effectively promote condensation reactions.[18, 28, 29, 33-35] These types of catalysts act in a similar way to enzymes in that multiple functionalities can interact with the reactant to promote the particular reaction. As these specific types of catalysts would be potentially advantaged for bio-oil applications, further focus will be on them.

Ordered silica catalysts such as SBA-15 and MCM-41 allow for the easy addition of acidic and/or basic functional groups. Therefore a significant amount of attention for bifunctional catalysts has involved these types of supports. For example, Hruby and Shanks investigated the Knoevenagel condensation using SBA-15 functionalized with either aminopropyl or dihydroimidazole groups to act as basic sites.[33] It was found that aminopropyl groups tethered onto the SBA-15 acted as much better catalysts than the corresponding homogeneous catalyst.[33] Capping of the silanol groups on the functionalized mesoporous silica surface also resulted in a significant decrease in catalyst activity.[33] These findings suggest that the silanol groups are actively participating in the condensation along with the basic groups through cooperative catalysis.[33] The Mark Davis group from Cal Tech has also investigated the synthesis and testing of bifunctional SBA-15 catalysts.[28, 29, 35] With their work, instead of attached basic amines cooperatively working with silanols, catalysts were synthesized that had both the base along with a sulfonic, phosphonic, or carboxylic acid group. Synthesis of SBA-15 containing both propylamine and sulfonic acid moieties demonstrated greatly enhanced activity over a homogeneous mixture as well as SBA-15 containing either one.[28] The cooperative mechanism proposed by Zeidan and Davis can be observed in Figure 4. As can be seen in the figure, the reaction begins through acid site promoted protonation of the nucleophile reactant

to form a carbocation. Abstraction of the α-hydrogen and the proton attached to the carbonyl results in an enolate anion. This enolate anion then attacks the aldehyde to form the ketol. Solvent effects were established to be of importance with these catalysts as more polar protic solvents stabilize the neutralized ion pair while non-polar aprotic solvents allowed the free acid and base to more easily exist.[28] When adding weaker acids such as those with phosphonic or carboxylic groups, it was found that the neutralization of the active sites does not as readily occur allowing for greater catalytic promotion of the reaction.[29]

Silica catalysts are not the only materials that have been examined for their cooperative nature in the aldol-reaction. Metal phosphate catalysts have also been found to contain both acid and base sites able to work together to catalyze the aldol condensation.[18, 34] Hasni et al. researched the aldol condensation of benzaldehyde with heptanal using zirconophosphates and galloaluminophosphates as catalysts.[34] The base sites on these types of metal phosphates can be tuned through a nitridation procedure involving the high temperature exposure of the material to flowing ammonia. Harsher conditions and longer times during this process allow for more basic nitrogen incorporation along with removal of acidic P-OH groups.[18, 36] Zirconophosphate was found to have more basic sites before nitridation than the galloaluminophosphate and was thus more active in the aldol reaction.[34] Nitridation of both catalysts resulted in an enhanced selectivity to the cross condensation between the aldehydes to form jasminaldehyde.[34] Climent et al. studied the aldol condensation of benzaldehyde with heptanal to form jasminaldehyde as well.[18] Catalysts used in their work consisted of aluminophosphate materials that had undergone different levels of nitridation.[18] Comparison of the non-nitrided aluminophosphate with other common aldol catalysts such as MgO showed that the aluminophosphate was far more

selective to the cross-condensation product than were the other more basic catalysts.[18] Further nitridation of the aluminophosphates correspondingly decreased selectivities to jasminaldehyde.[18] This demonstrated that both the weak acid sites and weak basic sites together promoted this cross-condensation reaction. A mechanism, as shown in Figure 5, was proposed by Climent et al. to explain this phenomena.[18] In the mechanism the phosphorol acid sites on the catalyst surface activate the carbonyl of the benzaldehyde while the bridged oxygen weak basic sites form a carbanion with heptanal. Activation of benzaldehyde makes it more vulnerable to nucelophilic attack by the heptanal carbanion.

1.7 Ketonization

1.7.1 General chemistry and mechanisms

Recently, ketonization has become a popular reaction of sorts due to the use of decarboxylative coupling for bio related applications.[37-39] Despite its modern relevance, the ketonization reaction has a long history. For instance, in 1858 Friedel discovered that acetone formed upon decomposition of calcium acetate.[40] However, it wasn't until 1895 that the ketonization of organic acids through a continuous flow system was discovered to be possible.[41] Demonstrating a great improvement in the ketonization process, Squibb found that barium carbonate effectively catalyzed the conversion of acetic acid to acetone without the formation of an intermediate barium acetate compound.[41] After this, ketonization flourished and was even used commercially for the production of acetone until World War I.[42] Interestingly, the process then, like more recently, involved the production of ketones from biorenewable resources. This is exemplified in that before and during WWI, acetone was produced by the dry distillation of calcium acetate acquired from the lime neutralization of wood distillates as well as by reactions with acetic acid from fermentation.[42] After more

cost effective biochemical and petrochemical routes of acetone production appeared, it seems that interest in the reaction waned before its more recent resurgence.

Despite the long history and extensive use of this reaction, the mechanism is not fully understood.[43] The lack of fundamental knowledge about this reaction is in large part due to the wide range of reaction conditions and catalysts explored. It appears to be hard to apply knowledge learned with one material and conditions to other situations. One thing that appears consistent through all ketonization work is the necessity of high reaction temperatures in order to allow the reaction to proceed. Even the most effective catalysts are rarely used under 300 °C, with common temperatures being in the 300-450 °C range.[44] Hence most work, especially with low molecular weight acids, like acetic acid, has been performed in the vapor phase. As described earlier, for pyrolysis oil, it would be advantageous to perform the upgrading in the condensed phase. Therefore a more active catalyst must be designed allowing for the reaction to take place at lower temperatures more conducive for the desired conditions. For this to occur, a more fundamental understanding of the ketonization reaction is needed, particularly in the condensed phase. Much of the research presented in subsequent chapters of this manuscript will focus on the goal of obtaining this type of information. The rest of section 1.7 will focus on recent developments and background on mechanistic theories and findings to help put the current work in context.

A large number of mechanisms have been proposed for the ketonization reaction. Yakerson et al. concluded that the reaction proceeded through different pathways depending on the catalyst used.[45] In that work, comparisons of results for quadrivalent oxides with previous research on group I and II carbonates and oxides was completed.[45] Quadrivalent oxides as well as BeO were found to not form bulk carboxylates unlike the group I and II

carbonates and oxides in the course of reaction.[45] The differences were proposed to be occurring due to the much higher lattice energy of the quadrivalent oxides than the group I and II oxides and carbonates.[45] As it appeared the reaction was not taking place through carboxylate decomposition, the authors concluded that the hydroxyl groups on the surface were acting as the catalytic sites for the MO_2 catalysts.[45] Yamada et al. recently probed acetic acid ketonization in the vapor phase over a number of rare earth oxides.[46] Agreeing with Yakerson et al. it was found that ceria did not undergo the formation of a bulk carboxylate.[46] However, it was discovered that some of the rare earth oxides such as La, Pr, and Nd did have acetate development.[46] Commonly, probing whether ketonization occurs through intermediate carboxylate formation is performed by comparison of reaction activation energies for metal carboxylates with the corresponding oxide. For example, a comparison of 3d metal acetate decomposition with ketonization over the equivalent oxide was reported by Bernal et al.[47] It was found that the activation energy and frequency factor for 3d metal oxide ketonization and acetate decomposition was the same.[47] Thus it was concluded that ketonization over these oxides occurred through decomposition of a carboxylate intermediate.[47]

Published in 1994, Rajadurai thoroughly reviewed mechanistic knowledge up to that point on the ketonization reaction.[48] The different pathways reviewed involve a number of various intermediates such as acid anhydrides, β-ketoacids, acyl carbonium ions, molecularly adsorbed acid, and ketene further exemplifying the lack of fundamental knowledge about the reaction.[48] After reviewing proposed mechanisms, Rajadurai concluded that the path of the reaction depends on the type of catalyst used, but the most likely mechanism is through interactions of two adsorbed carboxylate species or a carboxylate and an acyl carbonium

ion.[48] This theory is somewhat supported by findings that the reaction follows Langmuir-Hinshelwood kinetics—meaning that non-adsorbed gaseous acid does not participate in the mechanism.[48] Pathway of the reaction can apparently differ depending on the temperature the reaction is performed as well.[49] For instance, when examining the ketonization reaction of acetic acid in the vapor phase using chromia as a catalyst, it was found that the activation energy changed at ~400 °C signaling a potential change in the rate determining step.[49]

A significant, more recent investigation into the ketonization mechanism was done by Pestman et al.[43] Experiments in Pestman's work were performed in the vapor phase, using H_2 as the carrier gas, where continuous flow testing was done during a temperature ramp with periodic sampling.[43] Reactant concentration along with product evolution were plotted against temperature to help determine how the mechanism proceeded. For alumina, titania, chromia, and zirconia, H_2O, CO_2, and acetone all evolved at the same temperature corresponding with acid disappearance.[43] For titania this temperature was >300°C while for the other oxides T>400 °C.[43] However, for bismuth oxide, magnesium oxide, zinc oxide, and lead oxide, a sharp decrease in acid concentration occurred before product formation.[43] When acetone finally appeared, it occurred in a very narrow peak.[43] These results led Pestman et al. to conclude that the lead, magnesium, bismuth, and zinc oxides catalyzed the reaction through formation of intermediate bulk carboxylates while alumina, titania, chromia, and zirconia promoted the ketonization by a surface reaction.[43] To see if a ketene species was a reaction intermediate for the surface reaction, varying contact times were used and ketone/ketene content plotted during testing of a zirconia catalyst.[43] It was found that the ketone and ketene showed opposite trends—ketene decreasing and ketone concentration increasing with contact time.[43] Therefore, it was proposed that a ketene like

species was involved as a reaction intermediate during surface reactions.[43] Further reaction testing using C^{13} isotopes revealed that during mixed ketonization reactions of acetic acid and trimethylacetic acid, the ketone carbonyl group was solely evolved from the trimethylacetic acid of which no self ketonization occurred <450 °C.[43] It was concluded that an α-hydrogen is necessary for the reaction to proceed and that the additional alkyl group for the ketone product comes from a species in equilibrium with a ketene.[43] A final mechanism as seen in Figure 6 was proposed. In this mechanism, one acid molecule, through hydrogen abstraction, is adsorbed in a parallel fashion on the catalyst surface which allows for easy cleavage of the C-C bonds to form a methylene species.[43] This adsorbed species is proposed to be in equilibrium with a gaseous ketene.[43] The methylene species then reacts with a carboxylate in the immediate vicinity to form the ketone.[43] However, recently Nagashima et al. published a manuscript disagreeing with Pestman et al.'s mechanism claiming that the methylene intermediate would have formed methanol by interaction with water on the surface in addition to the ketone.[50] They then propose a mechanism involving radical and β-ketoacid intermediates (Figure 7).[50] Nagashima et al. don't have a ketene species in their proposed mechanism as many other authors have assumed to be an intermediate. Identification of the origin of ketene compounds can be complicated for ketonization as both acetone and acetic acid can thermally decompose to form ketene.[42] Clearly, there is still a considerable amount of debate about the correct mechanism for the surface catalyzed reaction—or for that matter if the surface reaction is even occurring differently than the bulk decomposition.

Only a few years ago, Mekhemer et al. published an article demonstrating that not only the lattice energy of metal oxides determined whether or not the reaction occurred

through bulk carboxylate formation or on the surface.[51] Studying vapor phase coupling of acetic acid promoted by magnesia, it was found that despite the supposed large lattice energy of the oxide, bulk acetate formation occurred after only 2 hours of acid exposure at room temperature.[51] This discrepancy was believed to occur because of the high basicity of MgO.[51] Catalytic , through surface acetates, as well as pyrolytic formation of acetone were discovered to occur at approximately the same temperature (300 °C).[51] It was therefore claimed that the reaction proceeded catalytically at temperatures >360 °C where the corresponding acetate and carbonate were unstable.[51]

Inhibition studies can also assist in learning about the reaction mechanism. Both carbon dioxide and water have been examined as potential inhibitors of the reaction. If water significantly decreases the catalyst activity it is likely that carboxylate intermediates are involved as water will hamper O-M bond formation through hydrolysis. CO_2 could potentially impede the reaction both through the promotion of a bulk metal carbonate as well as competing for possible surface active sites. This was exemplified by Gaertner et al. who found that co-feeding CO_2 with hexanoic acid over a ceria-zirconia catalyst led to significant inhibition of ketonization.[37] Activity was not regained after removal of the CO_2 leading the authors to propose that surface basic sites were the catalytic centers.[37] In the same study, water was also found to act as an inhibitor.[37] It was suggested that water binding to the active basic sites was also the reason for catalyst deactivation.[37] Contrasting results were reported by Deng et al. who claim that water had little influence on ketonization over their supported ceria and manganese catalysts.[13]

As knowledge of the ketonization mechanism is lacking, there has been significant speculation on what exactly are the catalytic active sites. As just mentioned, a number of

publications have claimed that basic sites are what promote the reaction.[37, 52] Other authors have implicated redox sites to be of importance. There is some evidence for these claims. For example, Rubinshtein et al. found that during ketonization of acetic acid on ceria the catalyst became reduced.[53] The ease of reduction of surface metal cations has also been proposed to explain why ceria>titania>alumina in terms of catalytic activity.[54] Catalyst surface structures have also been claimed to be of significance. This was first discussed by Kim and Barteau in 1990 for ketonization of acetic acid on titania single crystals.[55] During acetic acid TPD experiments, only {114} surface facets were found to promote acetone desorption.[55] Thus it was declared that for ketonization reactions to occur, an oxidized surface containing cations that are doubly unsaturated must be present.[55] Six years later, Stubenrauch et al. published results, again with single crystal acetic acid TPD studies, showing that ceria catalysts also have structure sensitivity for the ketonization reaction.[56] In ceria's case only {111} facets promoted acetone evolution.[56] Stubenrauch et al's findings are of significance because they contrast with the observations of Barteau and Kim as the Ce {111} surface does not have cations with multiple vacancies. Stubenrauch et al. suggest that methyl groups, from acetate decomposition, interact with other surface acetate species to form the ketone.[56] In a more industrially relevant probe of surface structure sensitivity, Kobune et al. tested ceria catalysts—with different faceting—in a fixed bed flow reaction of gas phase propanoic acid.[57] Ceria, containing the various facets, was created by varying catalyst calcination temperatures.[57] It was demonstrated that the use of higher calcination temperatures promoted the formation of larger ceria particles that exposed more of the {111} facets.[57] Using a constant surface area of catalyst, conversions over the different particles sizes were plotted, establishing that the larger particles with the {111}

facets were significantly more active on a surface area basis (Figure 8).[57] It should be noted that if the reaction can occur in the bulk, a surface area basis is not adequate for comparisons.

1.7.2 Heterogeneous catalysts

Ketonization reactions of carboxylic acids have been found to be catalyzed by a large number of metal oxides. A commonly cited manuscript demonstrating the breadth of oxides able to promote the reaction was published in 1995 by Glinski et al.[58] In that work, twenty different metal oxides were supported on silica and tested at different temperatures in acetic acid ketonization. As observed in Table 5, at temperatures >400 °C, the majority of catalysts showed significant activity. Many other manuscripts have investigated a number of oxide materials similar to these.[43, 59-63] However, it appears that ceria containing catalysts are among the best.[50, 64, 65]

Variations of these metal oxide catalysts—through changing of support or doping in another oxide—have also been examined. For example, since the ceria and manganese catalysts demonstrated superior performance, Glinski further probed these materials by using different supports. Alumina and titania supports showed noteworthy increases in activity over silica despite their lower surface areas.[58] However, no rational for why this was occurring was given in the paper. Mesoporous silica supports have also been probed for ceria and manganese catalysts.[52] Seemingly contradicting the work by Glinski et al, claims have been made that better dispersion of the active phase gives greater activity. In a review, Dooley asserts that supported ceria catalysts have an optimal loading around 0.7-0.9 mg/m^2 which corresponds to near one monolayer.[66] Sometimes during the course of ketonization, supported ceria catalysts will increase in activity, supposedly due to increasing dispersion of

ceria and the formation of mixed oxides with the support.[66] Doping of catalysts with small amounts of other species has been found to give varying results with the addition of alkali materials to supported ceria promoting undesired side reactions while alkali doped zirconia was reported to have enhanced activity.[60, 67] Mixed oxide catalysts have been examined as well. Nagashima et al. synthesized oxide catalysts containing 90 mol% ceria and 10 mol% of another oxide for testing in the ketonization of propanoic acid.[50] Mg, Mn, Fe, Co, Ni, Cu, and Zr oxide additions all led to significant catalytic enhancement over pure ceria while chromia completely deactivated the catalyst.[50] Manganese was the best additive and was further probed.[50] While pure manganese oxide gave greater conversions of propanoic acid to 3-pentanone than did pure ceria, mixing of the two oxides gave even higher activity.[50] Mn contents of ~60 mol% were found to be best for the particular ketonization reaction.[50] However, no explanation was given for the discovered enhancements. Ceria-zirconia mixed oxides have also commonly been used for ketonization reactions. Use of this material as catalyst has been largely driven by the James Dumesic group from the University of Wisconsin-Madison in the conversion of bio-derived compounds to liquid fuels.[37, 39, 68-70] This particular catalyst was described as being used due to its ability to inhibit coke formation because of more labile oxygen species and strong oxide-metal interactions.[71]

Examination of the literature demonstrates the need for further understanding of the ketonization process at a more fundamental level. Most research has tended to focus primarily on reaction testing and less on catalyst characterization. This leads to a lack of knowledge connecting the kinetics of product formation with fundamental understanding of what is occurring with the catalytic material. It is the hope that this work will provide some insights that may be used to help bridge this gap.

1.7.3 Ceria catalysts

Ceria, the most important rare earth oxide catalyst, is widely used in common applications and processes such as fluid catalyzed cracking, three way catalytic converters, ethylbenzene to styrene dehydrogenation, and catalytic wet air oxidation.[72] However, it is rarely used in pure form due to its higher cost than more common supports and because of its lower thermal stability which results in significant surface area losses at temperatures ~750 °C.[72] For further information, *Catalysis by Ceria and Related Materials*, a book giving a thorough review of ceria related catalyst properties and applications—edited by a leader in ceria science, Alessandro Trovarelli—is suggested.[73]

Knowledge of ceria's redox properties are of significance as most applications of the material take advantage of this characteristic. Likewise, prominent proposed ketonization mechanisms involve some sort of redox step.[66] Oxidation states of cerium in the metal oxide can transition between 3+ and 4+ resulting in oxide stoichiometries able to vary between Ce_2O_3 and CeO_2. However, the more reduced oxide is not stable under atmospheric O_2 pressures and thus characterization of this phase must be done in inert environments.[73] The fluorite crystal structure of the more stable CeO_2 oxide is maintained even through moderate reduction of the cerium.[73] When performing a temperature programmed reduction of ceria, it is common to see two peaks—one at a low temperature and a second broad reduction that occurs at high temperatures.[74] These peaks have been explained to be due to a more facile surface reduction and a more difficult bulk reduction.[75] Mixing different oxides with ceria can potentially result in drastically different reduction profiles. For example, it has been found that the addition of zirconia to make a mixed oxide allows for reduction of the bulk oxide to occur at lower temperatures.[74] This phenomenon transpires

as Zr^{4+} is a smaller ion than is Ce^{4+}, hence its addition allows for easier diffusion of oxygen within the mixed oxide.[76] It was found that like pure ceria, this mixed oxide lost a significant amount of surface area after reduction in temperatures up to 1000 ˚C.[74] However, the ceria-zirconia blend actually obtained improved oxidation-reduction cycling through the high temperature reduction and a subsequent oxidation while pure ceria's redox abilities were significantly hindered.[74] Other dopants than zirconia have been studied as well. A mixed ceria-alumina catalyst was found to have similar redox properties to mixed ceria-zirconia catalysts in that the bulk ceria was more easily reduced.[77] Addition of metals to the ceria surface can also cause noteworthy changes in reduction profiles. Findings have shown that gold drastically weakens the surface oxygen on ceria causing its reduction to occur hundreds of degrees lower than in the pure form while not affecting bulk ceria reduction temperatures.[78] This property has demonstrated catalytic relevance as reduction differences corresponded nicely to activity in the water gas shift reaction.[78] There, while pure ceria was not active below 300 ˚C, the gold dispersed on ceria catalysts had a light off temperature under 120 ˚C.[78] The addition of platinum was also found to lower the surface reduction temperature of ceria and correspondingly increase the rates of water gas shift.[79]

As described earlier, catalyst acid-base characteristics and surface faceting could also be of potential interest for ketonization applications. Cerium oxide is known to act as both a solid acid and a solid base.[80] However, as the degree of reduction of ceria containing catalysts changes, the acid-base properties of the catalyst can change as well.[71] As its been found that ceria can become reduced during ketonization, this influence could result in catalyst acid-base site quantities changing in the course of reaction.[53] Low index ceria surfaces decrease in stability as {111}, {110), and {100}.[81] Hence, generally ceria

exposes the more stable {111} surface. Surface structure influences of ceria for catalytic applications have been found to be of importance for other reactions as well. For example, exposure of the more reactive {100} and {110} facets has been found to result in greater CO oxidation activity.[82, 83] Further testing of this property in more realistic ketonization environments would be desirable, but to perform these types of experiments, ceria catalysts exposing the less stable {110} and {100} facets would need to be synthesized for comparison. Inabilities to easily create these types of materials in the past greatly limited further applications of highly idealized studies. Fortunately, recent focus on the creation of nanomaterials has advanced developments in synthesis techniques making it possible to create shape selective ceria nanocrystals that expose these highly reactive surfaces.[82, 84, 85] Of a number of methods used to create these types of catalysts, the hydrothermal synthesis technique is favored due to low costs, use of only a single step, and no organic solvents.[82]

Mechanisms for the formation of these types of shape selective ceria catalysts have been investigated by a couple of different researchers.[82, 86] Through an interesting vapor catalyzed hydrothermal synthesis technique, Niesz et al. found that at pH 7.3, the ceria {100} surface demonstrated enhanced hydrolytic activity thus stabilizing its surface with hydroxyl groups.[86] Since the {100} planes were of lower energy, the crystal structure grew in the [111] direction and formed the corresponding nanocubes.[86] Mai et al. found that both the basicity and temperature of the synthesis mixture played a role in determining the final shape and exposed facets of the catalysts.[82] In that work, ceria nanorods, nanocubes, and nanopolyhedra were all created.[82] The cerium precursor was also found to be of importance in that a Ce^{3+} precursor like cerium(III) nitrate allowed for shape specific

formation while Ce^{4+} precursors like ammonium cerium (IV) nitrate did not.[82] These results demonstrated that the anisotropic $Ce(OH)_3$ species was necessary for nanorod formation while the higher temperatures promoted the formation of CeO_2 from the $Ce(OH)_3$, leading to transformation of the nanorods to nanocubes.[82]

1.8 Thesis organization

This document contains a number of different chapters addressing different subtopics of the overall research subject. The first chapter consists primarily of a literature review and background of the project. This is followed by a more concise description of the goals for the research. Chapters 3-7 contain discussion along with results of completed research topics. Aldol condensations promoted through the use of acid-base cooperative catalysis are the focus of chapter 3 while chapters 4-7 all examine various aspects of the ketonization reaction. These chapters are standalone manuscripts and are therefore formatted in that manner. Finally chapters 8-9 contain general conclusions and lay out potential future work as well.

1.9 References

[1] Annual Energy Outlook 2010, U.S. Department of Energy, Washington DC. DOE/EIA-0383
[2] R. Brown, Biorenewable Resources, Blackwell Publishing, Ames, IA, 2003.
[3] Crude Oil and Total Petroleum Imports Top 15 Countries, US Energy Information Administration, Released Nov. 29, 2011. http://www.eia.gov/pub/oil_gas/petroleum/data_publications/company_level_imports/current/import.html. accessed 3/12/12.
[4] P. McKendry, Energy production from biomass (part 2): conversion technologies, Bioresource Technology, 83 (2002) 47-54.
[5] M.J.A. Tijmensen, A.P.C. Faaij, C.N. Hamelinck, M.R.M. van Hardeveld, Exploration of the possibilities for production of Fischer Tropsch liquids and power via biomass gasification, Biomass and Bioenergy, 23 (2002) 129-152.
[6] D. Mohan, C.U. Pittman, P.H. Steele, Pyrolysis of Wood/Biomass for Bio-oil: A Critical Review, Energy & Fuels, 20 (2006) 848-889.
[7] S. Czernik, A.V. Bridgwater, Overview of Applications of Biomass Fast Pyrolysis Oil, Energy & Fuels, 18 (2004) 590-598.
[8] J.P. Diebold, A review of the chemical and physical mechanisms of the storage stability of fast pyrolysis bio-oils, NREL/SR-570-27613, Jan. 2000.

[9] P.R. Patwardhan, J.A. Satrio, R.C. Brown, B.H. Shanks, Influence of inorganic salts on the primary pyrolysis products of cellulose, Bioresource Technology, 101 (2010) 4646-4655.
[10] W. Wang, Y. Yang, H. Luo, T. Hu, W. Liu, Amorphous Co-Mo-B catalyst with high activity for the hydrodeoxygenation of bio-oil, Catalysis Communications, 12 (2011) 436-440.
[11] Z. Su-Ping, Study of Hydrodeoxygenation of Bio-Oil from the Fast Pyrolysis of Biomass, Energy Sources, Part A: Recovery, Utilization, and Environmental Effects, 25 (2003) 57 - 65.
[12] M. Ahmad, F.R. Nordin, T. Azizan, Upgrading of bio-oil into high-value hydrocarbons via hydrodeoxygenation, American journal of applied sciences, 7 (2010) 746.
[13] L. Deng, Y. Fu, Q.-X. Guo, Upgraded Acidic Components of Bio-oil through Catalytic Ketonic Condensation, Energy & Fuels, 23 (2008) 564-568.
[14] S. Ege, Organic Chemistry: Structure and Reactivity, Houghton Mifflin Company, Boston, 2004.
[15] S. Patai, The Chemistry of the Carbonyl Group, Interscience, London, 1966.
[16] A.C. Cope, Organic Reactions, in, John Wiley and Sons, Inc., New York, 1968.
[17] H.O. House, Modern Synthetic Reactions, 2nd ed., W.A. Benjamin, Inc, Menlo Park, California, 1972.
[18] M. Climent, A. Corma, V. Fornés, R. Guil-Lopez, S. Iborra, Aldol Condensations on Solid Catalysts: A Cooperative Effect between Weak Acid and Base Sites, Advanced Synthesis & Catalysis, 344 (2002) 1090-1096.
[19] M. Hasni, G. Prado, J. Rouchaud, P. Grange, M. Devillers, S. Delsarte, Liquid phase aldol condensation of cyclopentanone with valeraldehyde catalysed by oxynitrides possessing tuneable acid-base properties, Journal of Molecular Catalysis A: Chemical, 247 (2006) 116-123.
[20] V.K. Díez, C.R. Apesteguía, J.I. Di Cosimo, Effect of the acid-base properties of Mg-Al mixed oxides on the catalysts deactivation during aldol condensation reactions, Latin American applied research, 33 (2003) 79-86.
[21] J.C.A.A. Roelofs, D.J. Lensveld, A.J. van Dillen, K.P. de Jong, On the Structure of Activated Hydrotalcites as Solid Base Catalysts for Liquid-Phase Aldol Condensation, Journal of Catalysis, 203 (2001) 184-191.
[22] D. Tichit, D. Lutic, B. Coq, R. Durand, R. Teissier, The aldol condensation of acetaldehyde and heptanal on hydrotalcite-type catalysts, Journal of Catalysis, 219 (2003) 167-175.
[23] S. Luo, J. Falconer, Aldol condensation of acetaldehyde to form high molecular weight compounds on TiO, Catalysis Letters, 57 (1999) 89-93.
[24] E.G. Doyagüez, F. Calderón, F. Sánchez, A. Fernández-Mayoralas, Asymmetric Aldol Reaction Catalyzed by a Heterogenized Proline on a Mesoporous Support. The Role of the Nature of Solvents, The Journal of Organic Chemistry, 72 (2007) 9353-9356.
[25] Y.-C. Chang, Y. Chang, Vapor phase reactions of acetaldehyde over type X zeolites, Applied catalysis. A, General, 190 (2000) 149.
[26] S.K. Bej, L.T. Thompson, Acetone condensation over molybdenum nitride and carbide catalysts, Applied Catalysis A: General, 264 (2004) 141-150.
[27] G.P. Dechaine, F.T.T. Ng, A New Coated Catalyst for the Production of Diacetone Alcohol via Catalytic Distillation, Industrial & Engineering Chemistry Research, 47 (2008) 9304-9313.
[28] R.K. Zeidan, S.-J. Hwang, M.E. Davis, Multifunctional Heterogeneous Catalysts: SBA-15-Containing Primary Amines and Sulfonic Acids, Angewandte Chemie International Edition, 45 (2006) 6332-6335.
[29] R.K. Zeidan, M.E. Davis, The effect of acid-base pairing on catalysis: An efficient acid-base functionalized catalyst for aldol condensation, Journal of Catalysis, 247 (2007) 379-382.
[30] G.G. Podrebarac, F.T.T. Ng, G.L. Rempel, A kinetic study of the aldol condensation of acetone using an anion exchange resin catalyst, Chemical Engineering Science, 52 (1997) 2991-3002.

[31] L. Gandia, L.M. Ganda, Gandia, Application of a new hydrogenated aluminophosphate oxynitride (ALPON) as a catalytic support for the one-step synthesis of methyl isobutyl ketone from acetone, Applied catalysis. A, General, 114 (1994) L1.
[32] S.-M. Yang, Y.M. Wu, One step synthesis of methyl isobutyl ketone over palladium supported on AlPO4-11 and SAPO-11, Applied Catalysis A: General, 192 (2000) 211-220.
[33] S.L. Hruby, B.H. Shanks, Acid-base cooperativity in condensation reactions with functionalized mesoporous silica catalysts, Journal of Catalysis, 263 (2009) 181-188.
[34] M.D. Hasni, S.; Rouchaud, J.; Grange, P., Adjustment of the acid-base properties of phosphates through nitridation, for increased selectivity in miexed aldol condensations, Silicates Industriels, 69 (2004) 77-84.
[35] E.L. Margelefsky, R.K. Zeidan, M.E. Davis, Cooperative catalysis by silica-supported organic functional groups, Chemical Society Reviews, 37 (2008) 1118-1126.
[36] M.J. Climent, A. Corma, V. Fornés, A. Frau, R. Guil-López, S. Iborra, J. Primo, Aluminophosphates Oxynitrides as Base Catalysts: Nature of the Base Sites and Their Catalytic Implications, Journal of Catalysis, 163 (1996) 392-398.
[37] C.A. Gaertner, J.C. Serrano-Ruiz, D.J. Braden, J.A. Dumesic, Catalytic coupling of carboxylic acids by ketonization as a processing step in biomass conversion, Journal of Catalysis, 266 (2009) 71-78.
[38] A. Corma, M. Renz, C. Schaverien, Coupling Fatty Acids by Ketonic Decarboxylation Using Solid Catalysts for the Direct Production of Diesel, Lubricants, and Chemicals, ChemSusChem, 1 (2008) 739-741.
[39] E.L. Kunkes, D.A. Simonetti, R.M. West, J.C. Serrano-Ruiz, C.A. Gartner, J.A. Dumesic, Catalytic Conversion of Biomass to Monofunctional Hydrocarbons and Targeted Liquid-Fuel Classes, Science, 322 (2008) 417-421.
[40] C. Friedel, Ueber s. g. gemischte Acetone, Justus Liebigs Annalen der Chemie, 108 (1858) 122-125.
[41] E.R. Squibb, Improvement in the manufacture of acetone, Journal of the American Chemical Society, 17 (1895) 187-201.
[42] A To Alkanolamines, M. Grayson (Ed.) Kirk-Othmer Encyclopedia of Chemical Technology, John Wiley and Sons, New York, 1978.
[43] R. Pestman, R.M. Koster, A. van Duijne, J.A.Z. Pieterse, V. Ponec, Reactions of Carboxylic Acids on Oxides: 2. Bimolecular Reaction of Aliphatic Acids to Ketones, Journal of Catalysis, 168 (1997) 265-272.
[44] L. Vivier, D. Duprez, Ceria-Based Solid Catalysts for Organic Chemistry, ChemSusChem, 3 (2010) 654-678.
[45]V.I. Yakerson, E.A. Fedorovskaya, A.L. Klyachko-Gurvich, A.M. Rubinshtein, Vapor Phase Catalytic Ketonation of CH3COOH over Oxides of Quadrivalent Metals and BeO, Kinetika i Kataliz, 2 (1961) 907-915.
[46] Y. Yamada, M. Segawa, F. Sato, T. Kojima, S. Sato, Catalytic performance of rare earth oxides in ketonization of acetic acid, Journal of Molecular Catalysis A: Chemical, 346 (2011) 79-86.
[47] S. Bernal, J. Cornejo, J.M. Criado, J.M. Trillo, Application of thermal methods in catalysis: ketonization of acetic acid on 3d and 4f metal oxides, Proc. Eur. Symp. Therm. Anal., 1st, (1976) 121-124.
[48] S. Rajadurai, Pathways for carboxylic acid decomposition on transition metal oxides., Catalysis Reviews-Science and Engineering, 36 (1994) 385-403.
[49] R. Swaminathan, J.C. Kuriacose, Studies on the ketonization of acetic acid on chromia : II. The surface reaction, Journal of Catalysis, 16 (1970) 357-362.
[50] O. Nagashima, S. Sato, R. Takahashi, T. Sodesawa, Ketonization of carboxylic acids over CeO2-based composite oxides, Journal of Molecular Catalysis A: Chemical, 227 (2005) 231-239.

[51] G.A.H. Mekhemer, S.A. Halawy, M.A. Mohamed, M.I. Zaki, Ketonization of acetic acid vapour over polycrystalline magnesia: in situ Fourier transform infrared spectroscopy and kinetic studies, Journal of Catalysis, 230 (2005) 109-122.
[52] A.D. Murkute, J.E. Jackson, D.J. Miller, Supported mesoporous solid base catalysts for condensation of carboxylic acids, Journal of Catalysis, 278 (2011) 189-199.
[53] A.M. Rubinshtein, A.A. Slinkin, V.I. Yakerson, E.A. Fedorovskaya, The reduction of CeO2 in the ketonization of ch3cooh, Russian Chemical Bulletin, 10 (1961) 2090-2092.
[54] M.A. Hasan, M.I. Zaki, L. Pasupulety, Oxide-catalyzed conversion of acetic acid into acetone: an FTIR spectroscopic investigation, Applied Catalysis A: General, 243 (2003) 81-92.
[55] K.S. Kim, M.A. Barteau, Structure and composition requirements for deoxygenation, dehydration, and ketonization reactions of carboxylic acids on TiO2(001) single-crystal surfaces, Journal of Catalysis, 125 (1990) 353-375.
[56] J. Stubenrauch, E. Brosha, J.M. Vohs, Reaction of carboxylic acids on CeO2(111) and CeO2(100), Catalysis Today, 28 (1996) 431-441.
[57] M. Kobune, S. Sato, R. Takahashi, Surface-structure sensitivity of CeO2 for several catalytic reactions, Journal of Molecular Catalysis A: Chemical, 279 (2008) 10-19.
[58] M. Glinski, J. Kijenski, A. Jakubowski, Ketones from monocarboxylic acids: Catalytic ketonization over oxide systems, Applied Catalysis A: General, 128 (1995) 209-217.
[59] R. Martinez, M.C. Huff, M.A. Barteau, Ketonization of acetic acid on titania-functionalized silica monoliths, Journal of Catalysis, 222 (2004) 404-409.
[60] K. Parida, H.K. Mishra, Catalytic ketonisation of acetic acid over modified zirconia: 1. Effect of alkali-metal cations as promoter, Journal of Molecular Catalysis A: Chemical, 139 (1999) 73-80.
[61] M. Glinski, J. Kijenski, Decarboxylative coupling of heptanoic acid. Manganese, cerium and zirconium oxides as catalysts, Applied Catalysis A: General, 190 (2000) 87-91.
[62] K. Okumura, Y. Iwasawa, Zirconium Oxides Dispersed on Silica Derived from Cp2ZrCl2, [(i-PrCp)2ZrH([mu]-H)]2, and Zr(OEt)4Characterized by X-Ray Absorption Fine Structure and Catalytic Ketonization of Acetic Acid, Journal of Catalysis, 164 (1996) 440-448.
[63] M. Jayamani, C.N. Pillai, Reaction of carboxylic acids with carbonyl compounds over alumina, Journal of Catalysis, 87 (1984) 93-97.
[64] M. Renz, Ketonization of Carboxylic Acids by Decarboxylation: Mechanism and Scope, ChemInform, 36 (2005).
[65] S.D. Randery, J.S. Warren, K.M. Dooley, Cerium oxide-based catalysts for production of ketones by acid condensation, Applied Catalysis A: General, 226 (2002) 265-280.
[66] K.M. Dooley, Catalysis of Acid/Aldehyde/Alcohol Condensations to Ketones, in: J.J.S.a.G.W. Roberts (Ed.) Catalysis, The Royal Society of Chemistry, Cambridge, 2004, pp. 293-319.
[67] K.M. Dooley, A.K. Bhat, C.P. Plaisance, A.D. Roy, Ketones from acid condensation using supported CeO2 catalysts: Effect of additives, Applied Catalysis A: General, 320 (2007) 122-133.
[68] E.I. Gürbüz, E.L. Kunkes, J.A. Dumesic, Integration of C-C coupling reactions of biomass-derived oxygenates to fuel-grade compounds, Applied Catalysis B: Environmental, 94 (2010) 134-141.
[69] C.A. Gaertner, J.C. Serrano-Ruiz, D.J. Braden, J.A. Dumesic, Ketonization Reactions of Carboxylic Acids and Esters over Ceria−Zirconia as Biomass-Upgrading Processes, Industrial & Engineering Chemistry Research, 49 (2010) 6027-6033.
[70] C.A. Gärtner, J.C. Serrano-Ruiz, D.J. Braden, J.A. Dumesic, Catalytic Upgrading of Bio-Oils by Ketonization, ChemSusChem, 2 (2009) 1121-1124.
[71] E.L. Kunkes, E.I. Gürbüz, J.A. Dumesic, Vapour-phase C-C coupling reactions of biomass-derived oxygenates over Pd/CeZrOx catalysts, Journal of Catalysis, 266 (2009) 236-249.
[72] A. Trovarelli, C. de Leitenburg, M. Boaro, G. Dolcetti, The utilization of ceria in industrial catalysis, Catalysis Today, 50 (1999) 353-367.

[73] A. Trovarelli, Catalysis by Ceria and Related Materials, in: G.J. Hutchings (Ed.) Catalytic Science Series, Imperial College Press, 2002.
[74] F. Fally, V. Perrichon, H. Vidal, J. Kaspar, G. Blanco, J.M. Pintado, S. Bernal, G. Colon, M. Daturi, J.C. Lavalley, Modification of the oxygen storage capacity of CeO2-ZrO2 mixed oxides after redox cycling aging, Catalysis Today, 59 (2000) 373-386.
[75] H.C. Yao, Y.F.Y. Yao, Ceria in automotive exhaust catalysts : I. Oxygen storage, Journal of Catalysis, 86 (1984) 254-265.
[76] C. de Leitenburg, D. Goi, A. Primavera, A. Trovarelli, G. Dolcetti, Wet oxidation of acetic acid catalyzed by doped ceria, Applied Catalysis B: Environmental, 11 (1996) L29-L35.
[77] L. Ilieva, G. Pantaleo, I. Ivanov, A.M. Venezia, D. Andreeva, Gold catalysts supported on CeO2 and CeO2-Al2O3 for NOx reduction by CO, Applied Catalysis B: Environmental, 65 (2006) 101-109.
[78] Q. Fu, S. Kudriavtseva, H. Saltsburg, M. Flytzani-Stephanopoulos, Gold-ceria catalysts for low-temperature water-gas shift reaction, Chemical Engineering Journal, 93 (2003) 41-53.
[79] G. Jacobs, U.M. Graham, E. Chenu, P.M. Patterson, A. Dozier, B.H. Davis, Low-temperature water-gas shift: impact of Pt promoter loading on the partial reduction of ceria and consequences for catalyst design, Journal of Catalysis, 229 (2005) 499-512.
[80] K. Tanabe, Misono, M. , Ono, Y., Hattori, H., New Solid Acids and Bases, Elsevier, Amsterdam, 1989.
[81] M. Baudin, M. Wójcik, K. Hermansson, Dynamics, structure and energetics of the (111), (011) and (001) surfaces of ceria, Surface Science, 468 (2000) 51-61.
[82] H.-X. Mai, L.-D. Sun, Y.-W. Zhang, R. Si, W. Feng, H.-P. Zhang, H.-C. Liu, C.-H. Yan, Shape-Selective Synthesis and Oxygen Storage Behavior of Ceria Nanopolyhedra, Nanorods, and Nanocubes, The Journal of Physical Chemistry B, 109 (2005) 24380-24385.
[83] E. Aneggi, J. Llorca, M. Boaro, A. Trovarelli, Surface-structure sensitivity of CO oxidation over polycrystalline ceria powders, Journal of Catalysis, 234 (2005) 88-95.
[84] R.F.-S. Si, Maria;, Shape and crystal-plane effects of nanoscale ceria on the activity of Au-CeO2 catalysts for the water-gas shift reaction, Angewandte Chemie, International Edition, 47 (2008) 2884-2887.
[85] F. Dang, K. Kato, H. Imai, S. Wada, H. Haneda, M. Kuwabara, Characteristics of CeO2 Nanocubes and Related Polyhedra Prepared by Using a Liquid−Liquid Interface, Crystal Growth & Design, 10 (2010) 4537-4541.
[86] K. Niesz, C. Reji, J.R. Neilson, R.C. Vargas, D.E. Morse, Unusual Evolution of Ceria Nanocrystal Morphologies Promoted by a Low-Temperature Vapor Diffusion Based Process, Crystal Growth & Design, 10 (2010) 4485-4490.
[87] R.W. Snell, Elliot Combs, Brent H. Shanks., Aldol Condensations Using Bio-oil Model Compounds: The Role of Acid-Base Bi-functionality, Topics in Catalysis, 53 (2010) 1248-1253.

1.10 Tables and Figures

Table 1. Top exporters of crude oil to the US.[3]

Country	Crude Oil Imports (1000s Barrels/day Sep. 2011)
Canada	2324
Saudi Arabia	1465
Mexico	1099
Venezuela	759
Nigeria	529
Colombia	510
Iraq	403
Ecuador	299

Table 2. Common aldehydes in bio-oil[8]

Compound	Bio-oil wt%
Acetaldehyde	0.1-8.5
Ethanedial	0.9-4.6
Formaldehyde	0.1-3.3
2-propenal	0.6-0.9
Pentanal	0.5
2-methyl-2-butenal	0.1-0.5

Table 3. Common ketones in bio-oil[8]

Compound	Bio-oil wt%
Acetone	2.8
MEK	0.3-0.9
3-methyl-2-cyclopenten-2-ol-1-one	0.1-0.6
Trimethylcyclopentenone	0.1-0.5
2,3, Pentenedione	0.2-0.4
2-Ethyl-cyclopentanone	0.2-0.3
Dimethylcyclopentanone	0.3

Table 4. Common acids in bio-oil[8]

Compound	Bio-oil wt%
Acetic	0.5-12
Formic	0.3-9.1
Propanoic	0.1-1.8
Hydroxyacetic	0.1-0.9
Pentanoic	0.1-0.8
Butanoic	0.1-0.5
4-Oxypentanoic	0.1-0.4
Heptanoic	0.3
Benzoic	0.2-0.3
Hexanoic	0.1-0.3

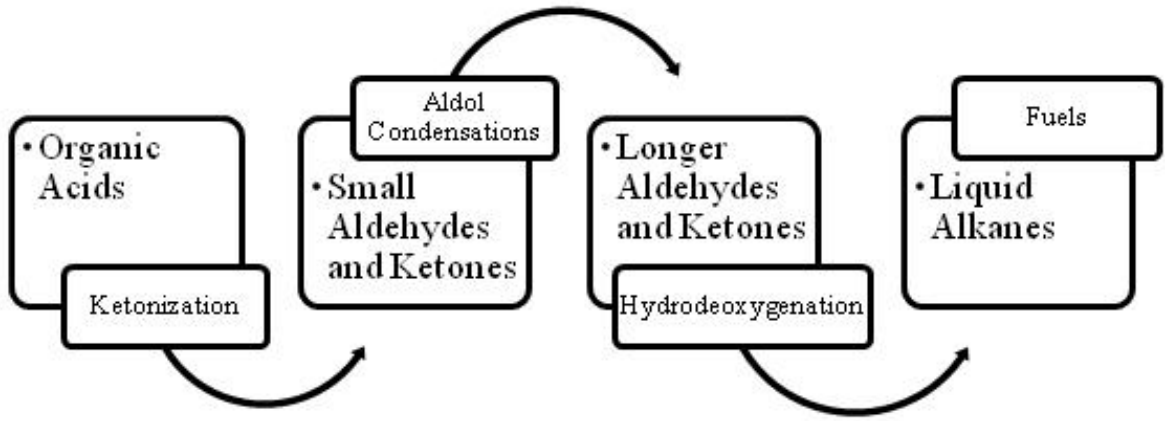

Figure 1. Potential bio-oil upgrading scheme.[87]

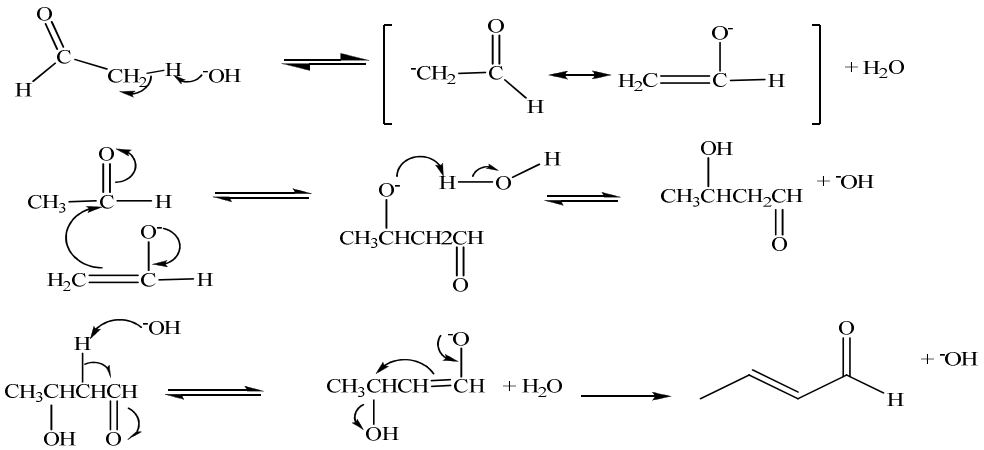

Figure 2. Base catalyzed mechanism for the aldol condensation of acetaldehyde followed by dehydration.

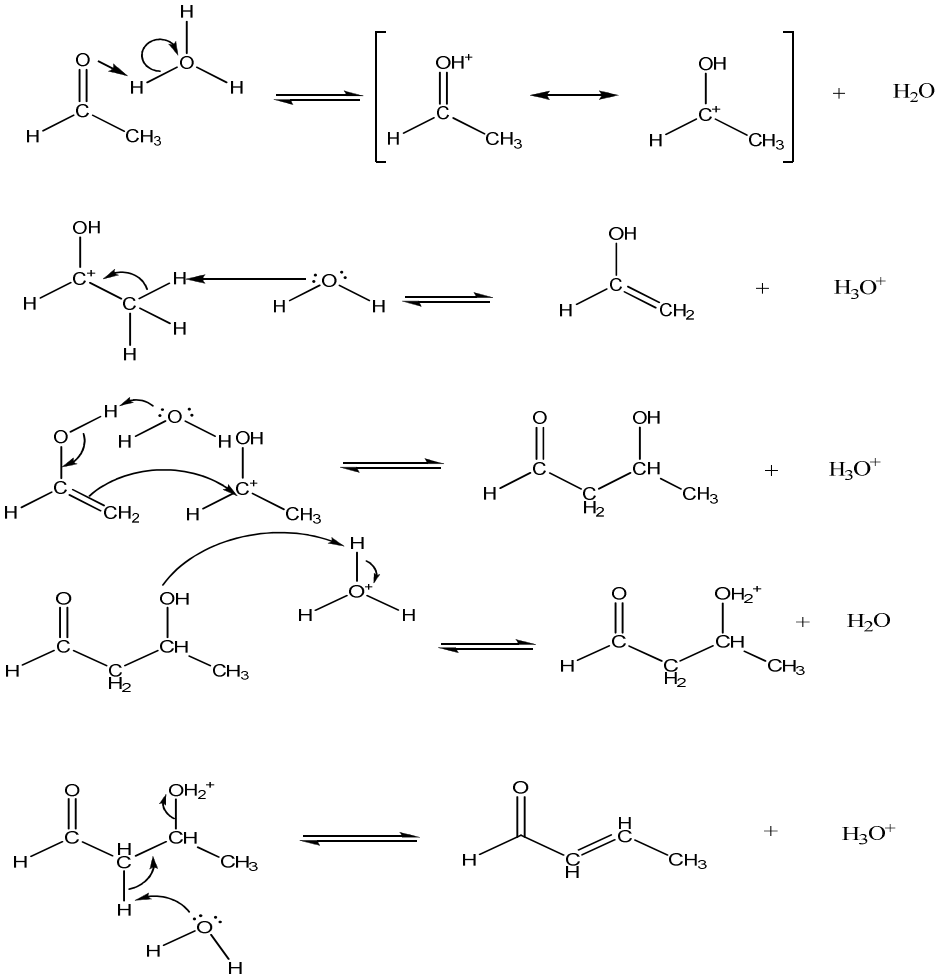

Figure 3. Acid catalyzed mechanism for the aldol condensation of acetaldehyde followed by dehydration.

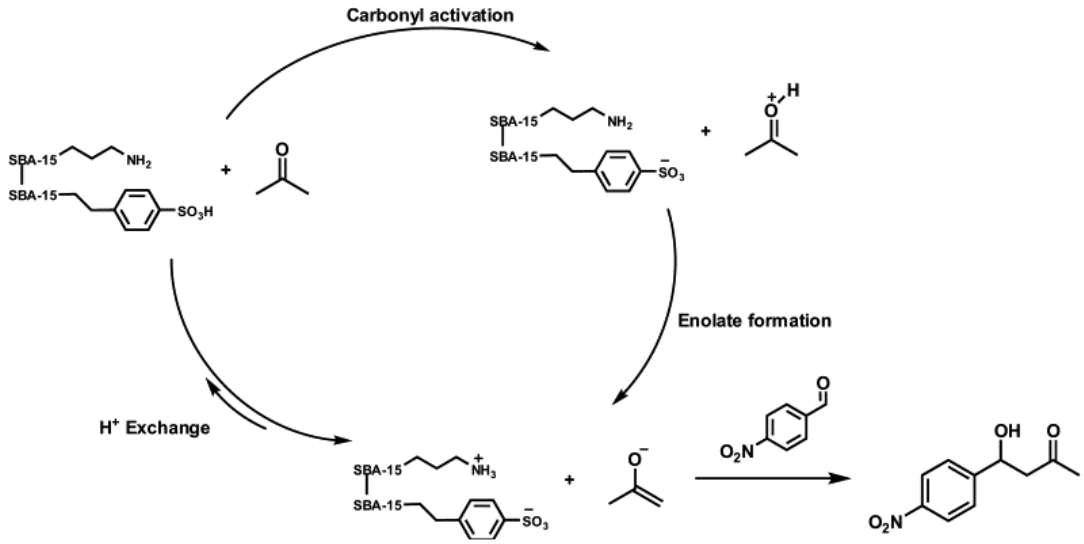

Figure 4. Zeidan and Davis's SBA-15 proposed acid-base cooperative mechanism.[29]

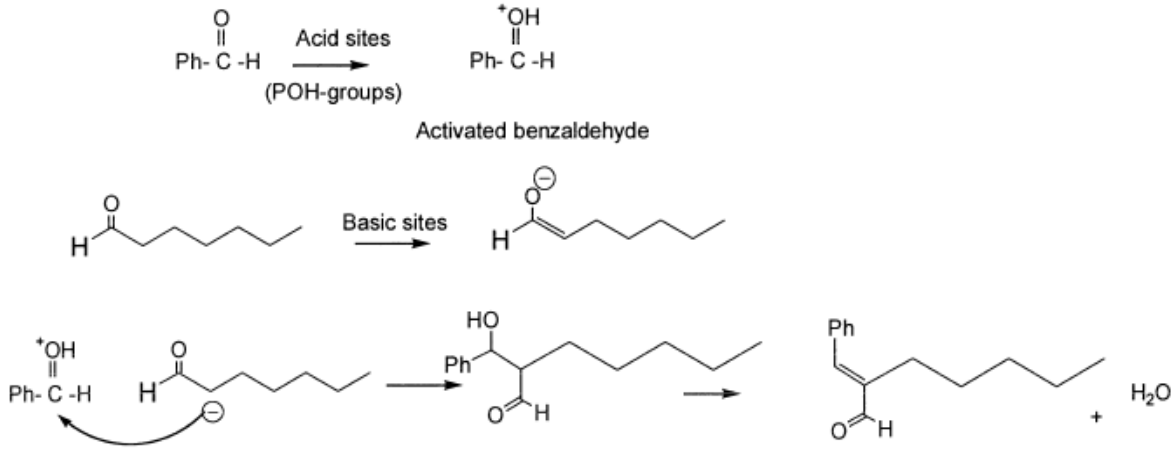

Figure 5. Climent et al. proposed aluminophosphate acid-base cooperative mechanism.[18]

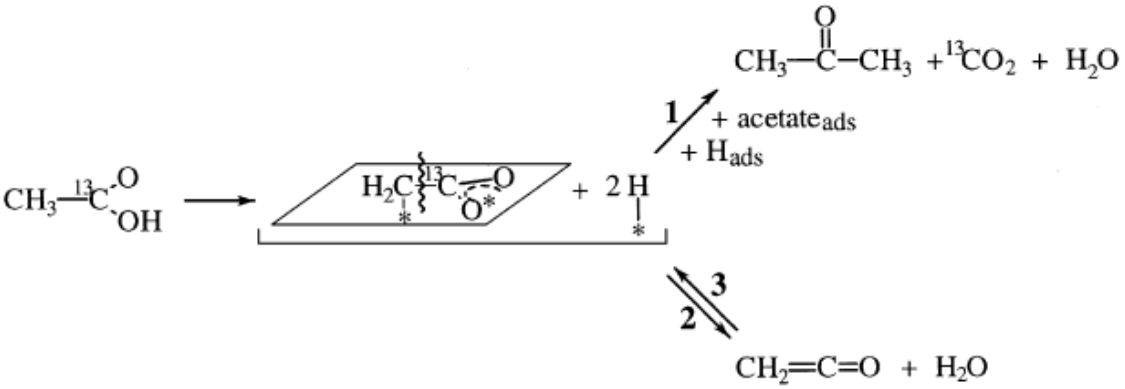

Figure 6. Surface ketonization mechanism as proposed by Pestman et al.[43]

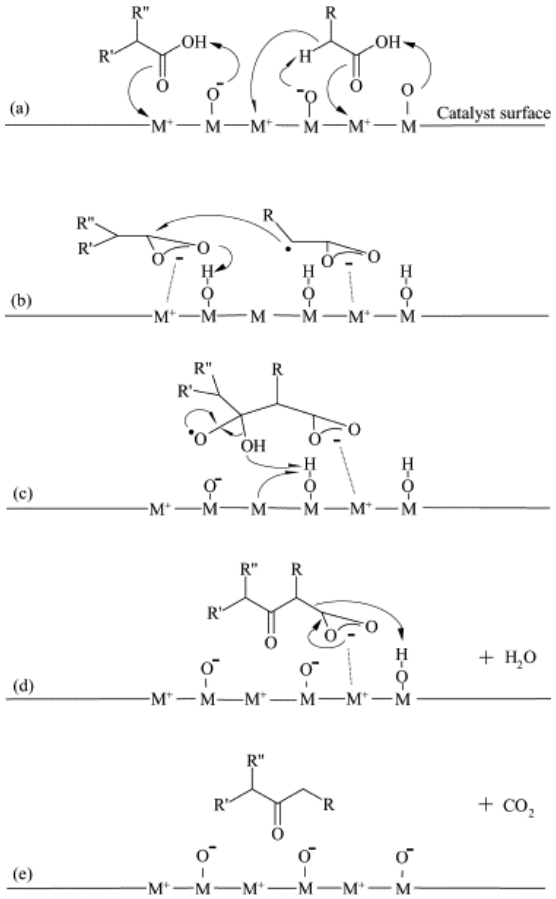

Figure 7. Ketonization mechanism of carboxylic acids over ceria-manganese mixed oxide catalysts as proposed by Nagashima et al.[50]

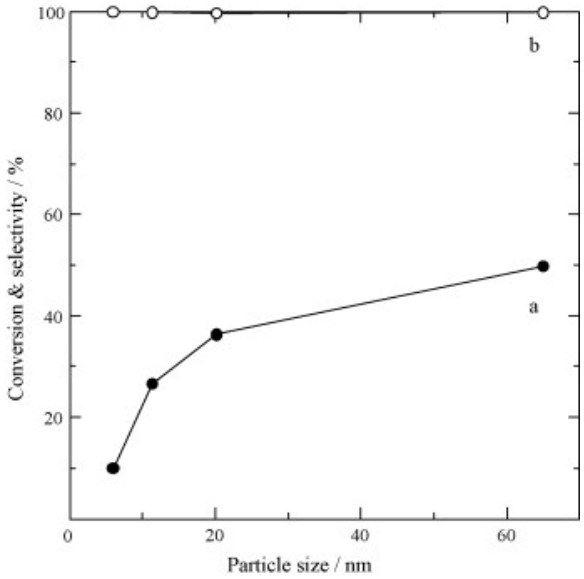

Figure 8. Propanoic acid conversion and selectivities to ketone over a constant surface area of ceria catalysts of different particle size and surface faceting as performed in experiments by Kobune et al.[57]

Table 5. Acetone yields for acetic acid ketonization over various oxides supported on silica as reported by Glinski et al.[58]

Active phase	Yield of acetone (%)						
	573 K	598 K	623 K	648 K	673 K	698 K	723 K
–[a]	2	2	3	4	5	20	32
B_2O_3	2	2	2	2	3	6	7
MoO_3	2	2	1	4	5	5	5
WO_3	2	4	6	6	5	5	6
P_2O_5	1	1	6	10	12	9	5
V_2O_5	3	4	4	9	21	29	24
Bi_2O_3	10	6	5	11	18	28	44
NiO[b]	7	9	10	31	–[b]	–[b]	–[b]
Al_2O_3	0	0	4	15	37	45	52
CuO[c]	5	5	6	29	39	43	50
ZnO	6	9	10	19	33	54	67
PbO	6	10	15	36	76	79	75
Cr_2O_3	1	8	52	48	39	46	54
Fe_2O_3	13	32	39	66	59	60	52
CoO	13	15	48	50	63	64	68
MgO	7	20	39	53	59	68	74
Nd_2O_3[d]	3	3	6	22	61	70[f]	–
La_2O_3	3	12	14	50	87[f]	–	–
MnO_2	18	22	34	72	96[f]	–	–
CdO[e]	6	27	73	76	94[f]	–	–
CeO_2	9	24	31	96	97[f]	–	–

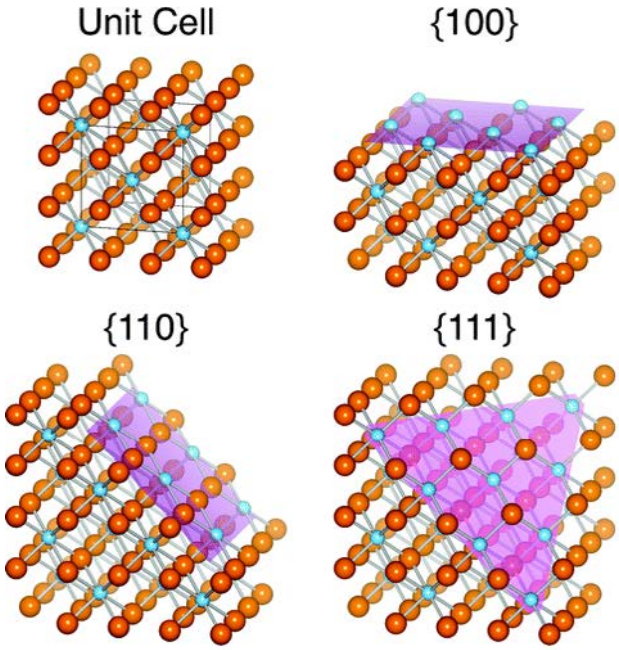

Figure 9. Ceria unit cell as well as bulk terminated low index surfaces. Small spheres are cerium cations while larger spheres are oxygen anions (image from Niesz et al.).[86]

Chapter 2

Research objectives

As was described in chapter 1, the creation of a clean, renewable, and cheap source of energy—particularly in the form of a liquid—is extremely important. Biorenewable resources are a particularly promising option to explore when attempting to tackle this issue as they supply a renewable carbon source. Fast pyrolysis in particular has demonstrated potential as a technique for transforming biomass into a more useable form. Unfortunately there are a number of difficulties that need to be addressed before pyrolysis oil can be efficiently and cheaply converted to a fuel capable of broad use. The field of catalysis is particularly situated to help in developing cost effective solutions to these problems. It was with this in mind that the current project was undertaken. Due to the complex composition of bio-oil as well as the lack of knowledge available about catalytic reactions involving common components, this is not a trivial task. When probing potential beneficial transformations of pyrolysis oil compounds, it can be seen that the formation of carbon-carbon bonds would be helpful. Therefore research of reactions completing this undertaking is especially pertinent. Aldol condensation and ketonization are two common carbon-carbon bond forming reactions. However, despite being widely known and mature reactions, there has been little research into their use with bio-oil compounds as well as in the conditions that would be preferred for upgrading. Therefore the goal of this research is to gain knowledge about aldol condensations and ketonization that can be applied to bio-oil applications. More explicitly, the goal of this work is to gain an understanding of the desirable catalytic traits for this particular exploitation of ketonization and aldol condensations through the synthesis, characterization, and testing of a variety of different materials.

Chapter 3

Aldol condensations using bio-oil model compounds: the role of acid-base bi-functionality

A paper published in Topics in Catalysis

Ryan W. Snell[1], Elliot Combs[1], Brent H. Shanks[1]

[1]Department of Chemical and Biological Engineering, Iowa State University

Authorship roles:

Snell: Primary author

Combs: Provided help with reaction testing

Shanks: Principal investigator

Abstract

The aldol condensation of acetaldehyde, acetone, and methyl ethyl ketone, which represent model bio-oil compounds, in the condensed phase, was performed using a bi-functional aluminophosphate catalyst. It was found that increasing the number and strength of the basic sites while decreasing acid sites on the catalyst caused a reduction in yield of the condensation products. In contrast, the addition of organic acids such as acetic acid at low concentrations to the catalyst-containing reaction mixture was found to increase activity. The presence of both acid and base sites was found to be necessary and their relative number was important for both the activity and selectivity of the condensation reaction. A mechanism explaining the observed phenomena was proposed.

*Keywords***:** Aldol condensation; Aluminum phosphate; Enolization; Bio-oil; Bi-functional catalyst

3.1 Introduction

With traditional energy sources becoming more difficult and less economical to obtain, it is crucial that new alternatives be developed. A promising source of renewable energy is fuels derived from biomass. Fast pyrolysis, involving high heating rates with temperatures around 450-500 °C and rapid cooling of vapors in an inert environment, has received increasing attention in recent years.[1-4] The liquid product from fast pyrolysis, which is known as bio-oil, is a complex mixture of many different functionalized molecules consisting largely of organic acids, ketones, aldehydes, alcohols, guaiacols, syringols, phenols, furans and various other oxygenates.[3]

The large number of molecules containing oxygen functionalities in bio-oil presents a clear disadvantage for using these liquids as a fuel since they significantly lower the energy density. It has been found that in general, bio-oil has about half of the energy density of crude oil.[5] Another difficulty with bio-oil is its high content of organic acids. These acids give the oil a pH of 2-3 which can cause storage issues due to corrosion with widely used materials such as aluminum and carbon steel.[6] Storage of the oil is also difficult as many reactions can occur between the highly functionalized molecules, causing the viscosity to increase as well as instigating phase separations.[3]

Hydrodeoxygenation is a conversion method that could be used to upgrade the bio-oil. However, as shown in Table 1, there are large numbers of small aldehydes and ketones that would become unusable for liquid fuels during this upgrading process. In order to preserve the carbon from these low molecular weight molecules in the liquid phase, it would be advantageous to perform condensed phase catalytically controlled reactions to increase carbon chain length prior to hydrodeoxygenation. An upgrading schematic similar to what

has been proposed by Deng et. al. can be seen in Figure 1.[7] Here, the organic acids in the oil would be removed first by ketonization reactions. Secondly, aldol condensations would be performed in order to create longer chain length molecules out of the many small aldehydes and ketones present in the bio-oil. Finally, hydrodeoxygenation would be done before use as a fuel. The work discussed here is relevant to the aldol condensation step in the upgrading scheme.

Aldol condensation is a well documented reaction that is common to most organic chemistry texts. The reaction involves condensing either two aldehydes, two ketones, or a mixture of the two. However, the condensation of two ketones typically does not occur to a great extent as it is not thermodynamically favored.[8-10] These reactions can be catalyzed by both acids and bases. While aldol condensations have historically been catalyzed with homogeneous acids and bases, due to environmental and economic concerns, more current literature has focused on heterogeneous catalysts. These heterogeneous catalysts are typically basic catalysts such as hydrotalcites[11], anion exchange resins[12], or MgO[13] among others. Recently, it was demonstrated that heterogeneous catalysts were able to effectively catalyze condensation reactions through acid-base cooperative catalysis.[14-16]

As strong acids and bases can catalyze a number of undesirable side reactions in bio-oil, it would be ideal to use a bi-functional catalyst allowing for more mild acids and bases to catalyze the desired aldol condensation. The acid and base containing catalyst aluminum phosphate (ALPO) was chosen because it allows for modification of its base site strength and density thus permitting for the study of acid-base cooperative catalysis. Nitrogen can replace oxygen on the catalyst through nitridation with ammonia at high temperatures. It is well documented that ALPO, containing both acidic P-OH groups and basic oxygen sites, will

lose acid sites and gain a greater basic character as more nitrogen is incorporated into the catalytic material.[14, 17-21] Not only does longer nitridation time increase the number of basic sites, it also increases the strength of the sites.[17] Since the correlative effect of nitrogen incorporation with basicity for this system has been thoroughly studied, the current work used increasing nitrogen weight percents synonymously with an increase in catalyst basicity. This catalyst or similar catalysts have been reported to be active in the aldol condensation of cyclopentanone with valeraldehyde[19] and heptanal with benzaldehyde[14]. In literature, the increase in basicity due to nitridation of the catalyst has had differing effects on the aldol condensation reaction. Climent et al. found that in the aluminum phosphate catalyzed condensation of heptanal and benzaldehyde low incorporation of nitrogen caused a decrease in activity while higher levels caused an increase.[14] It was also discovered that there was a decrease in selectivity to the cross condensation product with increased nitridation. Hasni et al. found that increased nitridation of their galloaluminophosphate material led to an increase in activity and in selectivity to the cross condensation product in the same reaction.[22] However, there has been little investigation into the catalysis of aldol condensations involving the small aldehydes and ketones found in bio-oil and particularly not in the condensed phase, which will likely be required for bio-oil upgrading. Here, the studies were performed on the aldol condensations of model bio-oil compounds in the liquid phase. The particular reactions studied were the condensations of methyl ethyl ketone (MEK) and acetaldehyde as well as acetone and acetaldehyde. The role of the catalytic acid and base groups on the reaction products were also probed.

3.2 Experimental section

The base aluminum phosphate catalyst was made in a method similar to Lindblad.[23] To an Erlenmeyer flask, 200 ml of deionized water along with 1 ml of 15.8 N nitric acid (Fisher) was added. In the flask 15.45 g of $Al(NO_3)_3 \cdot 9H_2O$ (Acros 99+%) and 5.43 g of $(NH_4)_2HPO_4$ (Fisher 99.7%) was dissolved with stirring. Concentrated ammonia (Fisher) was added dropwise until a pH of 8.74. The mixture was then stirred for one hour, vacuum filtered, and washed with copious amounts of water. The catalyst was dried at 120 °C for 16 h and calcined at 500 °C in air for 30 minutes. To lower the acidity and increase the basicity of the catalyst, nitridation was performed. The nitridation was done in a tube furnace by first purging with N_2, then flowing 240 ml/min NH_3 along with 230 ml/min N_2 over the catalyst for either 16 (ALPON-16), 24 (ALPON-24), 48 (ALPON-48) or 72 (ALPON-72) hours at 800 °C. After nitridation, the catalyst was moved to an oven and kept under vacuum at 150 °C overnight to remove physisorbed ammonia. Surface areas of the catalysts were measured on a Micromeritics ASAP 2020 using the BET method for N_2 adsorption isotherms. Nitrogen content of the catalysts was found using a Perkin-Elmer 2400 Series II CHN/S elemental analyzer. A summary of the catalyst properties can be found in Table 2.

Reactions were performed in 60 ml pressurized stirred batch reactors (Parr Series 4590, Parr Instrument Company) and analyzed by gas chromatography (Agilent 7890A) with a flame ionization detector using 1,4 dioxane as an internal standard. Prior to reaction the catalysts were heated overnight at 150 °C to remove adsorbed water. A reactant to catalyst weight ratio of 20 was used. The typical reaction procedure involved adding 2.00 g of acetaldehyde (Acros 99.5%), 2.00 g acetone (Fisher 99.7%) or 2.00 g MEK (Fisher 99.8%), 3.2 g of 1,4 dioxane (Fisher 100.0%), along with 44 ml of solvent, toluene (Fisher 99.9 %),

into the reaction vessel with 0.200 g of catalyst. The reactor was then pressurized to 350 psig with nitrogen to keep the reactants in the condensed phase and heated to 150 °C. A stir rate study was done and 800 rpm was chosen as it appears to prevent external transport limitations and the catalyst was finely ground to prevent internal mass transfer issues. Reaction samples were collected in cold toluene to limit the loss of reactants due to vaporization. Products were identified by injecting purchased standards. Yields were defined for cross products as $Yield = \frac{moles\ product\ formed\ during\ reaction}{initial\ moles\ of\ ketone\ reactant}$ and for crotonaldehyde as $Yield = \frac{moles\ crotonaldehyde\ formed\ during\ reaction}{\frac{1}{2}\ initial\ moles\ of\ acetaldehyde}$. Carbon balances over the entire reaction time were typically near 95%.

3.3 Results and discussion

In this work, the primary products of the aldol condensation of acetaldehyde (**1**) with acetone (**2**) were found to be the self condensation product (Figure 2) of (**1**), crotonaldehyde (**3)**, along with the cross condensation (Figure 3) of (**1)** and (**2**), 3-penten-2-one (**4**). The condensation of (**1**) with MEK (**5**) gave (**3**) along with 3-methyl-3-penten-2-one (**6**) and 4-hexen-3-one (**7**) (Figure 4). The reaction results for the two reactant systems are shown in Tables 3 and 4. As can be seen in the tables, the more basic the catalyst the lower was the yield for the cross condensation formation of (**4**), (**6**), and (**7**). In contrast, the yield of (**3**) did not decrease as significantly with increasing basicity.

Acid and base catalyzed aldol condensations are known to have different mechanisms. The acid catalyzed mechanism involves the formation of an enol, which then acts as a nucleophile, attacking a protonated carbonyl, which serves as an electrophile. For the base catalyzed mechanism, an enolate anion is formed, which then acts as a nucleophile

in the attack on the electrophilic carbonyl. A bi-functional acid-base cooperative mechanism has also been proposed where basic sites form an enolate that acts as a nucleophile while the electrophile is activated by acidic site protonation of its carbonyl group.[14]

As can be seen in Figure 5, the ability to catalyze cross condensations of the ketone and aldehyde compared to self condensation of the aldehyde significantly decreased with a loss of acid sites and an increase in basic sites. This result is important in the bio-oil upgrading scheme (Figure 1) as after the ketonization of organic acids, there will be an increase in the amount of less reactive low molecular weight ketones. Since ketones have less acidic α-carbons due to the electron donating methyl or methylene carbons, it was somewhat surprising that the more basic catalysts did not have greater activity in the cross condensation of the ketone and aldehyde.

Any of the three steps in the overall aldol condensation reaction, e.g. enolization, addition, or dehydration, could in principle be rate limiting in the overall reaction. Under the conditions used in the current work, kinetic studies found that the formation of (**6**) and (**7**) were zero order with respect to (**1**) while the formation of (**3**) was first order (Figure 6). While it is possible that these responses occurred due to competitive adsorption effects, a possible explanation is that the enolization step was rate limiting. Either acids or bases can catalyze enolization and it is known with either type of catalyst that the rate limiting step is the abstraction of the proton from the α-carbon.[24] The base catalyzed mechanism begins directly with this deprotonation, while the acid catalyzed mechanism requires protonation of the carbonyl followed by proton abstraction catalyzed by the conjugate base. If the enolization of (**5**) was following a base catalyzed mechanism, the reaction rate for the

crossed condensation should have increased as the aluminophosphate catalyst became more basic. However, as seen in Tables 3 and 4, this was not the case.

The ratio of the yields for products (**6**) and (**7**) were also found to be dependent on the basic character of the catalyst. As seen in Figure 7, when the nitrogen content increased in the catalysts, the ratio of (**7**) to (**6**) grew larger. It has been shown that different catalyst systems can produce branched or linear products preferentially in nonsymmetrical ketones. Catalysts differ as base catalysts typically form carbon-carbon bonds at the methyl carbon while acid catalysts generally yield carbon-carbon bonds at the methylene carbon giving either linear or branched molecules.[25] The difference could be due to kinetic differences in rates of dehydration, addition or enolization. Stiles et al. found for the alkaline catalyzed condensation of benzaldehyde and butanone that different rates of dehydration to the two product isomers caused the straight chain product to form preferentially whereas differences in the addition step caused the primary product to be the branched isomer with a strong acid catalyst.[26] Previous work has also shown that base catalyzed enolate formation occurs faster at the less sterically hindered methyl carbon and in contrast the rate of acid catalyzed enol formation is much greater at the methylene carbon due to the stabilizing effect of the added substituent.[27] Since the reactions in the current work may be rate limited by enolization, it seems possible that as nitrogen content in the catalyst was decreased, the enolization mechanism became more similar to the acid-catalyzed behavior, thus causing a decrease in the ratio of yields for (**7**) to (**6**).

To better understand the acid and base properties of the catalyst, small amounts of acetic acid were added to the reaction solution with the ALPO catalyst. At low addition levels the organic acid was found to enhance the reaction rate, but larger additions caused

decreases in activity (Figure 8). An inference from this result was that this bi-functional catalyst may have been limited by the number of acid sites even though base sites were needed as well. To test this theory, small amounts of a base, propylamine, were added to the reaction solution. Indeed, the addition of base caused a significant reduction in yields. The addition of the homogeneous acid also appeared to cause an increase in the ratio of cross to self condensation and a decrease in the ratio of yields for (**7**) to (**6**) as shown in Figure 9. The addition of acid to ALPO-72 reactions gave similar results.

The proposed acid-base bi-functional mechanism for cross-condensation given in Figure 10 could explain the phenomena seen in the reaction studies between (**1**) and (**2**) or (**1**) and (**5**). In this mechanism, the acidic P-OH sites on the catalyst activate the carbonyl of the ketone, drawing electrons and causing the α-carbon to become more acidic. The basic sites on the catalyst then facilitate the enolization of the activated ketone. The enol intermediate subsequently attacks the activated aldehyde in the addition step. Carbonyl activation of the aldehyde should occur as the enol is a weaker nucleophile than is an enolate anion. This proposed mechanism explains the significant decrease in activity for the cross condensation but not the self condensation with nitridation as the loss of acid groups retards the activation of the carbonyl groups. As (**1**) is more acidic than (**2**) or (**5**), activation of the carbonyl is not as imperative in self condensation of the aldehyde. This mechanism is very similar to the homogeneous acid catalyzed condensation. However, in the homogeneous acid catalyzed mechanism the acid's conjugate base deprotonates the α-carbon while in the heterogeneous catalyzed mechanism separate basic sites do this deprotonation. Therefore, the heterogeneous catalyst is advantaged as it can contain both the needed acid groups as well as separate stronger basic sites.

3.4 Conclusions

ALPO was found to be an effective catalyst for the aldol reaction of acetaldehyde with acetone or MEK. It was found that an increase in basicity caused by the incorporation of nitrogen through nitridation had a negative impact on the activity of the catalyst. The weak acid groups were found to play a crucial role in the condensation reaction, particularly with the cross condensation of the ketone and the aldehyde. These results were explained through the proposal of a mechanism in which the carbonyl of the nucleophile was activated by the acid sites. Further, the catalyst system appeared to be limited by the number of acids sites as the addition of dilute amounts of organic acids to the reaction mixture led to increased activity.

3.5 Acknowledgements

This work was supported in part by ConocoPhillips and by the U.S. DOE's Science Undergraduate Laboratory Internship (SULI) program at the Ames Laboratory.

3.6 References

[1] A.V. Bridgwater, G.V.C. Peacocke, Fast pyrolysis processes for biomass, Renewable and Sustainable Energy Reviews, 4 (2000) 1-73.
[2] P. McKendry, Energy production from biomass (part 2): conversion technologies, Bioresource Technology, 83 (2002) 47-54.
[3] J.P. Diebold, A review of the chemical and physical mechanisms of the storage stability of fast pyrolysis bio-oils, NREL/SR-570-27613, Jan. 2000.
[4] D. Mohan, C.U. Pittman, P.H. Steele, Pyrolysis of Wood/Biomass for Bio-oil: A Critical Review, Energy & Fuels, 20 (2006) 848-889.
[5] C.A. Mullen, A.A. Boateng, Chemical Composition of Bio-oils Produced by Fast Pyrolysis of Two Energy Crops†, Energy & Fuels, 22 (2008) 2104-2109.
[6] S. Czernik, A.V. Bridgwater, Overview of Applications of Biomass Fast Pyrolysis Oil, Energy & Fuels, 18 (2004) 590-598.
[7] L. Deng, Y. Fu, Q.-X. Guo, Upgraded Acidic Components of Bio-oil through Catalytic Ketonic Condensation, Energy & Fuels, 23 (2008) 564-568.
[8] S. Ege, Organic Chemistry: Structure and Reactivity, Houghton Mifflin Company, Boston, 2004.
[9] R. Mahrwald, Modern Aldol Reactions, in, Wiley-VCH Verlag GmbH and Co. KGaA, Weinheim, 2004.
[10] P. Sykes, A Guidebook to Mechanism in Organic Chemistry, 4 ed., Wiley, New York, 1975.

[11] K.K. Rao, M. Gravelle, J.S. Valente, F. Figueras, Activation of Mg-Al Hydrotalcite Catalysts for Aldol Condensation Reactions, Journal of Catalysis, 173 (1998) 115-121.
[12] G.G. Podrebarac, F.T.T. Ng, G.L. Rempel, A kinetic study of the aldol condensation of acetone using an anion exchange resin catalyst, Chemical Engineering Science, 52 (1997) 2991-3002.
[13] J.I. Di Cosimo, V.K. Díez, C.R. Apesteguía, Base catalysis for the synthesis of [alpha],[beta]-unsaturated ketones from the vapor-phase aldol condensation of acetone, Applied Catalysis A: General, 137 (1996) 149-166.
[14] M. Climent, A. Corma, V. Fornés, R. Guil-Lopez, S. Iborra, Aldol Condensations on Solid Catalysts: A Cooperative Effect between Weak Acid and Base Sites, Advanced Synthesis & Catalysis, 344 (2002) 1090-1096.
[15] R.K. Zeidan, M.E. Davis, The effect of acid-base pairing on catalysis: An efficient acid-base functionalized catalyst for aldol condensation, Journal of Catalysis, 247 (2007) 379-382.
[16] S.L. Hruby, B.H. Shanks, Acid-base cooperativity in condensation reactions with functionalized mesoporous silica catalysts, Journal of Catalysis, 263 (2009) 181-188.
[17] M.J. Climent, A. Corma, V. Fornés, A. Frau, R. Guil-López, S. Iborra, J. Primo, Aluminophosphates Oxynitrides as Base Catalysts: Nature of the Base Sites and Their Catalytic Implications, Journal of Catalysis, 163 (1996) 392-398.
[18] A. Massinon, J.A. Odriozola, P. Bastians, R. Conanec, R. Marchand, Y. Laurent, P. Grange, Influence of nitrogen content on the acid-base properties of aluminophosphate oxynitrides, Applied Catalysis A: General, 137 (1996) 9-23.
[19] M. Hasni, G. Prado, J. Rouchaud, P. Grange, M. Devillers, S. Delsarte, Liquid phase aldol condensation of cyclopentanone with valeraldehyde catalysed by oxynitrides possessing tuneable acid-base properties, Journal of Molecular Catalysis A: Chemical, 247 (2006) 116-123.
[20] J. Wang, Q. Liu, Synthesis, characterization, and base-catalytic performance of ordered mesoporous aluminophosphate oxynitride materials, Journal of Materials Research, 22 (2007) 3330-3337.
[21] R. Conanec, R. Marchand, Y. Laurent, Ph. Bastians, P. Grange, Synthesis and acid-base properties of "ALPON" nitrided aluminophosphates, Materials Science Forum, 152-153 (1994) 305-308.
[22] M. Hasni, S. Delsarte, J. Rouchaud, P. Grange, Adjustment of the acid-base properties of phosphates through nitridation, for increased selectivity in miexed aldol condensations, Silicates Industriels, 69 (2004) 77-84.
[23] T. Lindblad, B. Rebenstorf, Z.-G. Yan, S.L.T. Andersson, Characterization of vanadia supported on amorphous AlPO4 and its properties for oxidative dehydrogenation of propane, Applied Catalysis A: General, 112 (1994) 187-208.
[24] E.D. Anslyn, DA., Modern Physical Organic Chemistry, University Science Books, Sausalito, CA, 2006.
[25] S. Patai, The Chemistry of the Carbonyl Group, Interscience, London, 1966.
[26] M. Stiles, D. Wolf, G.V. Hudson, Catalyst Selectivity in the Reactions of Unsymmetrical Ketones; Reaction of Butanone with Benzaldehyde and p-Nitrobenzaldehyde, Journal of the American Chemical Society, 81 (1959) 628-632.
[27] F.A. Carey, R.J. Sundberg, Advanced Organic Chemistry Part A: Structure and Mechanisms, 3 ed., Plenum Press, New York, 1990.

3.7 Tables and Figures

Table 1. Common aldehydes and ketones found in bio-oil.[3]

Aldehyde or Ketone	Bio-Oil wt %
Acetaldehyde	0.1-8.5
Ethanedial	0.9-4.6
Formaldehyde	0.1-3.3
Acetone	2.8
2-Propenal	0.6-0.9
Methyl Ethyl Ketone	0.3-0.9
Pentanal	0.5

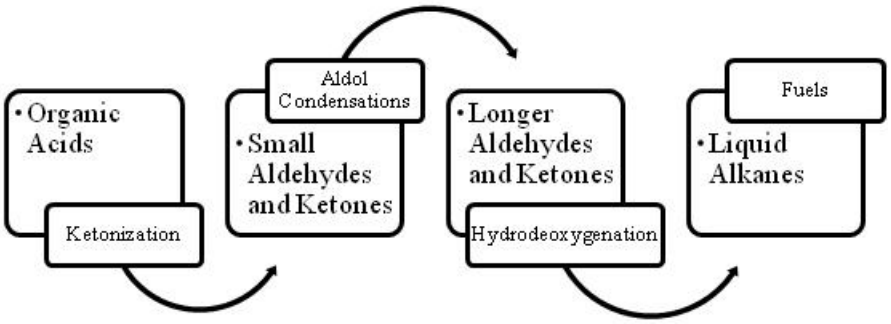

Figure 1. Possible bio-oil upgrading scheme.

Table 2. Characterization of the aluminophosphate catalysts.

Catalyst	Surface Area	N wt%
ALPO	177	--
ALPON-16	165	3.9
ALPON-24	165	4.9
ALPON-48	161	8.1
ALPON-72	165	8.5

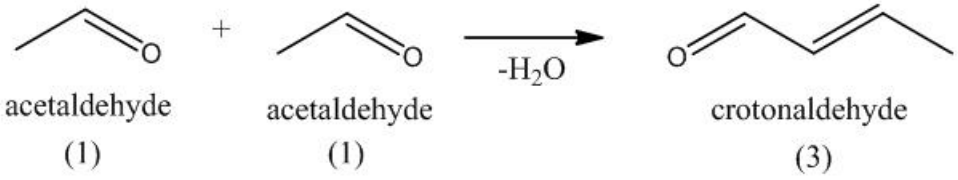

Figure 2. Self condensation of acetaldehyde.

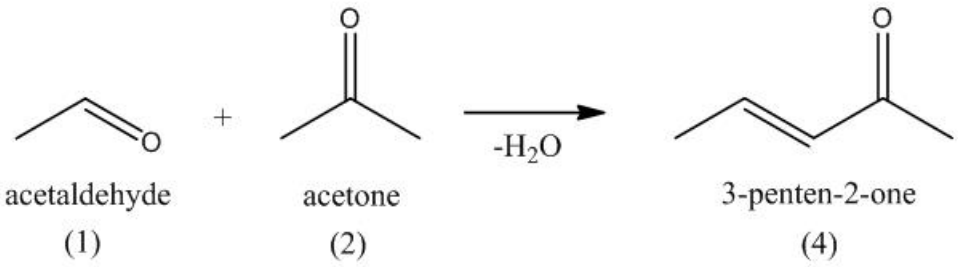

Figure 3. Cross condensation of acetaldehyde and acetone.

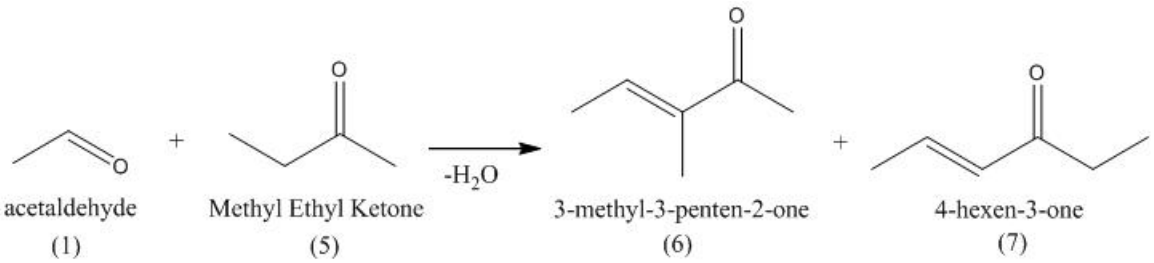

Figure 4. Cross condensation of acetaldehyde and MEK.

Table 3. Yields for the aldol condensation of acetaldehyde with acetone after 3 hours.

Catalyst	Yield (%) (**3**)	Yield (%) (**4**)
ALPO	21.52	7.44
ALPON-16	19.02	2.78
ALPON-24	20.14	2.69
ALPON-48	18.08	1.36
ALPON-72	13.98	0.70

Table 4. Yields for the aldol condensation of acetaldehyde with MEK after 3 hours.

Catalyst	Yield (%) (**3**)	Yield (%) (7)	Yield (%) (**6**)
ALPO	22.77	1.72	5.74
ALPON-16	21.85	0.83	1.99
ALPON-24	20.89	0.68	1.50
ALPON-48	20.00	0.34	0.62
ALPON-72	18.48	0.32	0.49

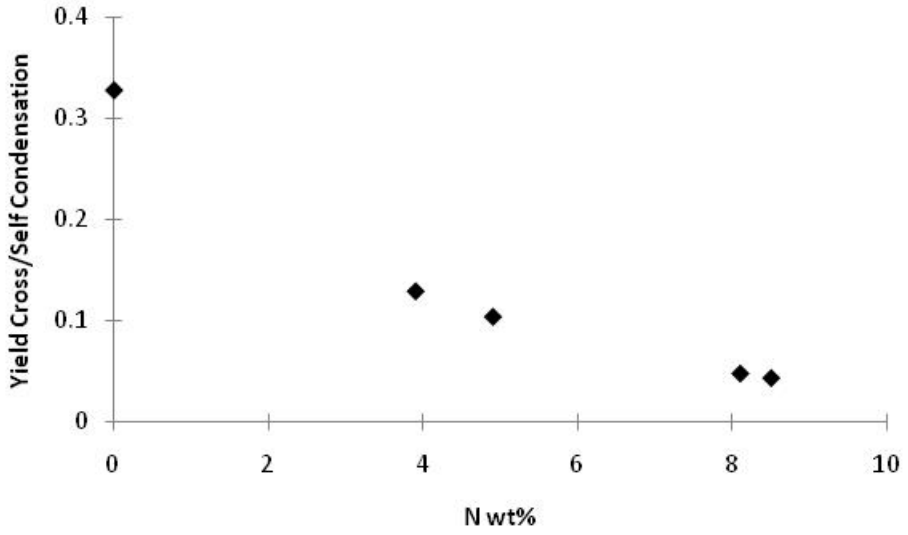

Figure 5. Effect of catalyst basicity on the ratio of cross/self condensation in the reaction of MEK and acetaldehyde after 3 hours.

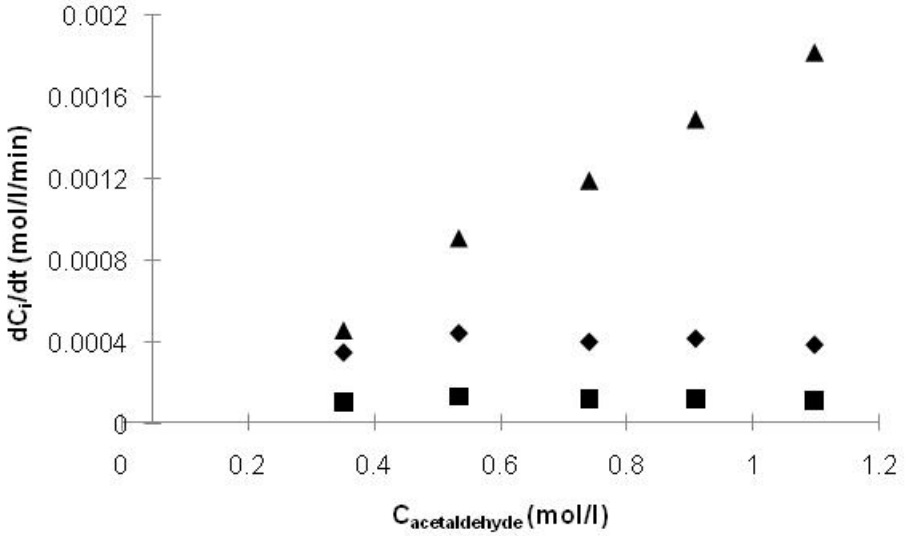

Figure 6. Reaction order calculations showing that the formation of 4-hexen-3-one (■) and 3-methyl-3-penten-2-one (♦) are zero order with respect to acetaldehyde and the production of crotonaldehyde (▲) is first order with respect to acetaldehyde.

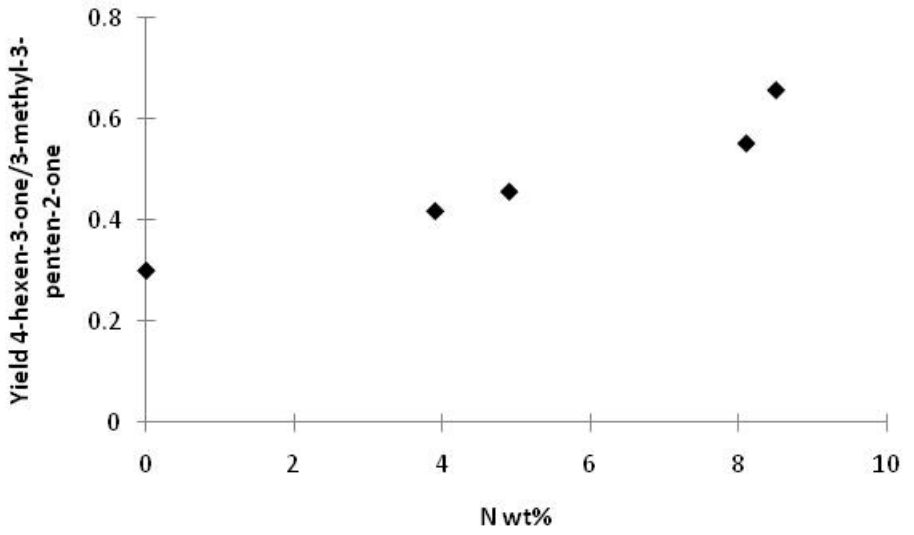

Figure 7. Role of base in determining if condensation occurs at methyl or methylene carbon in the condensation reaction of MEK and acetaldehyde after 3 hours.

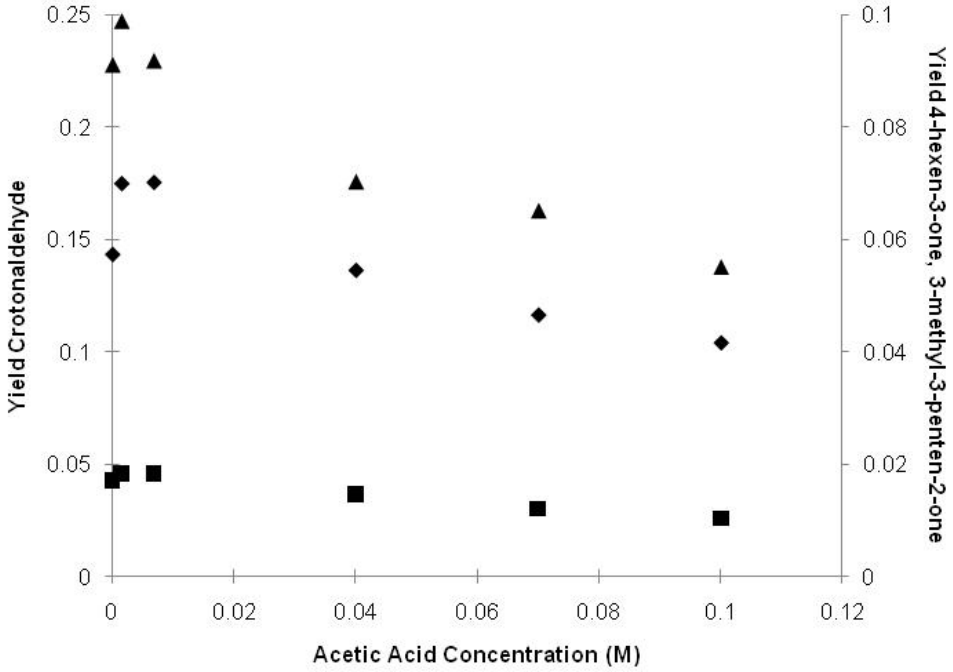

Figure 8. Effect of the addition of acetic acid on the yields of crotonaldehyde (▲), 4-hexen-3-one (■) and 3-methyl-3-penten-2-one (♦) after 3 hours in the condensation of MEK and acetaldehyde.

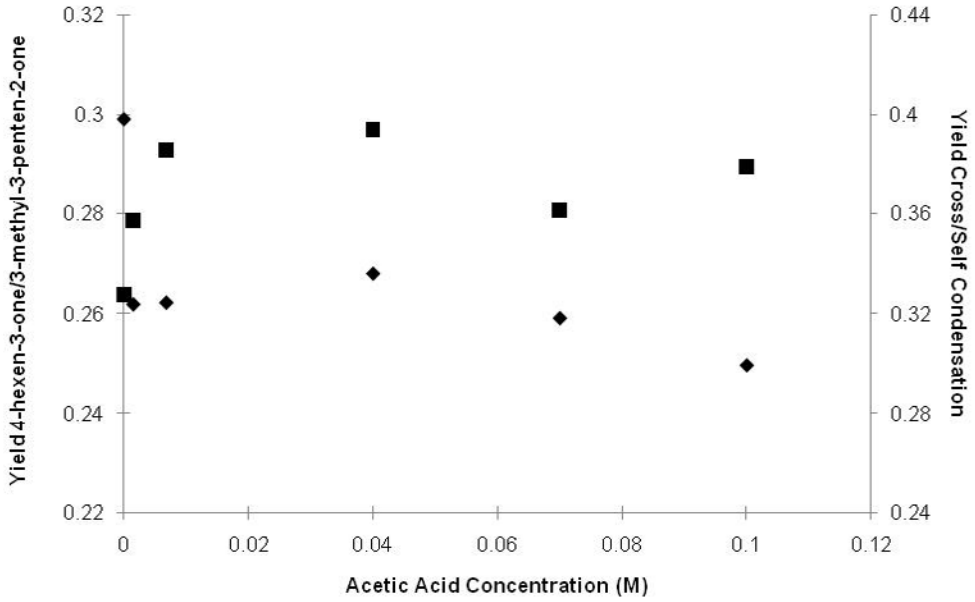

Figure 9. Effect of the addition of acetic acid on the ratio of cross to self condensation (■) and on the ratio of yields for 4-hexen-3-one to 3-methyl-3-penten-2-one (♦) in the reaction of MEK and acetaldehyde after 3 hours.

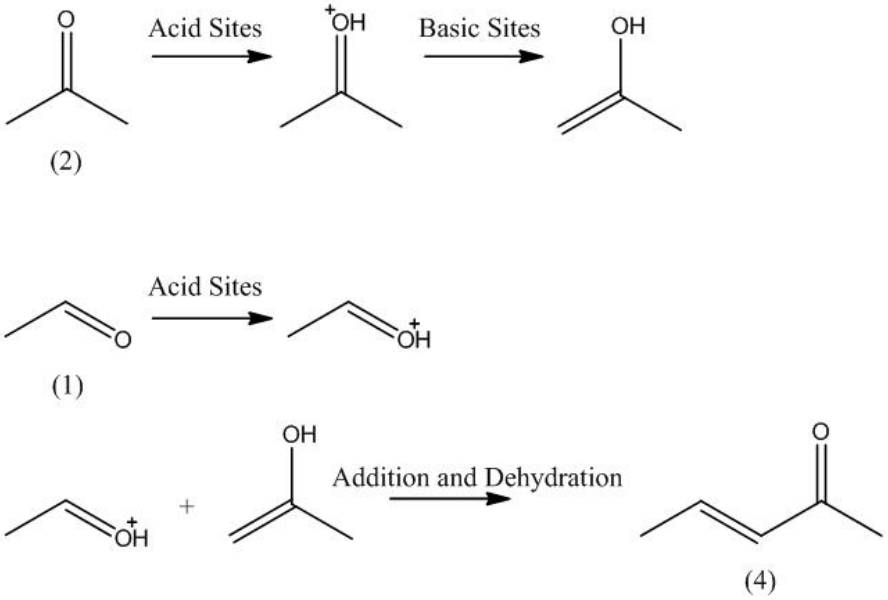

Figure 10. Proposed acid-base mechanism.

Chapter 4

Ceria calcination temperature influences on ketonization: bio-oil applications and mechanism insights

A paper to be submitted to Applied Catalysis A: General

Ryan W. Snell[1] and Brent H. Shanks[1]

[1]Department of Chemical and Biological Engineering, Iowa State University

Authorship roles:

Snell: Primary author

Shanks: Principal investigator

Abstract

The ketonization of carboxylic acids is an attractive method of removing undesirable acidity and oxygen from biorenewable fuels. However, in order to be more industrially relevant the temperature of reaction needs to be lowered. Unfortunately, ketonization is not fully understood making this task far from trivial. In this work, it was found that the calcination temperature changes the type of interactions that the good ketonization catalyst—cerium oxide— has with the model bio-oil compound acetic acid. Through extensive pre and post reaction characterization the calcination temperature was determined to influence catalyst final morphology, crystallinity, and oxidation state. It appears that at least in the condensed phase, the respectively enhanced reaction rates found on high temperature calcined catalysts are in part due to loss of surface area of ceria calcined at lower temperatures.

Keywords: Ketonization; Ceria; Bio-oil; Calcination; Cerium Acetate

4.1 Introduction

Ketonization reactions have been gaining interest due in large part to their relevance with biorenewable fuels and chemicals.[1-4] Fast pyrolysis, involving the rapid heating of biomass in the absence of oxygen, creates a bio-oil rich in small organic acids like acetic acid that would be good candidates for ketonization applications.[5] To avoid undesirable issues with bio-oil upgrading such as excessive coking and thermal decompositions, it would be preferred to perform these ketonization reactions in the condensed phase. However, the high temperatures necessary for ketonization to occur make this impractical. Therefore a more active catalyst needs to be developed allowing for lowering of the temperature at which significant conversion occurs.

Ketonization is a mature reaction being the industrial technique used for acetone production in the early 20^{th} century.[6] It also has its roots in biorenewable applications as this process occurred through the thermal decomposition of calcium acetate derived from the mixing of lime with wood distillates.[6] Despite its long history, the mechanism and desirable catalyst properties are still largely unknown.[7] This lack of knowledge makes it difficult to rationally engineer a more effective catalyst and necessitates extensive pre and post reaction characterization in order to isolate important material properties for ketonization.

A number of different catalyst properties have been implied to be of importance for ketonization. For example there is evidence that basicity might be expected to be of particular weight in the ketonization reaction.[4, 8-10] This was seen by Gaertner et al. in which co-feeding CO_2 during the ketonization of hexanoic acid greatly reduced reaction

rates.[4] Basic sites on the utilized ceria-zirconia catalyst were then proposed to be the active sites for ketonization.[4] Murkute et al. reached a similar conclusion when investigating the ketonization of propionic acid and butyric acid catalyzed by MnO_x/CeO_2 supported on mesoporous silica.[9] Catalyst basicity could also influence the reaction mechanism. In the ketonization of acetic acid in the vapor phase, catalyzed by MgO, it was found that the reaction occurred through multiple pathways.[10] When initially exposed to acetic acid, the strongly basic MgO formed metal acetates in the bulk of the material despite its high lattice energy.[10] It was established that at lower temperatures, the reaction proceeded through the decomposition of these metal acetates while at higher temperatures ketonization was surface catalyzed.[10]

Catalyst acid sites may also be of substance in the ketonization reaction. This is possibly the case as Lewis acid sites on the surface are needed to form carboxylate species commonly suspected as intermediates in the ketonization mechanism. Reducible Lewis acid sites are proposed by Hasan et al. to be of particular importance when examining the ketonization mechanism occurring on ceria, titania, and alumina.[11]

Redox properties of ceria could be expected to be of significance in the ketonization reaction as well. It makes sense that a catalyst commonly used for its oxygen mobility in applications such as catalytic converters could potentially use these same special traits for other reactions.[12] Moreover, a number of publications have hinted at the potential impacts of catalyst redox abilities. Rubinshtein et al. examined the oxidation state of ceria during the ketonization of acetic acid in the vapor phase using magnetic susceptibility techniques.[13] It was found that the catalyst became reduced during the course of reaction leading the authors to conclude that a redox process was taking place.[13] Reducibility has also been implicated

in partially explaining the enhanced activity of ceria over titania and titania over alumina for ketonization.[11] Likewise, most commonly cited mechanisms of ketonization tend to involve some sort of redox step.[14] For example, in the ketonization mechanism proposed by Nagashima et al. the redox cycle of the surface metal is proposed to be a necessary part of the formation of C-C bonds.[15] It may be speculated that some reduction of the catalyst could be of potential benefit as partially reduced ceria are good at dehydrogenating, thus perhaps being valuable in mechanisms with a ketene intermediate.[14]

Another catalyst property that has been shown to be of impact in the ketonization reaction is surface structure. This was demonstrated more than 20 years ago by Kim and Barteau whom found that {114} facets of titania were the only surfaces able to catalyze the ketonization reaction during studies of carboxylic acids on single crystal TiO_2(001).[16] The authors concluded that ketonization requires an oxidized surface with doubly unsaturated cations allowing for two acetates to be coordinated with one cation.[16] Stubenrauch et al. researched the reactions of adsorbed carboxylic acids on different ceria surfaces.[17] Acetone was found as a product with the ceria (111) surface but not the (100).[17] This result is interesting as the (111) surface has only cerium cations with a single coordination vacancy and hence can't accommodate two acetates as Kim and Barteau found was necessary for ketonization on titania. Recently, Kobune et al. examined a number of reactions, including the ketonization reaction over ceria catalysts that they calcined at different temperatures.[18] They discovered in the gas phase ketonization of propanoic acid at 350 °C, that higher temperatures used for calcination created a catalyst more active for ketonization on a surface area basis.[18] It was proposed that larger particles have more {111} facets which are more active for ketonization.[18]

While the previously mentioned studies all contain helpful insights into ketonization, there have not been investigations into calcination temperature influences on ceria catalyzed ketonization of the prevalent bio-oil compounds like acetic acid in the condensed phase as would be preferred for upgrading. With this in mind, here research focuses on determining if calcination temperature influences ceria catalysis in the condensed phase ketonization of acetic acid. Multiple characterization methods were utilized in order to determine the influence of calcination temperature on catalyst properties. If differences in catalyst attributes or activities are noticed, it is hoped that what can be learned from these observations may allow for greater understanding of ketonization catalysis in general.

4.2 Experimental section

4.2.1 *Synthesis of CeO_2*

Ceria was synthesized through the thermal decomposition of cerium(III) nitrate hexahydrate (Aldrich 99.99%) at either 450, 600, 750, or 900 °C in air with a Carbolite AAF 1100 muffle furnace. Heating ramps were 2 °C/ min and once temperature was reached it was maintained for 3 h. The resulting cerium oxide was crushed with a mortar and pestle to a very fine powder and stored in a dessicator until use.

4.2.2 *Reaction testing and product analysis*

Reaction testing of the ceria catalysts took place using Parr Series 4598 75 ml stainless steel batch reactors. For all reactions toluene (Fisher 99.8%) was used as a solvent, acetic acid as reactant (Fisher 100%), and 1,4 dioxane (Fisher 100%) as an internal standard. For the 4 h 20 min reactions, 1.0 g of acetic acid, 0.5 ml dioxane, 50 ml toluene and 0.2 g of ceria were added to each reactor. The respective reactors were pressurized to 40 bar with N_2, stirred at 400 rpm, and then heated to 230 °C. Samples were taken into a liquid nitrogen cold

trap and analyzed on an Agilent 7890 GC-FID. For initial rate studies, a similar set up was used but the amount of catalyst was varied so as to keep the yield from being too great during the course of reaction. Before post reaction characterization, the spent catalysts were dried in air at 100 °C for 1 h.

4.2.3 *Materials Characterization*

BET surface area analysis was performed using a Micromeritics ASAP 2020 with a liquid nitrogen bath. All materials were degassed at 100 °C prior to an analysis using 8 points between P/P_o of 0.06-0.2. The ceria catalysts calcined at 450, 600, and 750 °C were always examined using N_2 adsorption while the low surface area of the 900 °C material was generally probed with Kr gas.

For TG activation energy analysis a Perkin Elmer STA 6000 was utilized with a 50-600 °C temperature program at varying ramp rates all under the flow of UHP N_2 at 50 ml/min. The method as proposed by Starink where $\ln\left(\frac{\beta}{T_f^{1.92}}\right) = -1.0008\frac{E}{RT_f} + C$ was used for calculation of E_a [19]. In the equation β is the temperature ramp rate and T_f the temperature at a fixed point in the reaction. The equivalence points in the reactions were found in this work through weight derivative peaks.

H_2 TPR, CO_2 TPD, and NH_3 TPD were all performed on a Micromeritics Autochem (II) Chemisorption Analyzer. The TPR testing began by heating the ceria at 10 °C/ min to 400 °C after which the temperature was maintained for 30 min all under the flow of 50 ml/min 10% O_2 in He. The sample was then purged with 50 ml/ min Ar for 10 min and cooled to 50 °C. Next, reduction took place using 20 ml/min of 10 % H_2 in Ar and a temperature ramp of 5 °C/min to 450 °C. After cooling, this oxidation and reduction process

was repeated except the reduction was examined up to 990 °C. Results were measured using a TCD detector.

CO_2 TPD studies began by heating the ceria at 10 °C/min up to 400 °C and holding at that temperature for 10 min before cooling to 45 °C all under the flow of 20 ml/min He. After this cleaning step, the catalysts were exposed to 50 ml/min CO_2 for 30 min. Next, purging was performed using 20 ml/min of He for 60 min. Finally analysis occurred through a temperature ramp of 10 °C/min up to 500 °C and measurement of product evolution through a TCD.

NH_3 TPD began by cleaning of the material through a temperature ramp of 10 °C/min to 400 °C and dwelling for 10 min. After cooling, 10 % NH_3 in He was led over the ceria at 50 ml/min for 30 min. 20 ml/min of He for 60 min was then used for purging. The analysis occurred through use of a TCD and a ramp rate of 10 °C/min.

XPS was performed on a Physical Electronics 5500 Multi-technique system. The sample was mounted on double sided tape and an Al Kα source was used. Peak location was normalized by setting the C1s peak to a binding energy of 284.6 eV. For estimates of the oxidation state of the cerium in the oxides, a Shirley background was applied.

X-ray diffraction (XRD) was performed on a Siemens D-500 with a 0.15 detector slit and operated at 45kV and 30mA with Cu Kα radiation. Typically a step size of 0.05 was used with a dwell time of 2 s. Scanning electron microscopy (SEM) was completed on a FEI Quanta FE-SEM after sputtering the sample with iridium. Transmission electron microscopy (TEM) studies occurred on a 2007 JEOL 2100 with 200kV. The catalyst was dispersed in acetone, sonicated, and deposited on a carbon film before imaging.

In-situ XRD studies were performed on a STOE theta-theta diffractometer using Cu Kα radiation and a scintillation counter. An Anton Parr XRK 900 high temperature reaction chamber was used to house the sample during the course of experiments. Scans before and after testing were taken from 2-65 2θ, step size of 0.05 and dwell of 2s while during the course of acetic acid exposure, the scans were only taken from 5-36 2θ. Acetic acid vapors were generated by bubbling 100 ml/ min of He through 40 °C acetic acid. While the catalyst was exposed to this vapor stream, continuous scanning occurred.

4.3 Results and discussion

4.3.1 BET and XRD results

Effects of calcination temperature on the surface area of the ceria catalysts were found to be quite drastic with lower temperature calcination resulting in surface areas of 80-90 m^2/g while higher temperature treated materials had only 1-2 m^2/g (Table 1). This phenomenon has been seen elsewhere in literature where various forms of cerium precursors or the oxide itself was exposed to high calcination temperatures.[18, 20] Modification in catalyst crystallinity is also evident from XRD results with greater calcination temperatures resulting in more ordered materials (Figure 1). As seen in Figure 1, the cerium oxide is primarily in the fluorite 4+ state.

4.3.2 CO_2 and NH_3 TPD analysis

As described earlier, it has been claimed that materials with high basicity can undergo bulk carboxylate formation during ketonization despite significant lattice energy.[10] However, cerium oxide is known to have lower basicity and even higher lattice energy than MgO so it may be assumed that this observation will not occur in our case. To understand catalyst basicity and how it changes with calcination temperature for pure ceria catalysts,

CO_2-TPD was performed. It was found that weak base sites with desorption temperatures ~90-150 °C were present on all the ceria catalysts showing little difference in the sites' strength. The strength of the measured sites here is typical of pure ceria catalysts.[21] In order to characterize the acid sites on the ceria catalysts synthesized in this work, NH_3 TPD was used. As reported elsewhere, ceria was determined to primarily contain weak acid sites—in our case with the primary desorption peak occurring ~100 °C.[22] We can therefore propose that any activity or other differences observed between the ceria catalysts is likely not due to acid or base characteristics.

4.3.3 H_2 TPR and XPS pre-reaction testing

The next catalyst property examined was ceria's redox ability. As ceria redox properties are typically known to be valuable; the ease of catalyst reduction is potentially important to investigate. This property was probed in the present work through the use of TPR. Depicted in Figure 2, both high and low temperature reductions were found to occur with the catalysts. For catalysts calcined at 450, 600, and 750 °C a low temperature reduction was evident. High temperature reductions occurred at roughly the same temperature for all four catalysts. This type of low and high temperature reduction profile is ordinary for ceria catalysts.[23] Typically, the low temperature peak is associated with surface reduction while the high temperature reduction is affiliated with the bulk of the material.[24] However, the true reasons for the two separate peaks may be more complex as recent literature has found that Frenkel oxygen defect concentrations, which change with temperature treatment, may be of meaning in oxygen storage capacity.[25] Moreover, at temperatures below 400 °C, ceria that was calcined at >600 °C demonstrated an ability to maintain reduction abilities through multiple redox cycles.

As catalyst redox state could be of importance, further characterization of this property is of interest. XPS can allow for the determination of cerium's surface redox states. However, there are many different methods of trying to measure the ratio of Ce^{3+} to Ce^{4+}.[26] It is known that both the Ce 3d and the O 1s spectra demonstrate differences depending on the oxidation state of cerium.[27, 28] For the O 1s spectra, the presence of Ce^{3+} results in a binding energy of 1-2 eV greater than does Ce^{4+}.[28] However, the Ce 3d spectrum is much more commonly used for quantification of cerium oxidation state than is the O 1s. Peak nomenclature for the Ce 3d spectra used here is in the standard way developed by Burroughs et al.[29] The u'" peak in the ceria 3d spectrum has been found to only occur for cerium in the 4+ state and is therefore commonly used for oxidation state calculations.[26] For example, Shyu et al. plotted % Ce^{4+} vs. % u'" and proposed that the determined correlation could then be used to find the cerium oxidation state in future samples.[30] It's been reported that a percentage of 13.7 u'" with regards to the total spectrum area occurs for a CeO_2 sample.[31] This number agrees closely to that found for 100% Ce^{4+} as determined in the linear correlation by Shyu et al.[30] Therefore, for a rough quantitative calculation of cerium's oxidation states, a linear correlation of % Ce^{4+}=7.3(% u'") could be used. For the fresh ceria catalysts, XPS results of the Ce 3d region can be seen in Figure 3. In the spectra, v' and u' are due to Ce^{3+} while the v, u, v", u", v'", and u'" peaks are from Ce^{4+}.[32] Quantitative estimates of the cerium oxidation states are presented in Table 1. From the data, it is clear that cerium in the catalysts exists primarily in the 4+ state.

4.3.4 SEM and TEM pre-reaction analysis

To examine the surface faceting of the catalysts in this work, TEM was employed. It is known that the lattice plane spacings of (111), (220), and (200) are 0.31, 0.19, and 0.28 nm

respectively.[33] For the materials, surface energies are expected to decrease in the order of {100} > {110} > {111}.[34] TEM results showed that the lower temperature calcined catalysts, 450 °C ceria, consisted of smaller crystallites (~10nm) than did the higher temperature catalysts, 900 °C ceria, agreeing with XRD results (Figure 1). Surface facets of both the 450 °C ceria and 900 °C ceria catalysts appeared to be primarily {111}, but the 450 °C ceria catalysts tended to be more rounded and hence likely contained more of the {100} facets than 900 °C ceria. The 900 °C ceria catalyst did contain {100} facets as well, found appearing at the top of truncated octahedral crystals. SEM imaging demonstrated that both low and high temperature calcined ceria catalysts consisted of non shape or size specific particles (Figure 4).

4.3.5 Acetic acid ketonization

As mentioned in the introduction, desirable catalyst properties and mechanisms are not well understood for ketonization and thus all the aforementioned catalyst traits could be of potential importance. Reaction testing at 230 °C, far below typical ketonization temperatures, with a constant mass of catalyst demonstrated greater acetone yields by lower temperature calcined catalysts (Figure 5). However, as this was not a fair comparison of the catalysts since the surface areas were significantly different, initial rate studies were performed. As seen in Table 2, initial rate studies with activities based on pre-reaction surface areas found greater activity for the higher calcined materials, as was discovered by Kobune et al. with vapor phase propanoic acid studies.[18] These findings imply that enhanced reducibility is not clearly beneficial for the reaction—as may be inferred from various literature sources—as the more easily reduced catalysts were not necessarily more

active. To further understand why activity differences were observed amongst the catalysts, extensive post reaction characterization was warranted.

4.3.6 Post reaction BET results

After reaction testing, the catalysts were separated and dried before measuring surface area through the BET technique. What was found can help explain why higher temperature calcined ceria gave greater reaction rates in that severe loss of surface area occurred with the lower temperature calcined materials (Table 1). Therefore the surface area determined before reaction—used for normalization of the reaction rate—is not the correct surface area to use. Since this is the case in our testing, instead of surface morphology describing the enhancement in rates, it may just be the simple case of more catalyst giving greater conversion. Moreover, it was found that acetic acid greatly enhanced the surface area loss of the ceria as the oxide calcined at 450 °C used with the same acetic acid/ceria ratio as in the initial rate testing at 290 °C had a post reaction surface area of 2 m^2/g while ceria put through the same environment without the acetic acid still maintained a surface area of 54 m^2/g.

4.3.7 Post reaction XRD analysis

As shown in Figure 6, the crystalline structure of the ceria catalysts was found to drastically vary after reaction depending on the calcination temperature of the material. The less crystalline, higher surface area ceria was found to lose its fcc structure likely forming metal acetates in the bulk of the catalyst while the ceria calcined at > 750 °C appeared to greatly maintain the cerianite form. This finding is of significant importance as previous manuscripts have claimed that ceria is a stable catalyst for ketonization of acetic acid.[11, 35] However, many studies exploring ceria catalysts in ketonization used purchased ceria or ceria

calcined at high temperatures thus preventing bulk changes from occurring during ketonization. The findings here are also of meaning for mechanistic reasons.

4.3.8 Mechanistic implications

Many different mechanisms have been proposed for ketonization. It has been largely believed, as proposed by Yakerson et al., that depending on the catalytic material, the reaction follows different pathways.[36] This claim came about as group I and II carbonates and oxides promoted ketonization through the formation of a bulk carboxylate while BeO and quadrivalent oxides did not.[36] The respective disparity in the lattice energy of the materials reportedly created this difference.[36] Pestman et al. have also reported important research into the ketonization mechanism as well.[7] In their work, it was concluded that low metal-oxygen bond strength materials such as zinc oxide, bismuth, and lead promoted ketonization by formation of a bulk carboxylate while high metal-oxygen bond strength catalysts like zirconia and alumina performed the reaction through a surface mechanism.[7] Recently, Mekhemer et al. claimed that other influences than the lattice energy of metal oxides can influence the bulk or surface route ketonization proceeds through.[10] That respective work was done by researching the MgO catalyzed vapor phase reaction of acetic acid and determining that bulk metal acetates were formed at room temperature despite the supposed high lattice energy of magnesia.[10] This purportedly happened due to magnesia's basicity.[10]

Therefore it is commonly believed that cerium oxide, with its high lattice energy, relatively low basicity, and reported stability promotes the ketonization reaction through a surface catalyzed mechanism. However, results shown here are novel in that they demonstrate that not only lattice energy and basicity influences whether bulk crystalline

changes occur during the course of ketonization. As the lower temperature calcined materials have a greater surface area than the higher temperature calcined ceria, it is possible that the differences seen in this work are due to mass transfer limitations. To test this thought, ceria calcined at 450 °C and 900 °C were used in low quantities in the ketonization reaction with greater amounts of acetic acid for more than 24 hours. Results of this experiment complimented those found with the shorter reaction times, demonstrating evidence that mass transfer is likely not the reason for the phenomenon. It therefore appears probable that catalyst crystallinity is also important in resisting this change in bulk structure.

As acetic acid ketonization has been performed almost exclusively in the vapor phase, it is a valid question to ask if the crystalline change occurring is exclusively a condensed phase event. In-situ vapor phase XRD was performed to examine this theory. For this particular study, acetic acid vapors were led over the ceria calcined at 450 °C at a constant temperature of 230 °C while continually scanning. As can be observed in Figure 7, the ceria underwent a similar bulk change during the course of reaction. This result shows that despite the reaction phase, acetic acid can potentially interact with cerium oxide to form an acetate species in the bulk of the catalyst. Likely, this conclusion was not discovered earlier as a number of studies that found ceria to be stable during ketonization used an oxide calcined at a high temperature.[35]

4.3.9 Post reaction SEM results

Bulk crystalline changes were not the only catalyst transformation that occurred during the course of ketonization. Figure 8 shows that overall material morphology also changed during the course of reaction. Low temperature calcined ceria formed large amounts of whisker shaped particles while the high temperature calcined ceria maintained a similar

macro morphology to that before reaction testing. As the bulk crystal structure of the whisker shaped material also was altered during reaction it is likely that the two phenomena are tied together. Potentially the formation of cerium acetate involves bridging bonds of the acetate species forming a type of polymeric whisker structure. As the ceria calcined at 900 °C did not form the bulk acetate, the whiskers could not form.

4.3.10 Post reaction XPS results

XPS examination of the catalysts after the 4 hr 20 min reaction showed that the cerium oxidation state remained primarily 4+ for all the ceria catalysts. However, as portrayed in Figure 9 after longer reaction times with more acid, the cerium from the 450 °C calcined ceria had been significantly reduced to 3+ while the 900 °C calcined ceria remained as before in the 4+ oxidation state. This is of interest since it seems unusual that the interaction of the catalyst with a highly oxidized species like acetic acid actually caused reduction of the ceria surface. Reduction of cerium during ketonization has been reported before.[32] Gangadharan et al. reported that the cerium in their ceria-zirconia was further reduced during ketonization of propanal when co-fed with propanoic acid.[32] This was attributed to acid catalyzed reactions on the surface.[32] It is known that heating of cerium(IV) acetate will result in incomplete decarboxylation and a resulting reduced cerium state.[37] Moreover, this may explain why reduction of cerium was observed in this work even after drying of the catalyst post reaction in air as cerium(IV) acetate would be reduced to the thermally stable cerium(III) acetate. As the 450 °C calcined ceria had formation of cerium acetate throughout the bulk in contrast to the 900 ° C catalyst, it would have greater acetate formation and subsequent cerium reduction.

4.3.11 Activation energies

Through initial rate studies, apparent activation energies for both the 450 and 900 °C calcined catalysts were found. As shown in Figure 10, for the high temperature material, the activation energy was determined to be 161 kJ/mol. This value is reasonable as it is similar to the activation energy of 132 kJ/mol Gaertner et al. arrived at for the ketonization of hexanoic acid on a ceria-zirconia catalyst.[4] However, for the 450 °C treated ceria, a significantly lower activation energy was found as can be seen in Figure 10 as well. As this material underwent bulk rearrangements it is possible that reaction testing is occurring in the internal mass transfer regime thus causing the activation energy to appear lower. The apparent activation energy is also near ½ of that determined for the 900 °C ceria supporting this mass transfer theory.

As it appeared that the lower temperature ceria was undergoing bulk transformations and thus may catalyze the ketonization reaction through the bulk decomposition mechanism, comparison of the activation energies to that of the decomposition of cerium acetate would be of interest. Using an isoconversion thermogravimetric technique this goal was achieved. The method used the equation $ln\frac{\beta}{{T_f}^{1.92}} = -1.0008\frac{E}{RT_f} + C$ where β is the heating rate, T_f the temperature at which an equivalent point in the reaction is reached, C is a constant, R the ideal gas constant, and E is the activation energy as proposed by Starink.[19] Thus decomposing cerium acetate at different temperature rates allowed for the plotting of $\ln\left(\frac{\beta}{{T_f}^{1.92}}\right)$ vs. $-1.0008/(RT_f)$ in order to determine the activation energy. As multiple reactions are occurring during the course of cerium acetate decomposition care must be taken when choosing the equivalence stage for analysis. Arii et al. studied the decomposition of Ce(III)

acetate and determined that reaction occurred in 6 different stages during which acetone was formed in stages 2, 3, and 4.[38] According to Arii et al. these 3 stages consist of the steps

Stage 2. $2Ce(CH_3CO_2)_3 \rightarrow Ce_2O(CH_3CO_2)_4 + (CH_3)_2CO + CO_2$

Stage 3. $Ce_2O(CH_3CO_2)_4 \rightarrow 2CeO(CH_3CO_2) + (CH_3)_2CO + CO_2$

Stage 4. $Ce_2O_2(CH_3CO_2)_2 \rightarrow Ce_2O_2CO_3 + (CH_3)_2CO$

An example of the mass loss curve from the TGA experiments can be seen in Figure 11 with activation energies reported for the 3 steps in Table 3. Despite bulk structure changes occurring during ketonization, it is unlikely that the oxide was fully converted into complete metal acetate and thus the reaction most likely resembles the acetate decomposition that takes place during steps 3 and 4. As shown in Table 3, the activation energies for these steps are quite close to that found for ketonization over the ceria calcined at the high temperature. Therefore it is possible that the mechanism for both the thermal decomposition of cerium acetate and ketonization over cerium oxide are the same regardless of if bulk transformations occur. Further research is currently underway to clarify this possibility.

4.4 Conclusions

Cerium oxide catalyzed ketonization of the model bio-oil compound acetic acid was performed in the condensed phase with special emphasis involved on examination of the influence of ceria calcination temperature. It was found that not only the lattice energy of the oxide, as previously reported, is important in determining if the mechanism proceeds through a bulk or a surface catalyzed route, but also the crystallinity of the oxide. Low temperature calcined ceria even underwent bulk restructuring in the vapor phase proving that the discovered phenomenon is not just a condensed phase effect. As commonly cited, higher temperature calcined materials gave significantly greater rates of ketonization based on a

surface area determined before reaction. However, as the low temperature calcined catalysts lost a significant amount of surface area during the testing, this difference is in reality not as great or potentially non-existent for our condensed phase conditions. Characterization of the spent ceria catalysts showed that reduction and macroscale restructuring occurs as a result of partial bulk transformation to the metal acetate. This may explain reports in literature of cerium reduction occurring after acid exposure. Finally through activation energy calculations, it appears possible that the proposed different mechanisms occurring through either bulk decomposition or surface catalysis may indeed be the same.

4.5 Acknowledgements

This work was supported by grants from NSF PIRE. Jim Anderegg was very generous in his time while performing XPS testing of the materials in this study. Undergraduate Dan Weis was also involved in reaction testing during the course of experiments.

4.6 References

[1] E.L. Kunkes, D.A. Simonetti, R.M. West, J.C. Serrano-Ruiz, C.A. Gartner, J.A. Dumesic, Catalytic Conversion of Biomass to Monofunctional Hydrocarbons and Targeted Liquid-Fuel Classes, Science, 322 (2008) 417-421.
[2] C.A. Gärtner, J.C. Serrano-Ruiz, D.J. Braden, J.A. Dumesic, Catalytic Upgrading of Bio-Oils by Ketonization, ChemSusChem, 2 (2009) 1121-1124.
[3] E. Karimi, C. Briens, F. Berruti, S. Moloodi, T. Tzanetakis, M.J. Thomson, M. Schlaf, Red Mud as a Catalyst for the Upgrading of Hemp-Seed Pyrolysis Bio-oil, Energy & Fuels, 24 (2010) 6586-6600.
[4] C.A. Gaertner, J.C. Serrano-Ruiz, D.J. Braden, J.A. Dumesic, Catalytic coupling of carboxylic acids by ketonization as a processing step in biomass conversion, Journal of Catalysis, 266 (2009) 71-78.
[5] J.P. Diebold, A review of the chemical and physical mechanisms of the storage stability of fast pyrolysis bio-oils, NREL/SR-570-27613, Jan. 2000.
[6] A To Alkanolamines, M. Grayson (Ed.) Kirk-Othmer Encyclopedia of Chemical Technology, John Wiley and Sons, New York, 1978.
[7] R. Pestman, R.M. Koster, A. vanDuijne, J.A.Z. Pieterse, V. Ponec, Reactions of carboxylic acids on oxides .2. Bimolecular reaction of aliphatic acids to ketones, Journal of Catalysis, 168 (1997) 265-272.

[8] M. Renz, Ketonization of Carboxylic Acids by Decarboxylation: Mechanism and Scope, ChemInform, 36 (2005).
[9] A.D. Murkute, J.E. Jackson, D.J. Miller, Supported mesoporous solid base catalysts for condensation of carboxylic acids, Journal of Catalysis, In Press, Corrected Proof.
[10] G.A.H. Mekhemer, S.A. Halawy, M.A. Mohamed, M.I. Zaki, Ketonization of acetic acid vapour over polycrystalline magnesia: in situ Fourier transform infrared spectroscopy and kinetic studies, Journal of Catalysis, 230 (2005) 109-122.
[11] M.A. Hasan, M.I. Zaki, L. Pasupulety, Oxide-catalyzed conversion of acetic acid into acetone: an FTIR spectroscopic investigation, Applied Catalysis A: General, 243 (2003) 81-92.
[12] A. Trovarelli, C. de Leitenburg, M. Boaro, G. Dolcetti, The utilization of ceria in industrial catalysis, Catalysis Today, 50 (1999) 353-367.
[13] A.M. Rubinshtein, A.A. Slinkin, V.I. Yakerson, E.A. Fedorovskaya, The reduction of CeO2 in the ketonization of ch3cooh, Russian Chemical Bulletin, 10 (1961) 2090-2092.
[14] J.J. Spivey, G.W. Roberts, K.M. Dooley, Catalysis of Acid/Aldehyde/Alcohol Condensations to Ketones, Catalysis, The Royal Society of Chemistry, Cambridge, 2004, pp. 293-319.
[15] O. Nagashima, S. Sato, R. Takahashi, T. Sodesawa, Ketonization of carboxylic acids over CeO2-based composite oxides, Journal of Molecular Catalysis A: Chemical, 227 (2005) 231-239.
[16] K.S. Kim, M.A. Barteau, Structure and composition requirements for deoxygenation, dehydration, and ketonization reactions of carboxylic acids on TiO2(001) single-crystal surfaces, Journal of Catalysis, 125 (1990) 353-375.
[17] J. Stubenrauch, E. Brosha, J.M. Vohs, Reaction of carboxylic acids on CeO2(111) and CeO2(100), Catalysis Today, 28 (1996) 431-441.
[18] M. Kobune, S. Sato, R. Takahashi, Surface-structure sensitivity of CeO2 for several catalytic reactions, Journal of Molecular Catalysis A: Chemical, 279 (2008) 10-19.
[19] M.J. Starink, The determination of activation energy from linear heating rate experiments: a comparison of the accuracy of isoconversion methods, Thermochimica Acta, 404 (2003) 163-176.
[20] E. Aneggi, J. Llorca, M. Boaro, A. Trovarelli, Surface-structure sensitivity of CO oxidation over polycrystalline ceria powders, Journal of Catalysis, 234 (2005) 88-95.
[21] S. Bernal, G. Blanco, A.E. Amarti, G. Cifredo, L. Fitian, A. Galtayries, J. Martín, J.M. Pintado, Surface basicity of ceria-supported lanthana. Influence of the calcination temperature, Surface and Interface Analysis, 38 (2006) 229-233.
[22] J.I. Gutiérrez-Ortiz, B. de Rivas, R. López-Fonseca, J.R. González-Velasco, Characterization of the catalytic properties of ceria-zirconia mixed oxides by temperature-programmed techniques, Journal of Thermal Analysis and Calorimetry, 80 (2005) 225-228.
[23] G. Rao, Influence of metal particles on the reduction properties of ceria-based materials studied by TPR, Bulletin of Materials Science, 22 (1999) 89-94.
[24] H.C. Yao, Y.F.Y. Yao, Ceria in automotive exhaust catalysts : I. Oxygen storage, Journal of Catalysis, 86 (1984) 254-265.
[25] E. Mamontov, T. Egami, R. Brezny, M. Koranne, S. Tyagi, Lattice Defects and Oxygen Storage Capacity of Nanocrystalline Ceria and Ceria-Zirconia, The Journal of Physical Chemistry B, 104 (2000) 11110-11116.
[26] A. Trovarelli, Catalysis by Ceria and Related Materials, in: G.J. Hutchings (Ed.) Catalytic Science Series, Imperial College Press, 2002.
[27] A.Q. Wang, P. Punchaipetch, R.M. Wallace, T.D. Golden, X-ray photoelectron spectroscopy study of electrodeposited nanostructured CeO[sub 2] films, Journal of Vacuum Science & Technology B: Microelectronics and Nanometer Structures, 21 (2003) 1169-1175.
[28] E. Preisler, Stability of cerium oxide on silicon studied by x-ray photoelectron spectroscopy, J. Vac. Sci. Technol. B, 19 (2001) 1611.

[29] P.A.H. Burroughs, Anthony F. Orchard, Geoffrey Thornton, Satellite studies in the x-ray photoelectron spectra of some binary and mixed oxides of lanthanum and cerium, Journal of the Chemical Society, Dalton Transactions, 17 (1976) 1686-1698.
[30] J.Z. Shyu, K. Otto, W.L.H. Watkins, G.W. Graham, R.K. Belitz, H.S. Gandhi, Characterization of Pd/[gamma]-alumina catalysts containing ceria, Journal of Catalysis, 114 (1988) 23-33.
[31] J.Z. Shyu, W.H. Webber, H.S. Gandhi, Surface characterization of alumina-supported ceria, Journal of Physical Chemistry, 92 (1988) 4964-4970.
[32] A. Gangadharan, M. Shen, T. Sooknoi, D.E. Resasco, R.G. Mallinson, Condensation reactions of propanal over CexZr1-xO2 mixed oxide catalysts, Applied Catalysis A: General, 385 (2010) 80-91.
[33] H.-X. Mai, L.-D. Sun, Y.-W. Zhang, R. Si, W. Feng, H.-P. Zhang, H.-C. Liu, C.-H. Yan, Shape-Selective Synthesis and Oxygen Storage Behavior of Ceria Nanopolyhedra, Nanorods, and Nanocubes, The Journal of Physical Chemistry B, 109 (2005) 24380-24385.
[34] M. Baudin, M. Wójcik, K. Hermansson, Dynamics, structure and energetics of the (111), (011) and (001) surfaces of ceria, Surface Science, 468 (2000) 51-61.
[35] Y. Yamada, M. Segawa, F. Sato, T. Kojima, S. Sato, Catalytic performance of rare earth oxides in ketonization of acetic acid, Journal of Molecular Catalysis A: Chemical, 346 (2011) 79-86.
[36] V.I. Yakerson, E.A. Fedorovskaya, A.L. Klyachko-Gurvich, A.M. Rubinshtein, Vapor Phase Catalytic Ketonation of CH3COOH over Oxides of Quadrivalent Metals and BeO, Kinetika i Kataliz, 2 (1961) 907-915.
[37] R.A. Sheldon, Jay K. Kochi, Photochemical and thermal reduction of cerium(IV) carboxylates. Formation and oxidation of alkyl radicals., Journal of the American Chemical Society, 90 (1968) 6688-6698.
[38] T. Arii, T. Taguchi, A. Kishi, M. Ogawa, Y. Sawada, Thermal decomposition of cerium(III) acetate studied with sample-controlled thermogravimetric-mass spectrometry (SCTG--MS), Journal of the European Ceramic Society, 22 (2002) 2283-2289.

4.7 Tables and figures

Table 1. BET surface area of ceria materials fresh and spent after reactions at either 230 °C or 290 °C. The reaction at 230 °C used an acetic acid/ceria ratio of 5 for all materials while the reaction at 290 °C used different acid/ceria ratios as in initial rates experiments. The ratios were 40, 40, 20, and 5 for the catalysts calcined at 450, 600, 750, and 900 °C respectively for the 290 °C test. XPS results for the % of peak u'" and the corresponding values of cerium oxidation state are shown in columns 5 and 6 respectively showing that all the materials primarily consist of oxidized cerium.

Catalyst $T_{calcination}$ (°C)	SA_{BET} (m^2/g) fresh	SA_{BET} (m^2/g) 230 °C, 4.3 h	SA_{BET} (m^2/g) 290 °C, 20min	%u"'	% Ce^{4+}
450	88	28	2	13.2	96
600	70	26	1	12.9	94
750	25	16	2	12.6	92
900	1.7	1.0	1	12.5	91

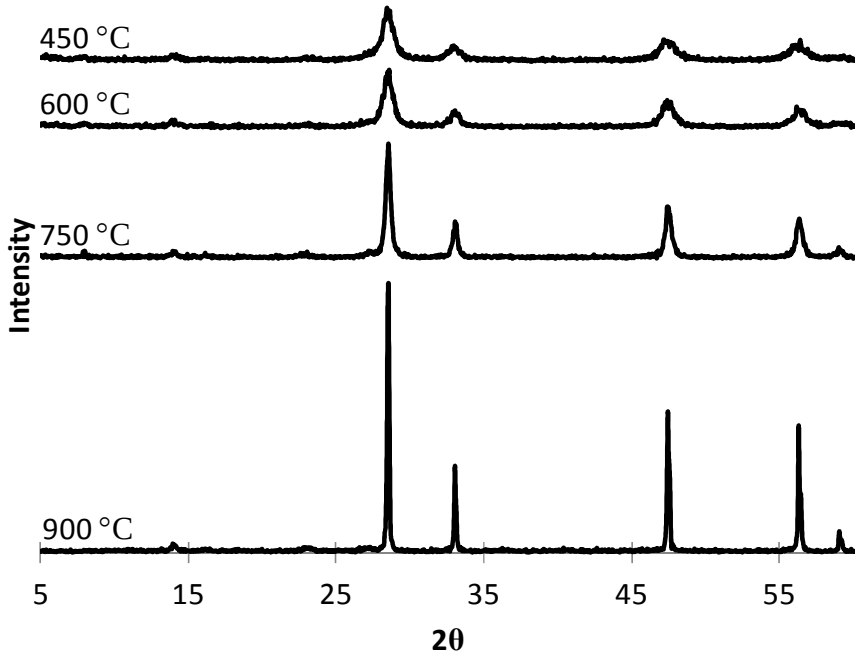

Figure 1. XRD patterns for ceria calcined at the different temperatures shown. The high temperature calcined materials demonstrated greater crystallinity.

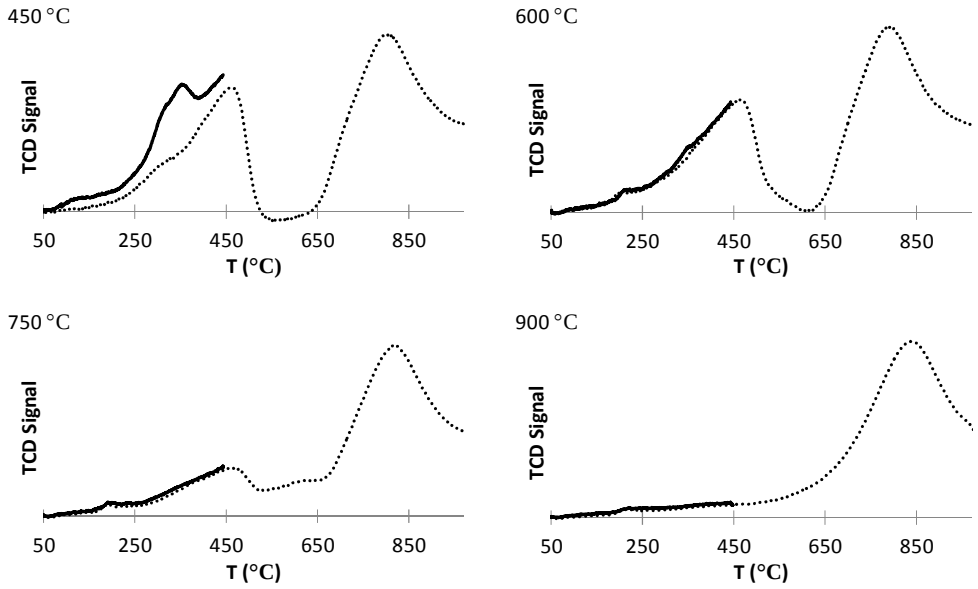

Figure 2. H_2 TPR of ceria calcined at different temperatures as shown in the top left corner. Each catalyst underwent two oxidation/reduction cycles where the first reduction is shown by a solid line while the dotted line represents the second reduction.

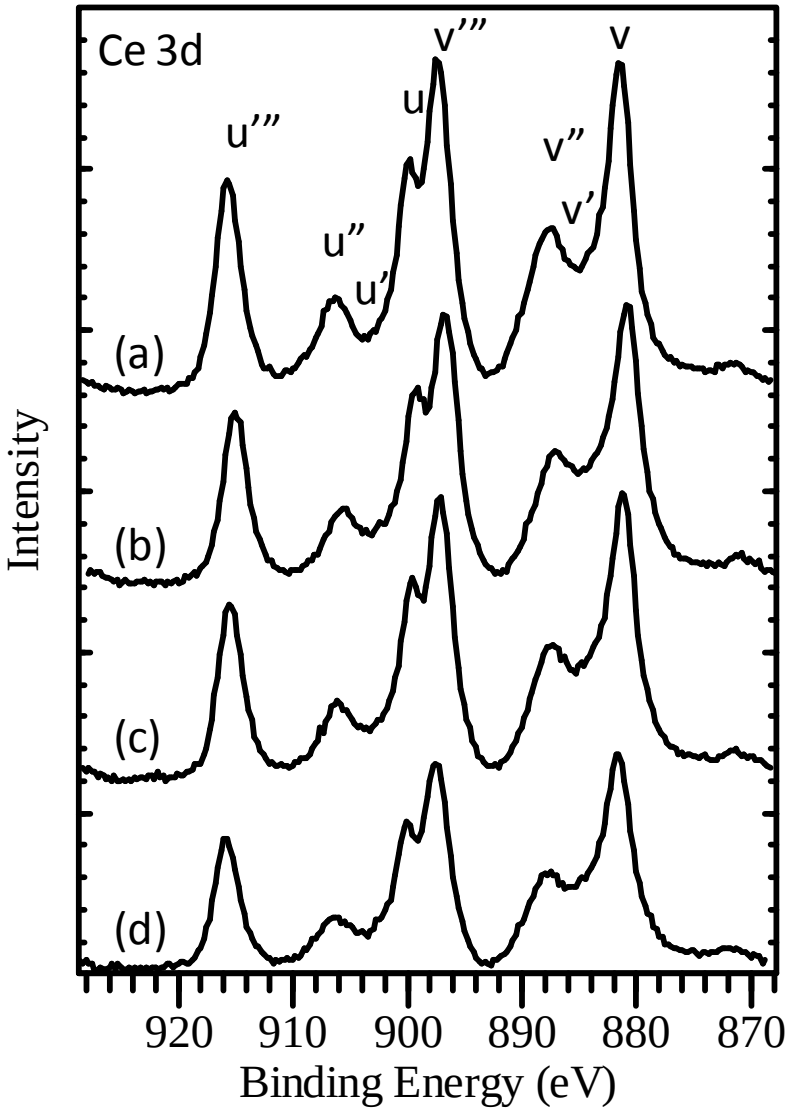

Figure 3. XPS spectra of Ce 3d for the fresh cerium oxide catalysts calcined at temperatures (a) 450 °C, (b) 600 °C, (c) 750 °C, or (d) 900 °C. Cerium was primarily in the 4+ state.

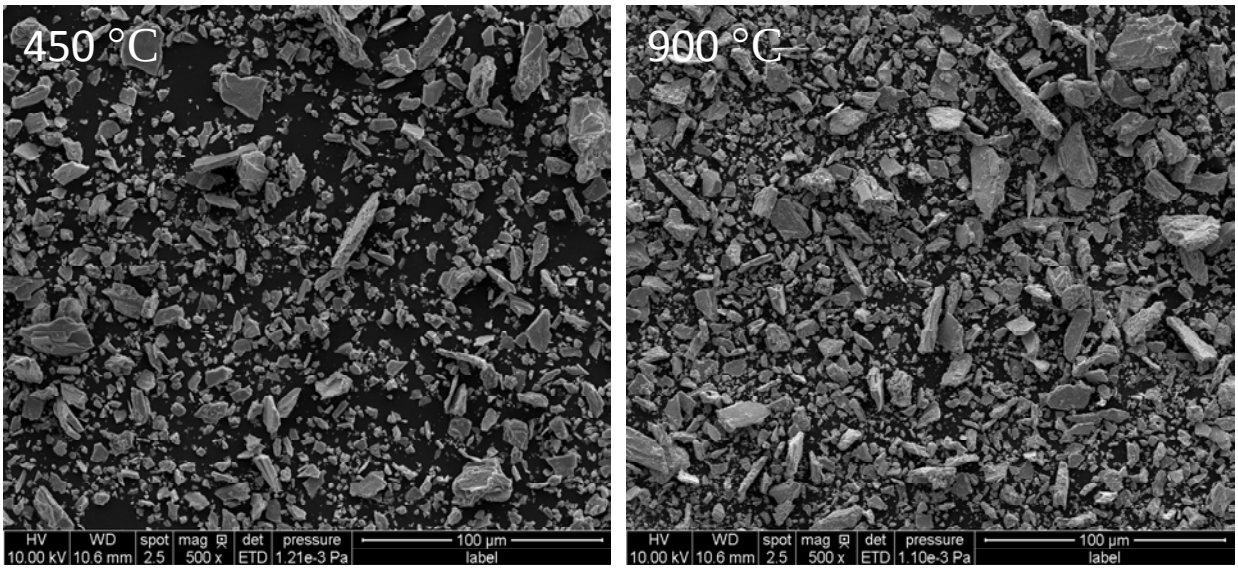

Figure 4. SEM images of ceria calcined both at low and high temperatures showing non uniform macro-morphology.

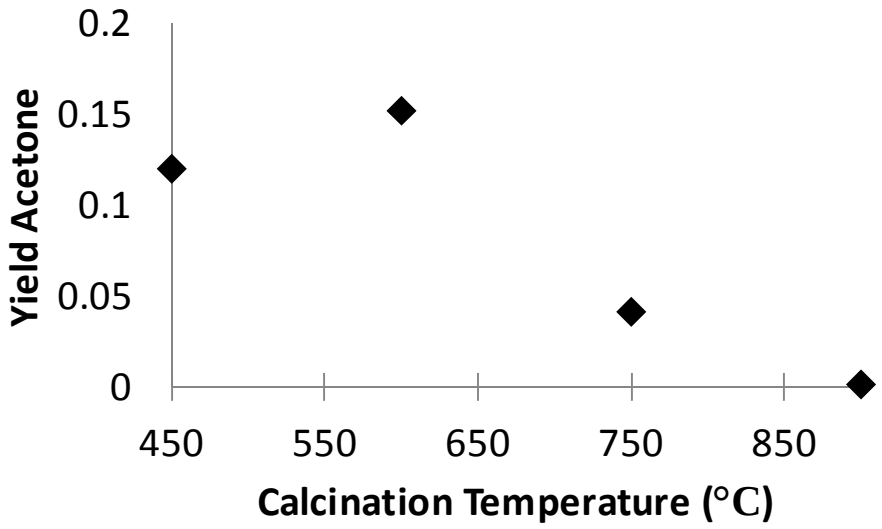

Figure 5. Acetone yields in the condensed phase ketonization of acetic acid run at 230 °C for 4 hours and 20 min with 1 g of acetic acid and 0.2 g of ceria.

Table 2. Initial rate studies for ceria catalysts showing a greater activity for higher temperature calcined ceria on a pre-reaction surface area basis.

Catalyst $T_{calcination}$ (°C)	Initial rate (µmol/m^2/h) at 543 K	Initial rate (µmol/m^2/h) at 563 K
450	52	333
600	94	408
750	258	835
900	267	1484

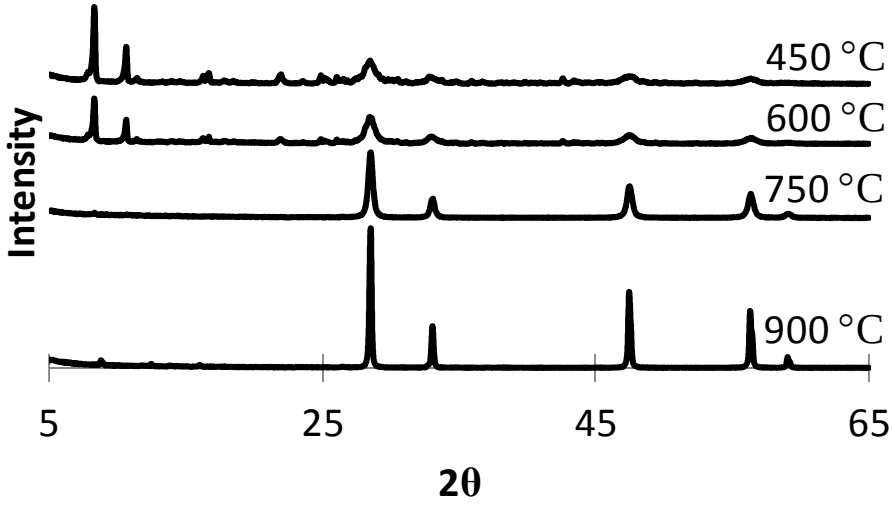

Figure 6. XRD profile of ceria catalysts after reaction testing for 4 h 20 min at 230 °C. Crystal structure disruption depended on calcination temperature.

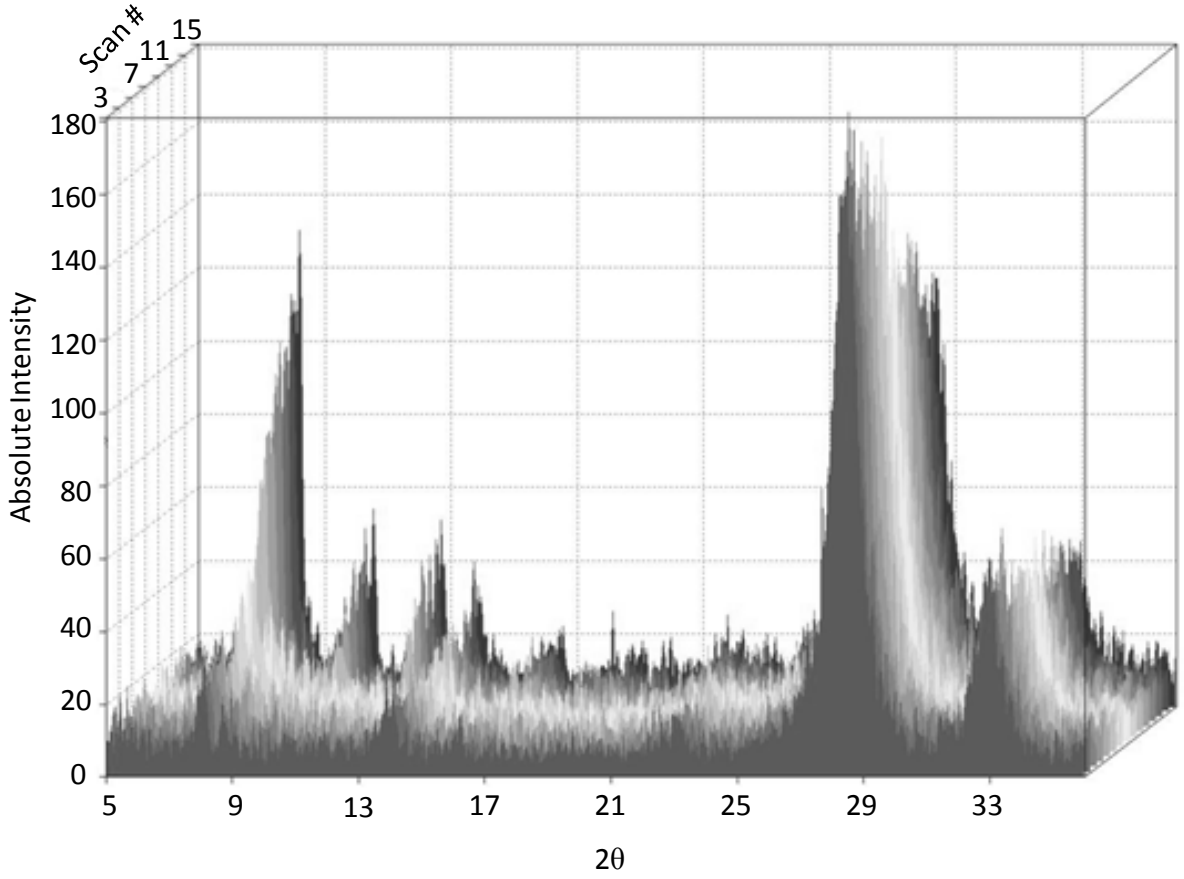

Figure 7. In-situ testing of ceria calcined at 450 °C. Acetic acid vapors were continuously led over the material during scans at 230 °C. It can be seen that by the higher scan #, the crystal structure was significantly changed.

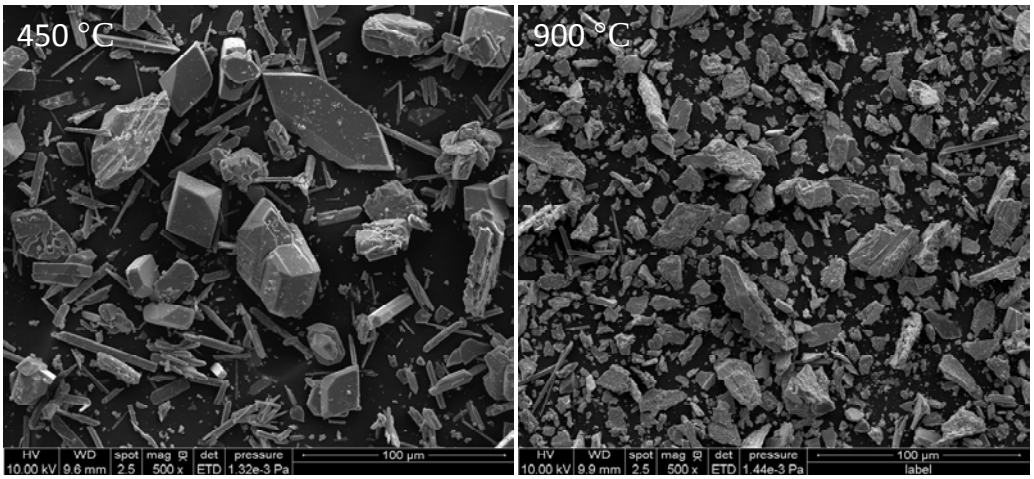

Figure 8. Post acetic acid ketonization (230 °C, 0.1 g catalyst, 2 g acetic acid, 24 h 45 min) SEM images of both low and high temperature calcined cerium oxide catalysts.

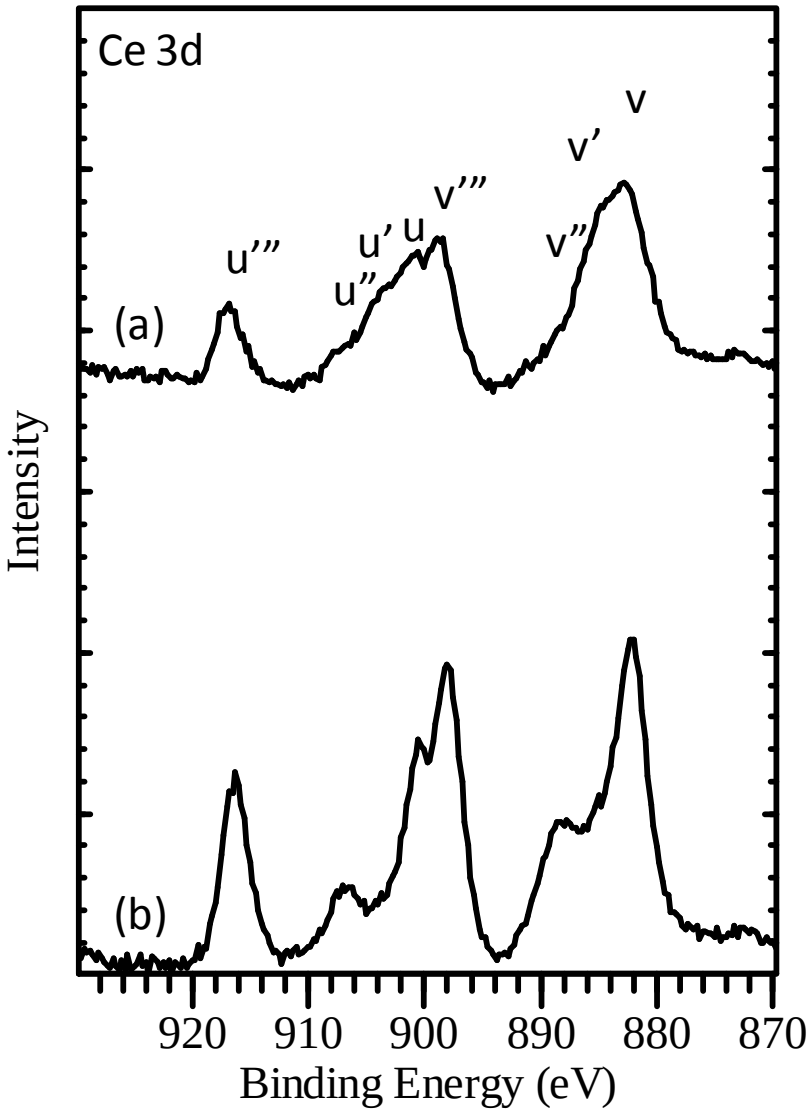

Figure 9. XPS spectra of ceria catalysts (a) 450 °C and (b) 900 °C after 24 h 45 min reactions with 2 g of acetic acid and 0.1 g catalyst at 230 °C. From the figure it is evident that the cerium on the oxide calcined at 450 °C has been significantly reduced. Rough calculations give the Ce^{4+} % to be 62% and 87% for the 450 and 900 °C materials respectively.

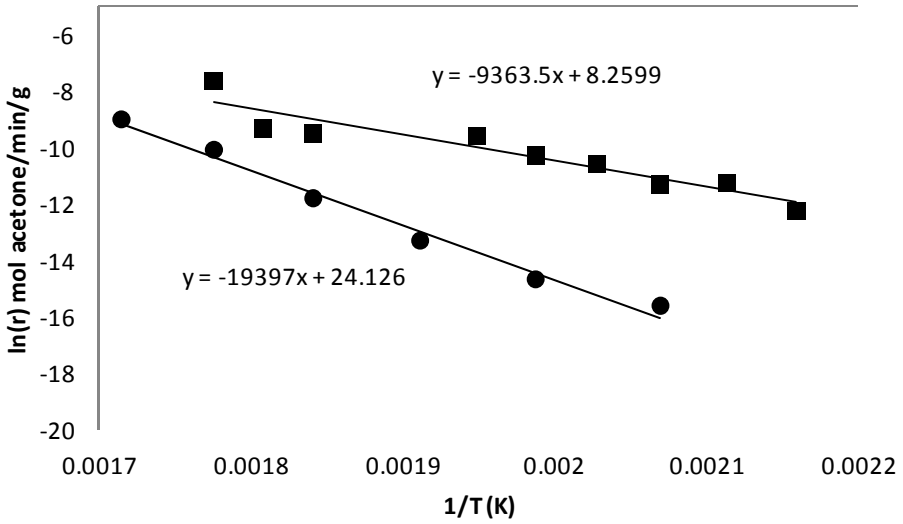

Figure 10. Arrhenius plots for both the 450 °C (■) ceria and the 900 °C (●) ceria in the condensed phase ketonization of acetic acid. Determined apparent activation energies are 161 kJ/mol for the 900 °C ceria and 78 kJ/mol for the 450 °C ceria.

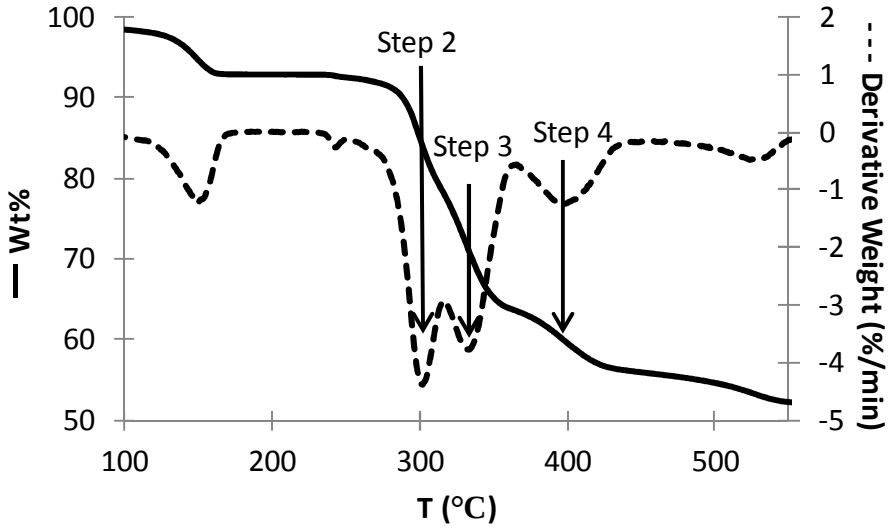

Figure 11. Example of a TGA decomposition plot of cerium(III) acetate hydrate. Labeled are the 3 decomposition steps of the metal acetate resulting in the production of acetone.

Table 3. Activation energies for the decomposition of cerium(III) acetate hydrate as determined from TGA experiments.

Step #	E_a (kJ/mol)
2	199±4
3	157±21
4	149±5

Chapter 5

Catalysis with ceria nanocrystals: biorenewable applications

A paper to be submitted to Journal of Molecular Catalysis A: Chemical

Ryan W. Snell[1], Sikander Hakim[2], James A. Dumesic[2], and Brent H. Shanks[1]

[1]Department of Chemical and Biological Engineering, Iowa State University

[2]Department of Chemical and Biological Engineering, University of Wisconsin-Madison

Authorship roles:

Snell: Primary author

Hakim: Performed vapor phase reaction testing

Dumesic, Shanks: Principal investigators

Abstract

The problems associated with the high content of organic acids present in bio-oil could potentially be alleviated through the use of the ketonization reaction. While there have been previous reports of ketonization reactions being sensitive to the surface morphology of the respective catalyst, these studies have largely been performed in idealized conditions. Here, shape selective ceria nano-catalysts were synthesized and examined in both vapor and condensed phase ketonization reactions of the model bio-oil compound acetic acid. It was found that in lower temperature condensed phase conditions the morphology of the catalyst may be of less importance due to crystal disruption from metal carboxylate formation. However, the bulk structure was maintained to a greater extent in the higher temperature vapor phase conditions. This work demonstrates that while the morphology of the catalyst may play a role in ketonization, its influence likely depends on the reaction conditions.

Keywords: Ketonization; Bio-oil; Nanocrystals; Reaction phase

5.1 Introduction

Recently, the creation of renewable fuels derived from bio-oil made from fast pyrolysis of biomass has generated increasing interest.[1-3] Unfortunately, upgrading is necessary as large amounts of organic acids exist in the bio-oil, thus lowering the pH to 2-3 and making storage and transportation difficult.[4] For this particular application the ketonization reaction is well suited as it converts two organic acids to a ketone, water and carbon dioxide.[5] Clearly a reaction like ketonization that efficiently removes oxygen to increase oil energy density along with raising the pH through removal of acids, is particularly beneficial. As correctly pointed out by Renz, this reaction is also environmentally friendly as it produces no harmful co-products.[6]

Interest in the ketonization reaction has increased in recent years largely due to its biorenewable applications.[7-9] Despite the surge in research involving ketonization, the catalyst mechanism remains undetermined.[10] However, a few publications have determined that there may be an influence of the catalyst surface structure.[11, 12] Kim and Barteau were among the first to find this type of dependence while performing TPD studies of acetic acid on titania single crystals.[11] Performing TPD experiments with acetic acid, it was discovered that acetone desorption occurred only from {114} surface facets.[11] It was then hypothesized that for ketonization to occur, a surface must be present that has doubly unsaturated cations and is oxidized.[11] Stubenrauch et al. also carried out acetic acid TPD experiments, except this time using ceria single crystals.[12] It was discovered that ceria only promoted ketone formation with {111} surfaces.[12] This finding is interesting because it seemingly contradicts the proposal from Barteau and Kim since the {111} surface of ceria

does not contain cerium with multiple vacancies. A mechanism where methyl groups, created from acetate decomposition, join with another surface acetate was proposed as the ketonization mechanism by Stubenrauch.[12]

While single crystal TPD studies occur in very controlled environments it would be preferred to study the role of surface structure in a more complex system beginning to approach that used for bio-oil upgrading. Ideally, recent advances in ceria nanocrystal synthesis allow for this potential. Mai et al. developed a hydrothermal method that allows for creation of ceria nanopolyhedra, nanorods, and nanocubes that preferentially expose either{111} and {100}, {110}and {100}, or {100} facets respectively.[13] Synthesis techniques like these allow for creation of ceria catalysts exposing the unfavorable {110} and {100} facets that can be subsequently used in reaction testing more complex systems than single crystal TPD studies will allow. This work examines ceria nanocrystals' use in the condensed and vapor phase ketonization reaction of acetic acid.

5.2 Experimental section

5.2.1 Catalyst synthesis

Synthesis of the shape selective nanocrystals used a similar hydrothermal technique to that proposed by Mai et al. as well as used by Si and Flytzani-Stephanopoulos.[13, 14] Ceria nanocrystals were made by first dissolving 8.68 g of cerium(III) nitrate hexahydrate (Aldrich 99.99%) into 50 ml of deionized H_2O. Next, NaOH—96g for ceria nanorods and nanocubes or 1.6g for nanopolyhedra—was added into 350 ml of deionized H_2O and dissolved. The solutions were then mixed together and stirred for 30 minutes at room temperature. After this aging step, the solution was put into a PFA bottle and sealed in a threaded stainless steel nipple (3" pipe size, 8" length). The SS nipple was then put into an

oven and heated to temperature—100 °C for nanorods or 180°C for nanocubes and nanopolyhedra—for 24 hours. After 24 hours, the oven was allowed to cool after which the nipple was removed and quenched in a bucket of water. Opening of the stainless vessel revealed the PFA bottle containing a layer of white precipitate that had settled on the bottom. The top liquid was decanted and the remaining amount with precipitate was put into 50 ml Corning centrifuge tubes. Centrifugation was used to separate the crystals from the mother liquor. After spinning, deionized water was used to wash the nanocrystals followed by more centrifuging. This washing step was performed 5x. After washing, the nanocrystals were put into a crucible and dried at 60 °C in air overnight. Finally, the crystals were calcined at 600 °C for 3 h before being finely ground to a powder and stored in a dessicator.

5.2.2 Reaction testing

Catalytic reactions were performed in Parr 4590 series 75 ml stainless steel batch reactors. Acetic acid (Fisher 99.9%) was used as the model bio-oil reactant, 1,4 dioxane (Fisher 100.0%) as the internal standard, and toluene (Fisher 99.9%) as solvent. Reactions were set up by mixing the acetic acid (typically 1.00g), 50ml toluene, ½ ml of 1,4 dioxane, and catalyst (typically 0.150g) into the stainless steel reactor vessel. After sealing the reactor, N_2 pressure was applied to 40 bar. The reactors were subsequently heated to 230 °C and stirred at 400 rpm. Final pressure at 230 °C was ~60 bar. Sampling occurred into a liquid nitrogen cold trap and products were analyzed on a GC-FID (Agilent 7890A). Yields were defined as $Yield = \frac{2*(Moles\ acetone\ produced)}{Initial\ moles\ of\ Acetic\ Acid}$ while conversion was defined as $Conversion = \frac{(Initial\ Moles\ Acetic\ Acid - Moles\ Acetic\ Acid\ Remaining)}{Initial\ Moles\ Acetic\ Acid}$. Before post reaction

characterization, the spent catalyst was separated by decanting off any liquids and drying in an oven under atmospheric conditions at 100 °C for 1 h.

The vapor phase reactions were performed in a fixed bed, down flow reactor consisting of a quarter-inch stainless steel tube. Approximately 50mg of CeO_2 catalyst was mixed with 2 g of crushed fused silica to maintain the bed height. The bed was held in place by quartz wool. The reactor was heated to the reaction temperature of 623K using aluminum blocks heated by a well-insulated furnace. The acetic acid feed (20wt% in water) was pumped using a syringe pump. The feed was preheated at a temperature of 403K in a stainless steel pressure vessel. Helium was used to sweep the vapors to the reactor through heated lines. A WHSV (weight hourly space velocity) of $40h^{-1}$ was used for all the reaction runs. The reactions were performed at atmospheric pressure. The ceria catalysts were kept on stream for 100 hours to study the catalyst stability. A gas-liquid separator at room temperature was used to collect the liquid-phase reaction effluent for analysis using HPLC. The gas-phase products were analyzed using on-line GC-TCD and GC-FID.

5.2.3 Ceria characterization

A Siemens D-500 operated at 45 kV and 30 mA with Cu Kα radiation was used for X-ray diffraction(XRD) with a 0.15 detector slit, step size of 0.05 and dwell time of 2 s. A FEI Quanta FE-SEM was used for the SEM imaging. The materials were examined after sputtering the sample with iridium. A 2007 JEOL 2100 with 200 kV was utilized for the TEM imaging. Before examination, the catalyst was dispersed in acetone, sonicated and deposited on a carbon film. For X-ray photoelectron spectroscopy (XPS) studies an Al Kα x-ray source was used on a Phi 5500 Multitechnique system. The C1s peak at 284.6 eV was used for corrections. Quantifications used Shirley backgrounds.

CO_2 and NH_3 temperature programmed desorption (TPD) and H_2 temperature programmed reduction (TPR) were done on a Micromeritics Autochem II Chemisorption Analyzer. For CO_2 and NH_3 TPD the sample was first degassed under the flow of 20 ml/min helium by ramping the sample temperature up to 400 °C at 10 °C/min and holding at 400 °C for 10 min. The samples were then cooled to 45 °C before being exposed to either 50 ml CO_2 or 50 ml 10% NH_3-He for 30 min. 20 ml/min of He was used to purge the sample containing quartz tube for 60 min. Finally the catalyst temperature was ramped up to 850 °C at a rate of 10 °C/min under the flow of 20 ml/min He.

Multiple oxidation-reduction cycles were used to investigate catalyst redox properties with TPR. First the sample was oxidized through increasing the temperature to 400 °C by 10 °C/min and holding for 30 minutes under the flow of 50 ml/min 10% O_2-He. Next, the catalyst was cooled to 50 °C under the flow of 50 ml/min Ar. Reduction then took place by flowing 20 ml/min 10% H_2-Ar during a temperature rise of 5 °C/min to 600 °C. The catalyst was subsequently cooled to 50 °C under the flow of 50 ml/min Ar. Another oxidation step, mirroring earlier, was subsequently performed. Finally after cooling, another reduction step was completed as earlier, except this time the temperature was increased to 1000 °C.

5.3 Results

5.3.1 SEM and TEM results of fresh ceria

SEM images of the hydrothermally synthesized ceria nanocrystals can be seen in Figure 1. As is demonstrated by the figure, nanocube synthesis resulted in a mixture of larger cubes around 100 nm per side along with a number of smaller less uniform cubes with side lengths ~10nm. The lack of uniformity in comparison to Mai et al. is likely the result of scaling up the synthesis to produce much more material per batch.[13] Nanorods were quite

long, ~100 nm, and narrow, ~10 nm, while the nanopolyhedra were very small, ~ 10-20 nm in diameter. TEM images of select particles demonstrated morphologies similar to those created by Mai et al.[13]

5.3.2 XRD analysis before reaction testing

XRD of the assorted materials demonstrated peaks related to the cubic fluorite crystal structure common to CeO_2. As shown in Figure 2, the diffraction peaks increased in sharpness from the nanopolyhedra to the nanorods to the nanocubes showing enhanced crystallinity. Use of the Scherrer equation with the {111} peak allowed for calculation of crystal sizes and determined them to be 48 nm for the nanocubes, 22 nm for the nanorods, and 17 nm for the nanopolyhedra. These dimensions roughly agree with those found by SEM.

5.3.3 BET analysis of fresh nanocrystals

BET surface areas and pore size distributions of the catalysts were determined through the use of nitrogen adsorption and desorption isotherms. The surface areas of the nanoparticles—in relation to each other—were similar to that reported by Mai et al. in that the nanopolyhedra (44 m^2/g) and the nanorods (43 m^2/g) had similar BET surface areas significantly higher than the nanocubes (11 m^2/g).[13] However the surface areas of all three nanoparticles was ~20 m^2/g less than determined by Mai et al.[13] This may also be a result of scaling up the synthesis procedure. Type IV isotherms, characteristic of mesoporous materials were seen for all the ceria samples. However, there were differences in the types of hysteresis loops for the catalysts. Ceria nanorods and nanocubes exhibited type 3 hysteresis loops usually occurring in materials that are macroporous or aggregated while the nanopolyhedra had a type 2 hysteresis loop.

5.3.4 TPR and XPS analysis of catalyst redox properties

Literature hints that ceria's redox properties could be of importance in ketonization. This is evidenced as proposed mechanisms typically involve a redox step.[15] Therefore characterization techniques that probe this property, such as TPR, are important for potential catalysts. If proposed mechanisms are correct, the catalyst would need to go through multiple redox cycles. TPR experiments should then examine catalyst modifications when going through multiple cycles as well. For the TPR results presented in this work, after an oxidation step at 400 °C, the catalyst was reduced up to 600 °C with H_2. Another oxidation was then performed followed by reduction up to 1000 °C. Results of these reductions are displayed in Figure 3. There appears to be two steps in the reduction process. These different steps are commonly explained as a surface reduction followed by a bulk reduction.[16] For the first reduction there was not a significant difference between the catalysts. However, the second reduction showed dissimilarities in that the low temperature peak for the polyhedra became much less intense and broad portraying decreased redox abilities. Nanocubes and the nanorods catalysts demonstrated enhanced ease of reduction after the first redox cycle as evidenced by the shift in peak location to lower temperatures. Apparently the more unstable {100} and {110} surface facets maintain redox stability more than {111} surfaces. It is also possible that the cubes and rods could have oxygen removal occurring from the bulk at these low temperatures. While this characteristic would be of value in applications such as three way catalytic convertors it is unknown if these properties are of worth in the ketonization reaction.

XPS is a well known technique that can be used to determine the oxidation state of cerium oxide.[17] Results for the ceria nanocrystals can be observed in Figure 4. Labeling of

the peaks, as seen in the figure, follows the now standard naming method coined by Burroughs et al.[18] As the ceria 3d spectra is quite complex only particularly noteworthy peaks are labeled here. Typically, the u'" peak at ~917 eV is associated only with Ce^{4+}. Shyu et al. found that oxidized ceria has a peak area at a binding energy of 917 eV that is roughly 13.7% and that there is a linear correlation between u'"% and the content of Ce^{4+}.[19, 20] Therefore for a rough estimation of the Ce^{4+} contained in the ceria, the equation Ce^{4+}%=7.3(area u"'/total area) can be used with the Ce 3d spectra. Labeled peaks u", u, v'", v", and v are also affiliated with Ce^{4+} while u' and v' are connected to ceria in the Ce^{3+} oxidation state.[21] As can be seen in Figure 4, the ceria is primarily in the 4+ oxidation state, but the v' and u' peaks in the polyhedra are significantly enhanced in comparison to the cubes and rods demonstrating that the polyhedra may have more vacancies.

5.3.5 NH_3 and CO_2 TPD

There have been a number of publications proclaiming the importance of catalyst acid and/or base sites for the ketonization reaction.[7, 22, 23] Here, NH_3 and CO_2 were used to examine either the acid or base site respectively. It was discovered that there were both acid and base sites found on the nanoparticles. Generally these were weak sites that are characteristic of ceria.[24] However, there were also some strong base sites found on the nanorods and nanocubes likely as the result of sodium from synthesis. XPS and EDS confirmed that trace amounts of sodium were on the cubes and rods. After condensed phase reaction testing, this sodium had disappeared.

5.3.6 Condensed phase reaction testing

A number of the compounds in bio-oil are thermally unstable making upgrading in the condensed phase the preferred method for bio-oil. As described earlier, the ketonization

reaction is well suited for bio-oil upgrading as it cleanly and efficiently removes oxygen and acidity from the oil. Unfortunately high temperatures, typically 300-450 °C, have been necessary to promote the reaction in an efficient manner.[25] Clearly this makes ketonization impractical to perform in the condensed phase without the development of a more active catalyst. With the long term goal of creating a better catalyst able to ketonize acids in the condensed phase, it was deemed necessary to probe the reaction in the liquid phase with currently utilized catalysts like ceria. Due to the high temperatures necessary for ketonization, few have performed ketonization in the condensed phase and to our knowledge this is amongst the first reports of liquid phase ketonization of small model bio-oil acids like acetic acid. Reaction phase can greatly influence testing results from a number of different directions including catalyst stability, chemical kinetics, and thermodynamics. For example, thermodynamic calculations demonstrate that ketonization in the gas phase is endothermic with an enthalpy of reaction ~12 kJ/mol while if the acid, water, and acetone are in the condensed phase, the reaction is even more endothermic with an enthalpy of reaction ~41 kJ/mol at 298 °C.[26]

Figure 5 shows the somewhat surprising reaction results. For a reaction using a constant surface area of catalyst, it was found that there was not necessarily a connection between surface faceting and activity as the cubes and rods with the more reactive surfaces did not appear to be either more or less active than the polyhedra. This demonstrates that surface morphology isn't necessarily important in the condensed phase ketonization of bio-oil compounds at these conditions. Initial rate experiments were conducted as well and found similar results with the cubes being the most active and the rods and polyhedra giving

similar rates on a surface area basis. However, as can be seen in Table 1, on a mass basis, rods and polyhedra were the best of the materials.

5.3.7 Post reaction SEM and XRD characterization

As this is to our knowledge the first application of shape selective nanocatalysts to the ketonization reaction, it is imperative that the stability of the materials be examined. It seemed that after condensed phase ketonization for two hours that the materials were relatively stable. At higher magnifications, after 24 h at 230 °C, it still looks as if the shapes are maintained. However, at lower magnifications it becomes clear that severe macro reordering of the nanocrystals occurred (Figure 6). What appear to be very long—up to ~50 μm—whiskers form with the loss of the shape selective materials. Moreover, XRD of the spent catalysts showed that a significant amount of the cerianite crystal structure had been destroyed (Figure 7). This was especially evident with the extra small ceria nanopolyhedra. Running a control reaction where no acid was used demonstrated that this phase change could be attributed to the acid while calcination of the spent polyhedra catalyst reformed its original cerianite structure establishing that this phase change is reversible. Although ceria has long been established as a stable oxide catalyst for the ketonization of organic acids, the nanocrystals appear to be easily transformed into what are likely some form of cerium oxyacetates in these condensed phase conditions.[27]

5.3.8 Post reaction XPS analysis

Examination of the spent catalysts after condensed phase reaction testing demonstrated that the polyhedra catalyst underwent significant reduction during the course of reaction (Figure 8). This is evident from the decrease in the size of the u’” peak and the formation of v’ and u’. Estimates of the oxidation state for the cerium in the spent catalysts

resulted in Ce^{4+} contents of 95%, 97%, and 55% for the ceria nanocubes, rods, and polyhedra respectively. Reduction of cerium during the course of ketonization has been reported before[28], but it is interesting that here, the different catalysts showed such different behaviors. As the XRD results of the tested ceria also showed a large change in the crystal structure of the polyhedra, it is likely that the two phenomena are connected in that bulk crystal changes are paired with surface reduction. Acetate stabilization of Ce^{3+} is the probable explanation. Perhaps the smaller particle size or the apparent additional oxygen vacancies of the polyhedra made them more susceptible to the attack by the acid. However, there was no clear correlation between activity and this reduction.

5.3.9 Vapor phase reaction testing

As ketonization of small organic acids has previously almost exclusively been performed in the vapor phase, it would be of interest to compare the results from the condensed phase to those in more typical conditions. As mentioned earlier, usual reaction temperatures are 300-450 °C [25] so in our vapor phase testing a temperature of 350 °C was applied. Ceria with non-uniform shapes made through the decomposition of cerium nitrate, called “bulk”, at 600 °C was also tested for comparison. As can be observed in Table 2 agreeing with condensed phase initial rate results, the ceria nanorods and polyhedra appeared to be more active than the cubes on a mass basis. The rods and polyhedra also appeared to be better than the bulk catalysts. Again, these results provide evidence that the catalysts preferentially displaying {111}—such as the bulk and the polyhedra—facets aren’t necessarily better than those with other surface structures.

As observed in Figure 9, the different catalysts showed varying rates of deactivation with their respective time on stream. While initially far more active than the other three

materials, the rods appear to more strongly deactivate at later times while the cubes, polyhedra, and bulk seemingly are closer to a steady state activity. Potentially these catalysts deactivated faster at shorter times on stream than did the rods so deactivation was not as readily seen at times > 1400 minutes.

5.3.10 Post-vapor phase reaction characterization

During the course of reaction there was generally a significant amount of ceria surface area lost. As observed in Table 2, the bulk ceria dropped from a pre-reaction BET surface area of 69 m^2/g to 36 m^2/g. The rods and polyhedra shape selective materials dropped a noteworthy amount of surface area as well, while the cubes only had a smaller surface area disappear. However, as displayed in Table 2 the variation in surface areas are not fully responsible for the differences between the catalysts, as even on an area basis, the rods and polyhedra appear more active.

Post reaction XRD profiles demonstrated that the crystalline phase of the ceria nano-crystals was not disrupted by exposure to the acetic acid reactant (Figure 10). This is in contrast to the results found after condensed phase reactions (Figure 7) hinting that there was not cerium oxyacetate formation in the material's bulk during testing in the vapor phase conditions. XPS established that acetic acid ketonization during the higher temperature vapor phase reactions did not result in significant reduction of the cerium. Moreover, SEM showed that the crystals largely maintained their shape specific structure (Figure 11). There also seems to be fewer of the whisker shaped particles formed after the vapor phase testing.

5.4 Discussion

It was found that shape selective ceria nanocrystals were active in both condensed and vapor phase ketonization reactions. Perhaps surprisingly, in both the condensed and

vapor phase reactions it was discovered that the shape selective materials preferentially exposing {111} facets were not necessarily far more active than the other ceria nanocrystals. Likewise in both phases the polyhedra and rod shaped materials were revealed to be the most active on a mass basis.

Despite these similarities between the results of the two different reaction phases, a number of differences were found as well. For instance, during lower temperature condensed phase testing, crystal structure disruption occurred while after gas phase testing, this phenomenon was not revealed. This change in the condensed phase is likely due to formation of metal acetates in the catalyst bulk through M-O bond breakage due to interaction with the organic acid. This type of reaction was reported for other rare earth oxides by Yamada et al. during gas phase reaction testing at 350 °C, but—consistent with our vapor phase testing—not for ceria.[29] They concluded that therefore surface crystal planes have no influence on ketonization catalyzed by these types of materials. This notion certainly appears to make sense for our conditions in the condensed phase as if the bulk structure of the ceria is being destroyed; the original surface is likely disrupted as well. XPS results would offer further evidence for this surface transformation as the polyhedra cerium was significantly reduced to the 3+ state. The single crystal TPD study on ceria by Stubenrauch et al. may have found influences of surface faceting to be important if the conditions during their work did not allow for enough energy during acid exposure for M-O bond breakage and the resulting bulk acetate formation thus maintaining the original ceria surface structure.[12]

However, in the vapor phase testing it did appear that there were activity disparities between the nano-crystals based on shape. Again, as the best catalysts were the rods and polyhedra, our results do not give evidence that a greater exposure of the {111} faceting is to

blame for this result. Furthermore, results from our characterization showed nothing that is intuitively obvious for explaining the finding. As it was found during condensed phase low temperature conditions that there was enough energy for the disruption of M-O bonds and the subsequent formation of a bulk metal acetate species, it makes sense that this could also occur during the higher temperature vapor phase reactions. However, bulk carboxylates were not observed, possibly due to the high temperature of reaction. Arii et al, studied the thermal decomposition of cerium(III) acetate hydrate and found that by 350 °C, the metal carboxylate was largely destroyed.[30] Perhaps the increased activity was due to the small crystallite size of the polyhedra or rods potentially allowing for easier formation and decomposition of the carboxylate into acetone. Regardless, it appears that even if the surface faceting of the catalyst does likely not influence the activity in our reaction conditions, the morphology of the catalyst may potentially play a role. Further research into this characteristic may be of interest particularly for those desiring to perform ketonization at higher temperatures where bulk carboxylate formation will not occur.

5.5 Conclusions

In a novel catalytic application of shape selective ceria nanocrystals the ketonization of the model bio-oil compound acetic acid was examined. It was discovered that ceria nanocubes, nanopolyhedra, and nanorods were all active for the respective reaction both in the condensed and in the vapor phase. During the course of condensed phase testing the materials' crystal structure was disrupted by the exposure to the acid, likely beginning to form a cerium carboxylate compound. Along with the metal acetate formation, reduction of the surface cerium occurred. However, in the vapor phase these changes did not take place adding to the stability of the nanocrystals-likely due to the decomposition temperature of the

resulting metal carboxylate. Rods and polyhedra shaped materials were found to be the most active demonstrating that the surface faceting is potentially not a critical influence in these types of conditions.

5.6 References

[1] A.V. Bridgwater, Review of fast pyrolysis of biomass and product upgrading, Biomass and Bioenergy, Biomass and Bioenergy, 38 (2012) 68-94.
[2] M.M. Wright, D.E. Daugaard, J.A. Satrio, R.C. Brown, Techno-economic analysis of biomass fast pyrolysis to transportation fuels, Fuel, 89 (2010) S2-S10.
[3] P.R. Patwardhan, J.A. Satrio, R.C. Brown, B.H. Shanks, Product distribution from fast pyrolysis of glucose-based carbohydrates, Journal of Analytical and Applied Pyrolysis, 86 (2009) 323-330.
[4] S. Czernik, A.V. Bridgwater, Overview of Applications of Biomass Fast Pyrolysis Oil, Energy & Fuels, 18 (2004) 590-598.
[5] M. Glinski, J. Kijenski, A. Jakubowski, Ketones from monocarboxylic acids: Catalytic ketonization over oxide systems, Applied Catalysis A: General, 128 (1995) 209-217.
[6] M. Renz, Ketonization of Carboxylic Acids by Decarboxylation: Mechanism and Scope, ChemInform, 36 (2005).
[7] C.A. Gaertner, J.C. Serrano-Ruiz, D.J. Braden, J.A. Dumesic, Catalytic coupling of carboxylic acids by ketonization as a processing step in biomass conversion, Journal of Catalysis, 266 (2009) 71-78.
[8] E.L. Kunkes, D.A. Simonetti, R.M. West, J.C. Serrano-Ruiz, C.A. Gartner, J.A. Dumesic, Catalytic Conversion of Biomass to Monofunctional Hydrocarbons and Targeted Liquid-Fuel Classes, Science, 322 (2008) 417-421.
[9] C.A. Gärtner, J.C. Serrano-Ruiz, D.J. Braden, J.A. Dumesic, Catalytic Upgrading of Bio-Oils by Ketonization, ChemSusChem, 2 (2009) 1121-1124.
[10] R. Pestman, R.M. Koster, A. van Duijne, J.A.Z. Pieterse, V. Ponec, Reactions of Carboxylic Acids on Oxides: 2. Bimolecular Reaction of Aliphatic Acids to Ketones, Journal of Catalysis, 168 (1997) 265-272.
[11] K.S. Kim, M.A. Barteau, Structure and composition requirements for deoxygenation, dehydration, and ketonization reactions of carboxylic acids on TiO2(001) single-crystal surfaces, Journal of Catalysis, 125 (1990) 353-375.
[12] J. Stubenrauch, E. Brosha, J.M. Vohs, Reaction of carboxylic acids on CeO2(111) and CeO2(100), Catalysis Today, 28 (1996) 431-441.
[13] H.-X. Mai, L.-D. Sun, Y.-W. Zhang, R. Si, W. Feng, H.-P. Zhang, H.-C. Liu, C.-H. Yan, Shape-Selective Synthesis and Oxygen Storage Behavior of Ceria Nanopolyhedra, Nanorods, and Nanocubes, The Journal of Physical Chemistry B, 109 (2005) 24380-24385.
[14] R. Si, M. Flytzani-Stephanopoulos, Shape and crystal-plane effects of nanoscale ceria on the activity of Au-CeO2 catalysts for the water-gas shift reaction, Angewandte Chemie, International Edition, 47 (2008) 2884-2887.
[15] J.J. Spivey, G.W. Roberts, K.M. Dooley, Catalysis of Acid/Aldehyde/Alcohol Condensations to Ketones, Catalysis, The Royal Society of Chemistry, Cambridge, 2004, pp. 293-319.
[16] H.C. Yao, Y.F.Y. Yao, Ceria in automotive exhaust catalysts : I. Oxygen storage, Journal of Catalysis, 86 (1984) 254-265.
[17] A. Trovarelli, Catalysis by Ceria and Related Materials, in: G.J. Hutchings (Ed.) Catalytic Science Series, Imperial College Press, 2002.

[18] P.A.H. Burroughs, Anthony F. Orchard, Geoffrey Thornton, Satellite studies in the x-ray photoelectron spectra of some binary and mixed oxides of lanthanum and cerium, Journal of the Chemical Society, Dalton Transactions, 17 (1976) 1686-1698.
[19] J.Z. Shyu, W.H. Weber, H.S. Gandhi, Surface characterization of alumina-supported ceria, The Journal of Physical Chemistry, 92 (1988) 4964-4970.
[20] J.Z. Shyu, K. Otto, W.L.H. Watkins, G.W. Graham, R.K. Belitz, H.S. Gandhi, Characterization of Pd/[gamma]-alumina catalysts containing ceria, Journal of Catalysis, 114 (1988) 23-33.
[21] D.R. Mullins, S.H. Overbury, D.R. Huntley, Electron spectroscopy of single crystal and polycrystalline cerium oxide surfaces, Surface Science, 409 (1998) 307-319.
[22] A.D. Murkute, J.E. Jackson, D.J. Miller, Supported mesoporous solid base catalysts for condensation of carboxylic acids, Journal of Catalysis, In Press, Corrected Proof.
[23] M.A. Hasan, M.I. Zaki, L. Pasupulety, Oxide-catalyzed conversion of acetic acid into acetone: an FTIR spectroscopic investigation, Applied Catalysis A: General, 243 (2003) 81-92.
[24] S. Bernal, G. Blanco, A.E. Amarti, G. Cifredo, L. Fitian, A. Galtayries, J. Martín, J.M. Pintado, Surface basicity of ceria-supported lanthana. Influence of the calcination temperature, Surface and Interface Analysis, 38 (2006) 229-233.
[25] L. Vivier, D. Duprez, Ceria-Based Solid Catalysts for Organic Chemistry, ChemSusChem, 3 (2010) 654-678.
[26] D.R. Lide, CRC Handbook of Chemistry and Physics in, CRC Press LLC, Boca Raton, 2003-2004.
[27] V.I. Yakerson, E.A. Feorovskaya, A.L. Klyachko-Gurvich, A.M. Rubinshtein, Vapor Phase Catalytic Ketonation of CH3COOH over Oxides of Quadrivalent Metals and BeO, Kinetika i Kataliz, 2 (1961) 907-915.
[28] A.M. Rubinshtein, A.A. Slinkin, V.I. Yakerson, E.A. Fedorovskaya, The reduction of CeO2 in the ketonization of ch3cooh, Russian Chemical Bulletin, 10 (1961) 2090-2092.
[29] Y. Yamada, M. Segawa, F. Sato, T. Kojima, S. Sato, Catalytic performance of rare earth oxides in ketonization of acetic acid, Journal of Molecular Catalysis A: Chemical, 346 (2011) 79-86.
[30] T. Arii, T. Taguchi, A. Kishi, M. Ogawa, Y. Sawada, Thermal decomposition of cerium(III) acetate studied with sample-controlled thermogravimetric-mass spectrometry (SCTG--MS), Journal of the European Ceramic Society, 22 (2002) 2283-2289.

5.7 Tables and figures

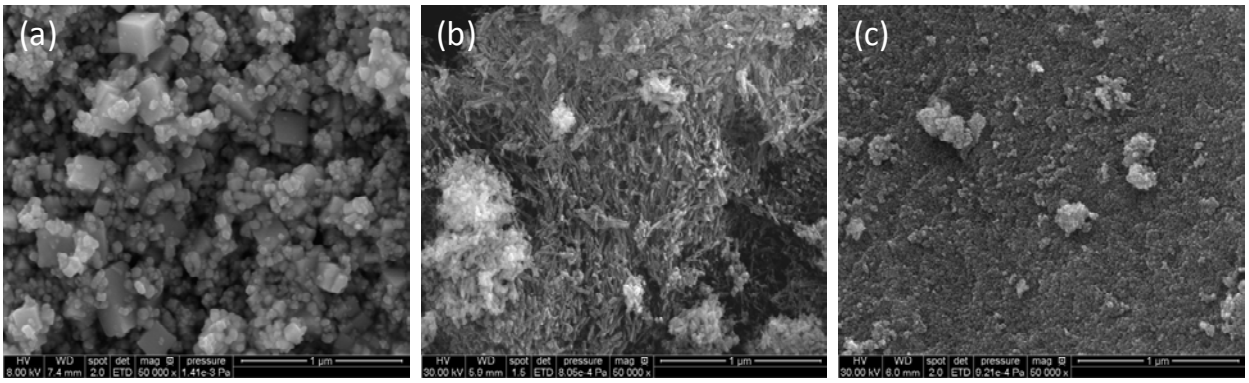

Figure 1. SEM images of fresh ceria (a) cubes, (b) rods, (c) polyhedra

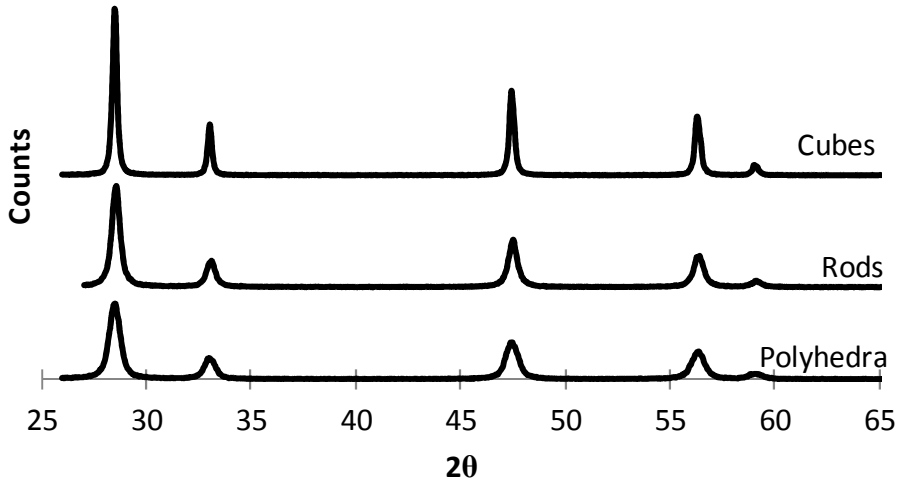

Figure 2. XRD plots of ceria nanocubes, rods, and polyhedra before reaction testing.

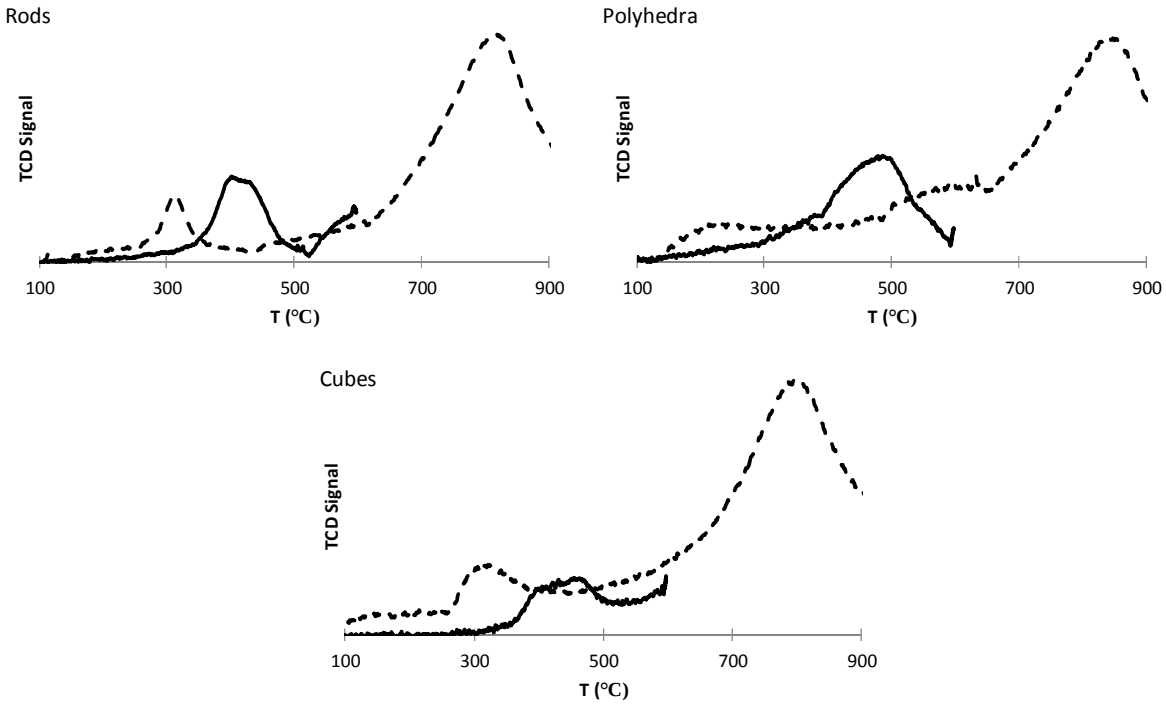

Figure 3. TPR of fresh ceria nanocubes, rods, and polyhedra. The solid line represents the first reduction step while the dotted line shows results from the second reduction.

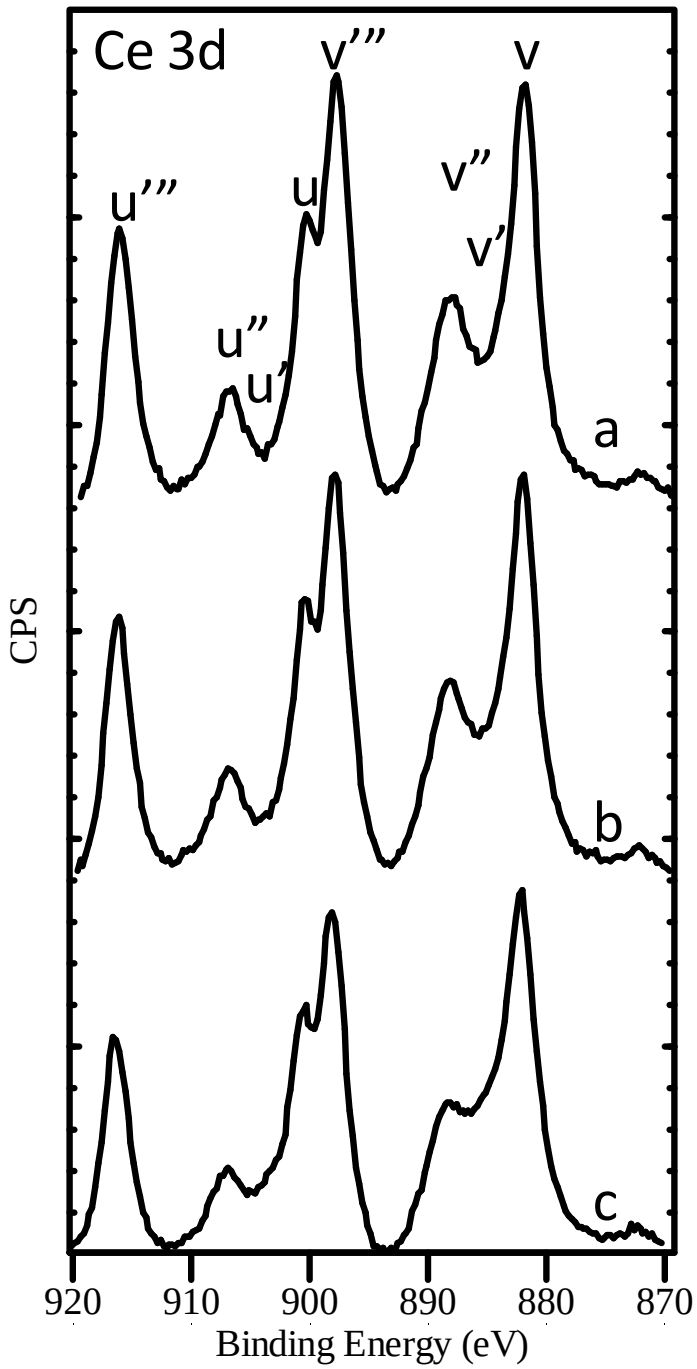

Figure 4. XPS spectra of fresh (a) nanocubes, (b) nanorods and (c) nanopolyhedra.

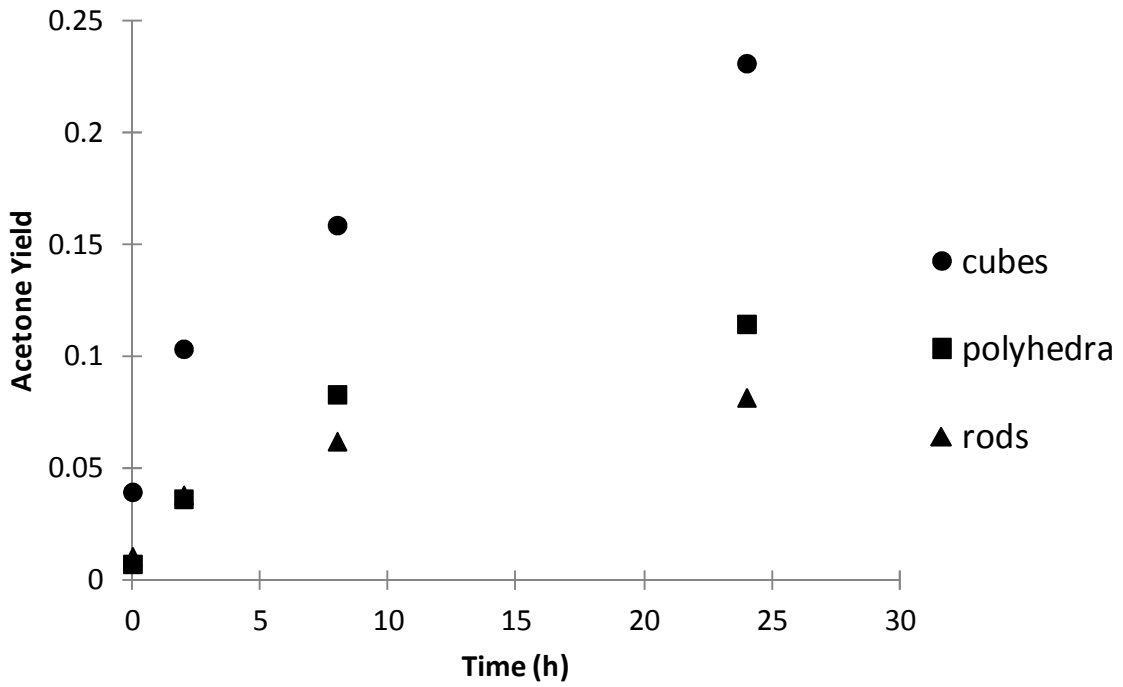

Figure 5. Acetic acid conversion during ketonization by 4 m^2 of ceria catalysts (230 °C, 60 bar).

Table 1. Initial rates for the condensed phase ketonization of acetic acid (230 °C, 60 bar, 0.15 g catalyst).

Catalyst	Rate (µmol/m²/h)	Rate (mmol/g/h)
Cubes	62	0.9
Rods	33	1.4
Polyhedra	29	1.2

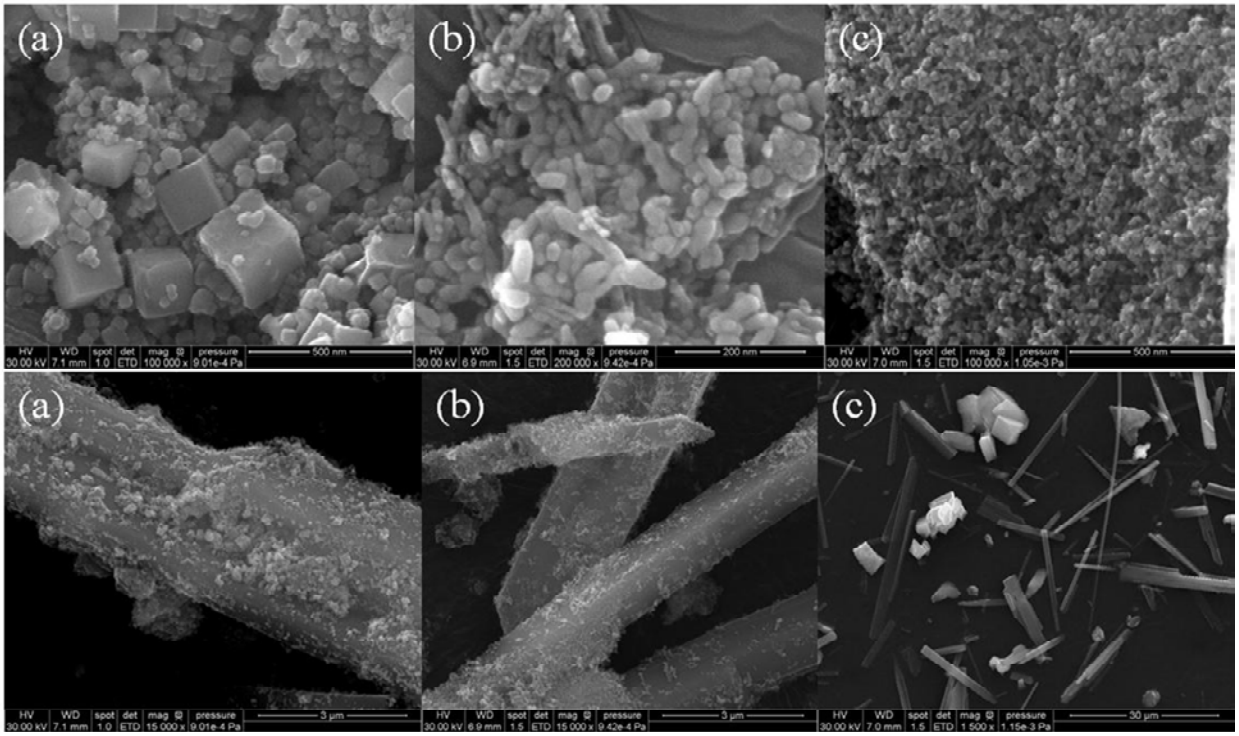

Figure 6. SEM images of nano-catalysts spent in 24 h reactions at higher (top) and lower (bottom) magnification (230 °C, 60 bar) (a) cubes, (b) rods, (c) polyhedra.

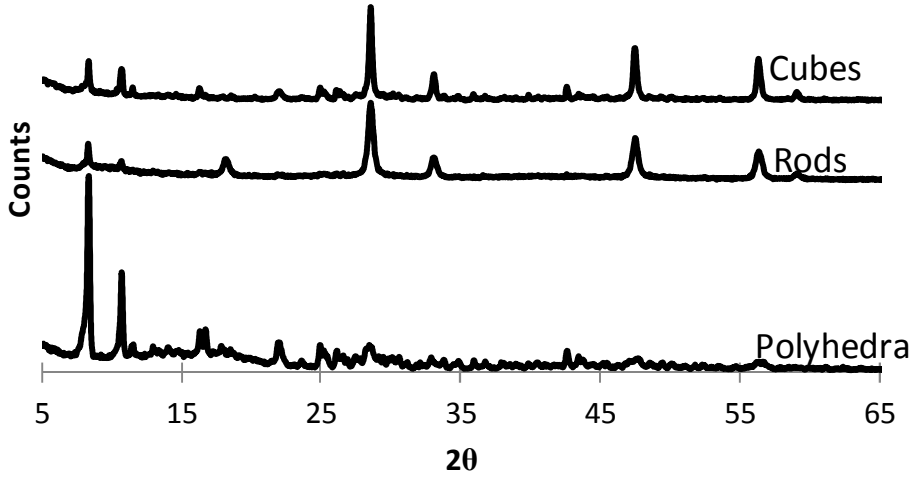

Figure 7. XRD patterns of spent (24h, 230 °C, 60 bar) ceria nanocatalysts in the condensed phase ketonization of acetic acid.

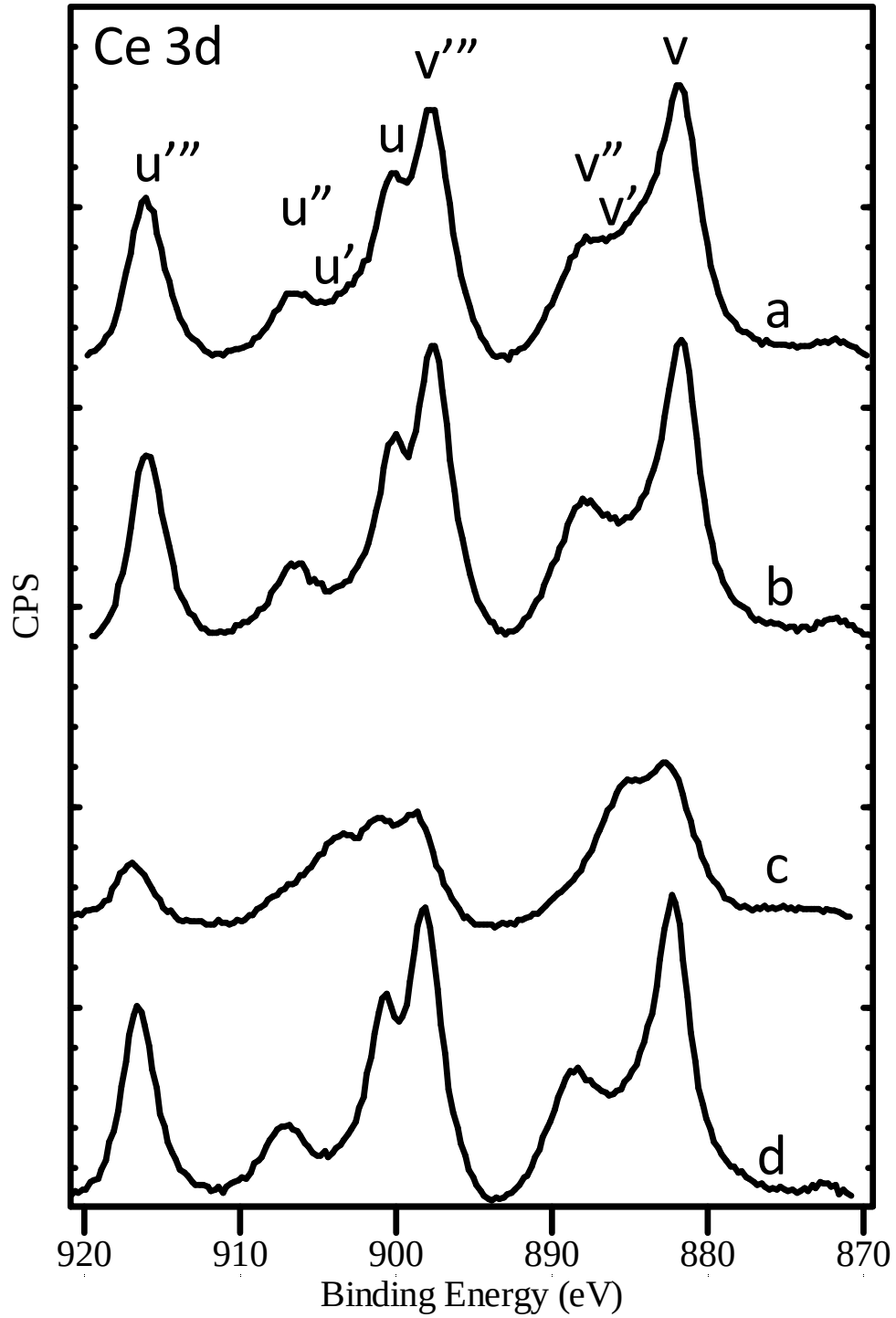

Figure 8. XPS results of spent ceria (a) nanocubes, (b) nanorods, and (c) nanopolyhedra after reaction in the condensed phase at 230 °C, 60 bar, 24 h. The control reaction (d) was performed in the same way as were the other reactions except no acetic acid was added to the reaction mixture.

Table 2. Gas phase reaction testing results of ceria nanocrystal materials (350 °C)

Catalyst	Pre reaction BET SA (m^2/g)	Post reaction BET SA (m^2/g)	CO_2 production (mmol/min/g cat)	CO_2 production (mmol/min/m^2)
Cubes	11	7	0.04	0.006
Rods	43	25	0.5	0.02
Polyhedra	44	8	0.2	0.03
Bulk	69	36	0.15	0.004

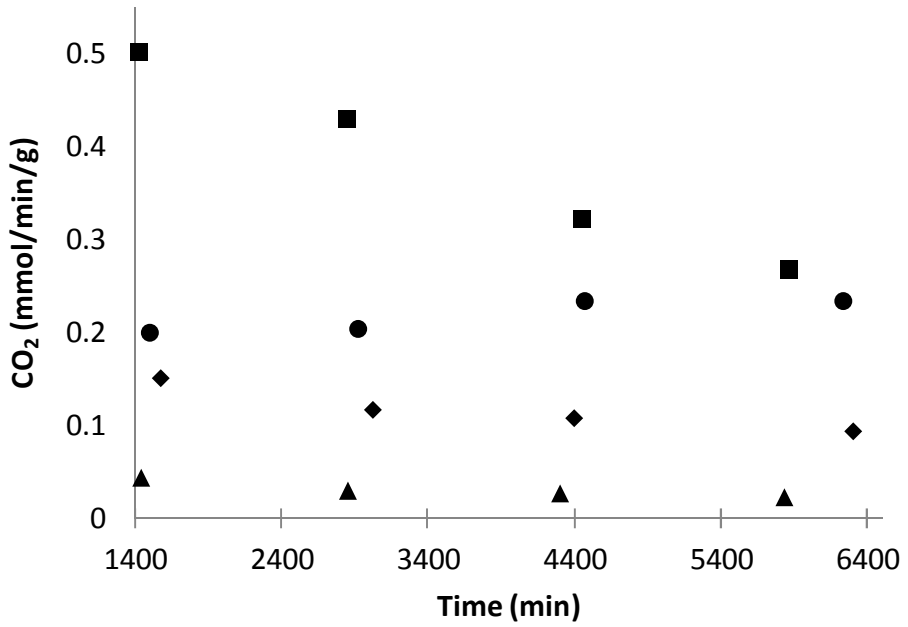

Figure 9. Deactivation with time on stream in the ketonization of acetic acid with ceria catalysts (■) rods, (●) polyhedra, (♦) bulk, (▲) cubes.

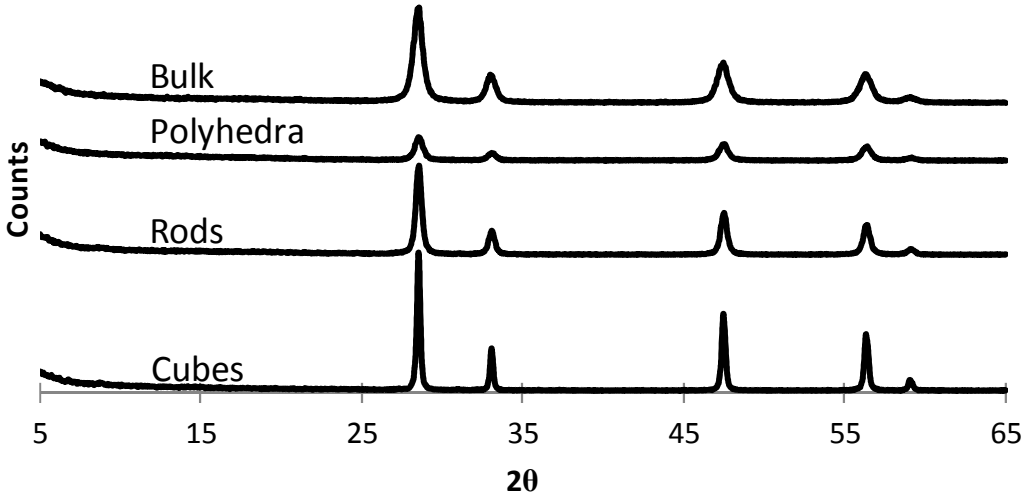

Figure 10. Post vapor phase reaction testing XRD images of spent ceria nanocrystals demonstrating maintenance of the original crystal structure.

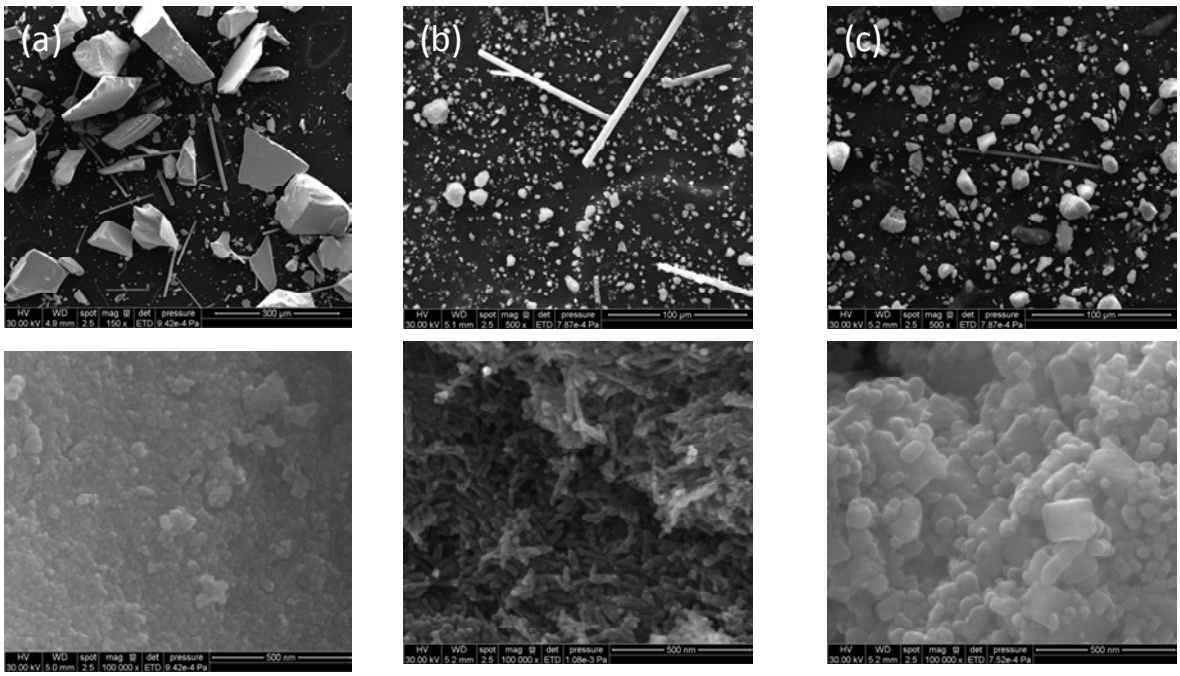

Figure 11. SEM images of the spent catalysts after vapor phase ketonization of acetic acid (a) polyhedra, (b) rods, (c) cubes.

Chapter 6

Insights into the ceria catalyzed ketonization mechanism for biofuels applications

A paper to be submitted to Journal of Catalysis

Ryan W. Snell[1] and Brent H. Shanks[1]

[1]Department of Chemical and Biological Engineering, Iowa State University

Authorship roles:

Snell: Primary author

Shanks: Principal investigator

Abstract

The ketonization of small organic acids is a valuable reaction for biorenewable applications. Ceria has long been used as a catalyst for this reaction. However, in both liquid and vapor phase conditions our work found that given the right temperature regime, cerium oxide—previously believed to be a stable catalyst for ketonization—can undergo bulk transformations. This, along with other literature reports, suggest that the long held belief of two separate mechanisms—for either bulk or surface ketonization reactions—may be of question. XPS, SEM, and TPD results supported the formation of metal acetates and explained the occurrence of cerium reduction as well as the formation of cerium oxide/acetate whiskers. After TG-MS and FTIR experiments a mechanism was proposed that can be applied to either surface or bulk reactions as well as with any active oxide catalyst.

6.1 Introduction

While a number of renewable energy alternatives such as solar and wind are increasingly being utilized, economic downturns have highlighted the potential difficulties that may be encountered while replacing a trillion dollar infrastructure built around liquid fuels. Therefore, in the near future, the creation of a renewable liquid fuel able to successfully make use of the current infrastructure would be extremely valuable. As biomass provides a renewable source of carbon, it is an attractive alternative to current petroleum use.

While there are a number of different techniques used for converting biomass to liquid fuels, fast pyrolysis has been increasingly discussed due to the simplicity of the process, direct creation of liquid bio-oil, and the flexibility of feedstock.[1] However, there are a number of undesirable characteristics of this oil such as a low pH and high oxygen content—both caused in part by its large quantity of small organic acids.[2] As the bio-oil contains a number of thermally unstable compounds, it would be preferred to perform condensed phase catalytic reactions so as to alleviate some of these difficulties.

One reaction that would be potentially beneficial is ketonization. The ketonization reaction has been attracting increasing attention for biorenewable fuel applications since Kunkes et al. reported its use during conversion of glucose to liquid fuels.[3] Regrettably the high temperatures, typically greater than 300 °C, utilized for the reaction make it impractical for condensed phase applications as would be preferred with bio-oil. Increasing catalyst activity is thus vital to obtaining reasonable liquid phase reaction conditions. To achieve this task, it would be helpful to have a good understanding of the reaction's fundamental chemistry. Unfortunately, despite recent advances, much about ketonization remains debated, including the catalyst mechanism[4] This is particularly true in regards to the reaction in the condensed phase. Here, our goal is to probe the ketonization of the model bio-oil compound

acetic acid in the condensed phase using ceria catalysts with the hope of gaining insight into the reaction mechanism.

6.2 Experimental section

6.2.1 Materials synthesis

Cerium oxide was made through thermal decomposition of cerium(III) nitrate hexahydrate (Aldrich 99.99%) at 600 °C in air using a Carbolite AAF 1100 muffle furnace. A 2 °C/min heating ramp to 600 °C was used after which the temperature was held steady for 3 h. After cooling, the ceria was finely powdered using a mortar and pestle before being kept in a dessicator.

A number of different cerium carboxylates were synthesized through reacting either cerium (III) nitrate hexahydrate (ROTH ≥99.5%) or cerium(III) carbonate hydrate (Aldrich 99.9%) with the respective acid-either acetic acid (Fluka 99.8%), propionic acid (AppliChem >99%), butyric acid (AppliChem ≥99%), isobutyric acid (Fluka ≥99.5%) or pivalic acid (Merck ≥99%). For cerium pivalate this consisted of first neutralizing the acid with ammonium hydroxide before mixing with the aqueous metal nitrate solution and adjusting the pH to 6-7 in a fashion similar to that proposed by Khudyakov.[5] The solution was then heated to 60 °C and stirred for a short time before being cooled and stirred overnight. Finally the carboxylate was filtered and dried at 110 °C in air. For cerium acetate, cerium propionate, and cerium isobutyrate, cerium carbonate was mixed directly with slight excess of the respective acid. This solution was then heated and stirred until the metal carboxylate gel was formed. After filtration the product was dried in air at 130 °C for 2 h.

6.2.2 Materials characterization

Thermogravimetric analysis of the metal carboxylates was performed on a Netzsch STA 449 Jupiter TGA-DSC under the flow of 70 mL/min argon with a ramp rate of 10 °C/min. Product evolution was evaluated with a connected mass spectrometer. BET surface area analysis was done on a Micromeritics ASAP 2020 at 77 K using N_2. Prior to testing the ceria was degassed at 100 °C. XPS was used for the measurement of cerium oxidation states and was executed on a Physical Electronics 5500 Multi-technique system using an Al Kα source and double sided tape for mounting. Peak binding energies were obtained by placing the binding energy of the C 1s peak to a location of 284.6 eV. XRD characterization of ceria catalysts both before and after reaction testing utilized a Siemens D-500 with a 0.15 detector slit and Cu Kα radiation. In-situ XRD tests involved use of a STOE theta-theta diffractometer with a scintillation counter and Cu Kα radiation. During the experiments the powdered sample was in an Anton Parr RK 900 high temperature reaction chamber. Scans during the tests were of a step size of 0.05 with a dwell time of 2s. Acetic acid vapors were led over the catalysts during these tests by bubbling 100 ml/min of He gas through acetic acid at 40 °C. SEM of materials used a FEI Quanta FE-SEM. TPD of spent ceria catalysts was done on a Micromeritics Autochem(II) Chemisorption Analyzer connected to a Microstar MS. The tests occurred using a 5 °C/min ramp from 80-700 °C under the flow of 20 ml/min argon. Finally FTIR transmission experiments were completed using a Bruker IFS 66 spectrometer. For cerium acetate tests, the sample was diluted in KBr, pressed into a self supporting wafer, and mounted in a heated quartz chamber under the constant flow of Ar. The sample was then dehydrated at 150 °C, cooled and the spectrum taken. A similar process was used for the in-situ cerium oxide FTIR experiments except the ceria was not diluted in KBr and was used by itself to form the wafer. The ceria wafer was then exposed to small amounts of acetic acid

vapor in flowing Ar at the given temperature and purged with pure Ar before cooling and taking the spectra.

6.2.3 Reaction testing

Reaction testing of the ceria catalyst was done at a variety of temperatures using 50 ml of toluene (Fisher 99.8%) as solvent, 1.0 g of acetic acid (Fisher 100%) or 1.7 g of pivalic acid (Aldrich 99%) as reactant, and ½ ml of 1,4 dioxane (Fisher 100%) as internal standard. The catalyst was then added along with the previously listed chemicals into a stainless steel Parr Series 4598 75 ml batch reactor. The reactor was subsequently pressurized with N_2 to 30-40 bar before heating in order to keep the reactants in the condensed phase. After pressurizing, the vessels were heated to the desired temperature while stirring at 400 rpm. A liquid nitrogen cold trap was used to collect samples and an Agilent 7890 GC-FID used for product analysis. Prior to characterization and after reaction, the catalysts were dried at 100 °C in air for 1 h.

6.3 Results and discussion

Before reaction testing, the ceria was characterized. It was found that the BET surface area of the synthesized cerium oxide was a relatively high 73 m^2/g. As demonstrated in Figure 1, XRD showed that the crystal structure of the catalyst was consistent with the cerianite form as expected. Agreeing with the XRD results, XPS showed that the cerium oxidation state consisted primarily of Ce^{4+} (Figure 2). SEM images (Figure 3) of the catalyst showed that the materials consist of non-uniformly shaped agglomerated crystals.

A large number of mechanisms have been discussed for the ketonization reaction.[6] It is our hope that through our work, the potential pathways for the reaction may be narrowed. For instance, a recent mechanism proposed the involvement of a radical

intermediate.[7] If this is true, toluene should act as an inhibitor since the radical likely would readily react with it. Therefore the use of toluene as a solvent should offer insight into the reaction mechanism. During the course of ceria catalyzed ketonization of acetic acid in toluene, small amounts of radical products like bibenzyl were found by GC-MS. However, as Figure 4 demonstrates, the ketonization reaction proceeded in toluene even at the comparatively low temperature of 230 °C, demonstrating that a radical intermediate is not likely. Exploring different reaction temperatures, it was found that at 150 °C, only traces of acetone were found after 24 h using an acid/ceria ratio of 5 while increasing the reaction temperature to 300 °C led to complete conversion in 30 minutes.

It has long been claimed that the ketonization reaction proceeds through different mechanisms depending on the catalyst used.[4, 8] For catalysts with a low metal-oxygen bond strength or low lattice energy, the reaction purportedly progresses through the formation of a bulk metal carboxylate which then acts as the working catalyst and whose thermal decomposition results in ketone production. In contrast, for catalysts with a high metal oxygen bond strength or large lattice energy, a surface catalyzed reaction is reported to promote the formation of acetone.[4] A comparison of lattice energies for potential ketonization catalysts can be observed in Table 1. However, there have been some conflicting reports with this simplified explanation. For instance, recently Mekhemer et al. published findings demonstrating that MgO, claimed to have a high lattice energy, underwent transformations to a bulk acetate during room temperature exposure to acetic acid.[9] This apparent deviation from the earlier explained two-pathway model was proposed to occur in this particular instance due to the basicity of the oxide. Moreover, it was found that at higher reaction temperatures the MgO promoted the reaction through surface adsorption.[9] It was

therefore claimed that the mechanism was different for low temperature ketonization—which purportedly progressed through the pyrolytic route—than at high temperatures which catalyzed the reaction through both acid and base surface sites.[9] However, as ceria is a superior ketonization catalyst to MgO, further focus on how the mechanism progresses on it is warranted.[10]

A number of manuscripts have reported the supposed stability of ceria as a catalyst in ketonization through post reaction characterization by XRD.[8, 11, 12] However, in the current work, post reaction XRD characterization of the ceria catalyst spent at 230 °C demonstrated that the oxide underwent bulk restructuring during the course of reaction. Further reactions were run to see if this crystal structure change would occur at lower temperatures as was found by Mekhemer et al. with MgO. Interestingly though, ceria's fluorite phase was maintained to temperatures lower than 200 °C, demonstrating that it is unlikely bulk absorbance of acid occurs at these temperatures. Crystal structure was also preserved at temperatures ~300 °C. Therefore as shown in Figure 5, there appears to be an intermediate temperature at which ceria restructuring occurs. This result is of note as it's been claimed that catalysts with metal-oxygen bonds weak enough to undergo bulk carboxylate formation are of low activity for ketonization.[13] Our results appear to contradict this statement as ceria, one of the most active ketonization catalysts, was found to undergo bulk crystal changes. Running a control, it was determined that it was unquestionably the addition of acid that caused the bulk changes as opposed to a solvent interaction.

In order to confirm that bulk metal acetate is indeed what is forming during the course of reaction, a temperature programmed decomposition (TPD) experiment was

performed in which the spent catalyst was heated at a specific rate and the evolved products measured through the use of a MS. As shown by Figure 6, acetone was evolved in two steps beginning ~250 °C and reaching a maximum ~300 °C, perhaps not coincidently near temperatures that the ketonization reaction tends to readily occur. For comparison, the same process was performed with purchased cerium acetate hydrate. Figure 7, demonstrates that a similar evolution of products came from cerium acetate and that acetone evolution appeared to occur at roughly the same temperature. However, there does appear to be 3 steps during which acetone was produced as opposed to two in the spent catalyst. This difference may occur as the ceria catalyst has not fully transformed into bulk acetate and is instead in an intermediate cerium oxyacetate form. As the catalyst spent at a temperature of 300 °C did not show the bulk restructuring during the course of reaction it would be of interest to see if this spent catalyst would also form acetone at similar temperatures. Figure 8 gives evidence that this is indeed the case.

XRD of cerium acetate hydrate did not result in a diffractogram similar to that found of the catalyst treated at 230 °C demonstrating again that during the course of our reactions ceria has not been transformed to a pure carboxylate but rather an intermediate form. Use of cerium acetate hydrate as catalyst in the reaction, or for that matter even cerium carbonate hydrate, did however result in a diffractogram very similar to that of our spent catalyst, lending more evidence to the formation of a metal-carboxylate intermediate during ceria catalyzed ketonization (Figure 9).

SEM imaging of the spent ceria catalysts demonstrated the formation of large rods or whiskers (Figure 10). Again, use of a control showed that this phenomenon is not the result of growth promoted by the solvent during reaction conditions but rather through interaction

with the acetic acid. Interestingly, after using cerium acetate hydrate as a catalyst, it too displayed the formation of rods, but in its case these were greatly aggregated. Therefore SEM results complemented our previous XRD and TPD findings in that some form of metal carboxylate is being created at these intermediate temperatures.

As ketonization of small organic acids has been almost exclusively performed in the gas phase due to the necessity of high temperatures, it is of importance to determine if the new findings presented here are a result of a condensed phase environment or if they are more generally applicable to the reaction as a whole. To probe this question, in-situ XRD was used in which acetic acid vapors were led over the ceria catalyst at different temperatures while continuously scanning over a specified 2θ range. As evidenced by Figure 11, different temperature regimes, in regards to acetate formation in the bulk of the catalyst, occurred in the vapor phase showing that what was seen in the condensed phase is a more global occurrence. One thing to note from Figure 11 is that at 300 °C, the diffractogram has not reverted back to the original ceria form as may be expected from our results in Figure 5. To understand this, a condensed phase reaction was performed at 230 °C with 1.0 g of acetic acid and 0.20g of ceria for 24 h. After reaction this catalyst was separated, analyzed by XRD, and then the spent ceria catalyst was baked in toluene for 1 h at 300 °C. Following this treatment, the ceria was again separated and examined by XRD. These results were then compared to catalyst spent in a reaction at 300 °C for 30 min with 1.0 g of acetic acid, and 0.2 g of ceria. Figure 12 shows that analogous results were found in the condensed phase as were discovered in the vapor phase. For both phases, after initial formation of metal carboxylates in the bulk, the ceria did not revert back to its original crystal structure at 300 °C. However, as shown in Figure 5 and Figure 13, in both vapor and liquid phase conditions,

exposure to acid only at 300 °C resulted in apparent bulk stability. As research reporting that ceria is a stable oxide for ketonization, hence promoting the reaction on the surface, usually test at temperatures near or greater than 300 °C, this bulk transformation isn't noticed.[8, 11]

From our work, it is apparent that the lack of carboxylate formation in the bulk at high temperatures is clearly not the result of metal-oxygen bond strength differences. The discovery thus shows that this material property alone does not dictate the route ketonization proceeds through. Furthermore, it was recently reported that oxides with even higher lattice energies than ceria such as La_2O_3 and Nd_2O_3 underwent partial bulk acetate formation during ketonization of acetic acid while ceria did not.[11] Again, ceria was found to be stable—likely due to the high temperature of reaction. Perhaps it is worth contemplating if there are even two different pathways to begin with. For over 150 years it has been known that the pyrolysis of select metal acetates can form acetone.[14] But, perhaps hard evidence that the surface mechanism is catalytic and different than the bulk thermal decomposition mechanism is lacking. Possibly, the surface catalytic pathway is just the pyrolysis of surface carboxylates. This theory would explain the XRD observations in Figure 5. At high temperatures metal carboxylate formation in the bulk would not occur due to thermal instability at these conditions. Moreover, properties of the particular oxide—potentially including traits such as lattice energy—could prevent the formation of carboxylates in the bulk until there is enough energy to break catalyst M-O bonds. If it takes enough energy to break the M-O bonds such that the temperatures needed for carboxylate formation in the bulk are higher than the value at which the metal-carboxylate decomposes, then disruption of the crystal structure will not be observed. However, this does not mean that the actual mechanism is different. Metal carboxylate formation would still occur on the surface or

depending on transport limitations, possibly even through the first few atomic layers. After formation, these carboxylates would pyrolytically decompose to form the ketone. Hence in either bulk or surface promoted cases, the intermediate species would be a metal carboxylate. A diagram explaining this theory is shown in Figure 14. Similar processes likely occur with other metal oxide catalysts but with different temperature regimes. For some oxides like MgO, the material apparently forms the bulk acetate near room temperature and decomposes at >360 °C.[9] However, for oxides like alumina, it is likely that the metal acetate would decompose at temperatures below at which there is enough energy to break the Al-O bonds and destroy the bulk crystallinity. Regardless, the mechanism would be the same for the various oxides. This concept is graphically demonstrated in Figure 15. If an oxide has a high activation energy for the formation of carboxylates in the bulk (E_{a1}), and a comparatively low activation energy for the decomposition of that intermediate (E_{a2}), the metal carboxylate will not be effectively observed. However, if the activation energy for formation of the metal carboxylate is quite low in comparison to the decomposition, the carboxylate will be easily found. A third option, representing ceria, is if the two energies are quite similar in which case there will be a narrow window in which the carboxylate phase in the bulk can be observed.

It has been commonly reported that an α-hydrogen is necessary for ketonization to proceed thus lending support to the formation of a ketene like intermediate.[4, 7] To see how this discovery fits into our theory of thermal carboxylate decomposition, the ketonization of pivalic acid (trimethylacetic acid) was attempted in the condensed phase. Consistent with literature, none of the expected product of ketonization (2,2,4,4 tetramethyl-3-pentanone) was found at temperatures of up to 315 °C for 24 h runs (1.7 g pivalic acid, 0.2 g catalyst). Moreover, when the spent ceria catalyst was separated from the reaction mixture through the

use of vacuum filtration and analyzed by XRD at temperatures up to 300 °C, the original cerianite structure was maintained. However, when ketonization was attempted at 315 °C, it was discovered that no heterogeneous catalyst remained post reaction. After drying off the solvent and reactant with air, a powder precipitated out. Averaging over four EDS spectra, the contents of Ce, C, and O in the powder were found to be 39, 43, and 17 weight % respectively. This composition is roughly that of cerium(III) pivalate (34% Ce, 43% C, 23% O). Pivalic acid's electron donating methyl groups, sterics, or lack of detecting solubilized catalyst could all explain the higher temperature necessary for discovery of bulk carboxylates. SEM images of the spent ceria catalyst from reaction did not demonstrate the production of the rod shaped ceria as was evident after reactions with acetic acid (Figure 16). This may be expected as apparently cerium pivalate is readily soluble in toluene while cerium acetate is not. XPS of this sample (Figure 17) showed the Ce^{4+} state had been fully reduced in the course of pivalate formation. This result may explain some reports of cerium reduction during the course of ketonization by demonstrating that reduction of the catalyst occurs during carboxylate creation and not necessarily evolution or further reactions of the ketone.[15, 16] This makes sense as for our experiments the spent catalyst was dried at 100 °C in air therefore likely oxidizing any reduced oxide that had formed as a result of any side reactions. However, the formation of cerium carboxylates could stabilize the material in the 3+ state and would not decompose in air at the low temperature used for drying.

The above mentioned experiments demonstrated that on cerium oxide no ketonization of pivalic acid occurred at temperatures up to 315 °C in the condensed phase. This result lends credence to the claim that an α-hydrogen is necessary. Again, our proposed mechanism, shown in Figure 14 for acetic acid ketonization, doesn't imply that it is

necessary to have an α-hydrogen, but only enough energy to thermally decompose the metal carboxylate formed either on the surface or throughout the bulk. If this theory is to be true, it must require higher temperatures to thermally decompose cerium pivalate than the corresponding acetate. As it has been shown that branching and thus a loss in the number of α-hydrogen atoms for a given acid compound decreases its activity[7] in the ketonization reaction, the thermal stability of metal carboxylates should increase in the series of acetate < propionate < isobutyrate < pivalate. Figure 18 shows that expected order of thermal stability is exactly what was found through the series of TG-MS experiments. Substitution of methyl groups for the α-hydrogen dramatically increased the stability of the carboxylate. Cerium acetate, propionate, and isobutyrate decomposed and appeared to form their corresponding ketone. However it is difficult to probe this ketone formation for cerium pivalate as it wasn't pyrolyzed until such a high temperature that it is likely if the ketone was formed it would have decomposed immediately. These results show that it is possible that the necessity for an α-hydrogen may be related to a pyrolytic more than a catalytic mechanism.

The question of how the ketonization reaction occurs on a more molecular scale than demonstrated by Figure 14 must now be addressed. Kinetic modeling have shown that Langmuir-Hinshelwood like kinetics result in a good fit which would be supporting our belief that two adsorbed species are what is reacting.[17, 18] Carboxylate species can bind with metal cations in a number of different confirmations.[19] This type of binding may influence the ease at which the intermediate metal acetate is thermally decomposed and is therefore desirous to know. Metal acetate infrared spectra and its connection to carboxylate coordination have previously been studied.[20] Differences in carboxylate bond symmetry occur depending on the type of binding—examples being unidentate, bidentate, or ionic.

These differences create varying locations for $\upsilon_{asym}(CO_2)$ and $\upsilon_{sym}(CO_2)$ thus changing the $\Delta_{asy\text{-}sym}$ values and potentially allowing for determination of carboxylate coordination.[20, 21] Some reports have shown that while there is some value in this method, caution should still be used so as to not reach unfounded conclusions [21-23]. Thus our assessments of the spectra will be quite generalized. The FTIR spectrum of cerium acetate after heating to 230 °C, is shown in Figure 19 along with the difference spectra of cerium oxide after exposure to small amounts of acetic acid vapor at either 230 °C or 300 °C. It is evident from the figure that while only one set of peaks appeared for cerium acetate, the asymmetric peak was split for the ceria compounds. From peak maxima, it was determined that $\Delta_{asy\text{-}sym}$=153 for the acetate, $\Delta_{asy\text{-}sym}$=109/129 for the 230 °C exposed ceria and $\Delta_{asy\text{-}sym}$=104/121 for the 300 °C ceria exposed to the acid. The acetate value agrees quite well with the previously reported $\Delta_{asy\text{-}sym}$ of 150 for cerium acetate hydrate while the $\Delta_{asy\text{-}sym}$ for ceria exposed to acetic acid at 300 °C is very close to the $\Delta_{asy\text{-}sym}$ of 105 determined by Hasan et al. after exposure of their ceria catalyst to acetic acid at the same temperature [12, 22] According to Deacon and Phillips generally $\Delta_{asy\text{-}sym}$>200 cm^{-1} corresponds to unidentate binding while $\Delta_{asy\text{-}sym}$ <150 cm^{-1} corresponds to bridging or chelating coordination and $\Delta_{asy\text{-}sym}$<105 cm^{-1} is typically more connected to chelating.[21] While cerium acetate is reported to have bridging carboxylate bonds, according to Stubenrauch et al, it is unlikely that acetic acid on the surface of ceria could coordinate in a bridging fashion as the bond length between Ce cation pairs is too great.[21, 24] Therefore one possibility is that the acid is binding in a chelating fashion on the surface of ceria. While ceria can expose crystallographic facets of {111}, {100}, and {110} typically the {111} surface is prevalent due to its enhanced stability.[25] As the ideal termination of the {111} surface exposes only cerium with one dangling bond, it

seems unlikely that a chelating coordination occurs without surface reconstruction. However, reconstruction of the surface seems quite feasible as Figure 5 shows even bulk crystallite changes can occur given the right conditions.

Carboxylate binding modes may explain some of the phenomena observed with the ceria catalysts during the course of reaction testing. Figure 10 demonstrated that as ceria began to form a bulk carboxylate, the overall macro structure advanced to whisker shapes. The bridging binding of cerium acetate could facilitate this type of elongation while chelating would not. The different form of metal carboxylate coordination may also help explain the slight differences in Figure 6, Figure 7 and Figure 8 with acetate and catalyst used at different temperatures. Ceria used at 230 °C, as would therefore be expected, decomposes in a pattern more closely resembling cerium acetate than does ceria used at 300 °C since the high temperature prohibits bulk acetate formation.

As described earlier, since ketonization readily occured in toluene, it is likely that radicals are not intermediates in the reaction. Since the reaction is assumed to proceed through the pyrolysis of either bulk or surface cerium carboxylates, this may be somewhat surprising as radical species are common in pyrolytic processes.[26] However, the very common pyrolytic elimination reaction does seem to explain much of our findings as well as many of those in literature. The mechanism as proposed in Figure 20 first involves the abstraction of an α-proton by a carboxyl group bound to the metal. Surface basic sites in a cerium oxyacetate or oxide may also perform this abstraction when available. This difference between the acetate/oxyacetate/oxide system may explain the enhanced stabilities of metal carboxylates observed in Figure 11 and Figure 12. The step would also explain the number of reports claiming the necessity of an α-hydrogen. Branched carboxylates would have greater

stability (Figure 18) as the added substituents are electron donors and thus lower the acidity. The mechanism proceeds through the formation of a six-membered ring intermediate before the simultaneous formation of CO_2 and acetone agreeing with Figure 6, Figure 7, and Figure 8. Water and carbon dioxide have been commonly cited as inhibitors for the ketonization reaction.[17] This would be logical for the proposed mechanism as water would hydrolyze the carboxylate bonds and carbon dioxide would competitively bind metal sites either in the bulk or on the surface. It should be noted that the proposed mechanism is somewhat similar to that of Pestman et al. in that a proton is initially removed from the α-carbon on the molecule whose carboxylate group will eventually form carbon dioxide. However Figure 20 also alleviates concerns that Nagashima et al. expressed about Pestman et al.'s mechanism in that our mechanism has the C-C cleavage occurring in the same step as ketone production thus prohibiting side products formation such as methanol.[7] It is important to emphasize that the proposed mechanism can be generalized to any type of catalyst as well as occur on a surface or throughout the bulk of the respective catalyst. Differences seen between catalysts can be explained through the formation of different types of carboxylate coordination as well as to the electronegativity of the respective metal creating discrepancies with the ease in which the C-C bond is broken. Strength of M-O bonds in the metal oxide are important as well in that strong M-O bonds will make it difficult to form the needed metal carboxylate groups while very weak M-O bonds may result in the formation of very thermally stable metal carboxylates.

6.4 Conclusions

Characterization techniques such as XPS, SEM, FTIR, and XRD of fresh and spent catalysts were found to be necessary to explain some of the phenomena—such as cerium

reduction and morphology changes—seen here as well as in previous reports with ketonization. Degradation of ceria's crystal structure was found to be dependent on the temperature regime used for the ketonization reaction. Therefore the long held belief that ketonization occurs through multiple catalytic routes based upon observance of a bulk carboxylate phase appears to be of question. A mechanism involving the coupling of two carboxylate species-either on the surface or throughout the bulk can explain a number of the phenomena reported in this paper as well as in other's previous work. While the proposal that pyrolytic decomposition of carboxylates is the sole mechanism for ketonization may appear to limit the ability of research to further develop effective catalysts for the reaction it is our belief that this is not the case. Different materials will result in different forms of carboxylate binding, CO_2 and H_2O inhibition, ability to form the metal carboxylate, and temperature of decomposition. Therefore further investigations into ketonization is warranted—especially in regards to more complex systems like supported or mixed metal oxides.

6.5 Acknowledgements

This research was funded by NSF PIRE grants. Jim Anderegg's help with XPS is much appreciated. Dan Weis, an ISU undergraduate was involved in reaction testing of materials.

6.6 References

[1] A.V. Bridgwater, Review of fast pyrolysis of biomass and product upgrading, Biomass and Bioenergy, 38 (2012) 68-94.
[2] S. Czernik, A.V. Bridgwater, Overview of Applications of Biomass Fast Pyrolysis Oil, Energy & Fuels, 18 (2004) 590-598.
[3] E.L. Kunkes, D.A. Simonetti, R.M. West, J.C. Serrano-Ruiz, C.A. Gartner, J.A. Dumesic, Catalytic Conversion of Biomass to Monofunctional Hydrocarbons and Targeted Liquid-Fuel Classes, Science, 322 (2008) 417-421.
[4] R. Pestman, R.M. Koster, A. van Duijne, J.A.Z. Pieterse, V. Ponec, Reactions of Carboxylic Acids on Oxides: 2. Bimolecular Reaction of Aliphatic Acids to Ketones, Journal of Catalysis, 168 (1997) 265-272.

[5] M. Khudyakov, Cerium(III) Pivalate [Ce(Piv)3(HPiv)3]2: Synthesis, Crystal Structure, and Thermal Stability, Russian journal of coordination chemistry, 28 (2002) 521.
[6] S. Rajadurai, Pathways for carboxylic acid decomposition on transition metal oxides., Catalysis Reviews-Science and Engineering, 36 (1994) 385-403.
[7] O. Nagashima, S. Sato, R. Takahashi, T. Sodesawa, Ketonization of carboxylic acids over CeO2-based composite oxides, Journal of Molecular Catalysis A: Chemical, 227 (2005) 231-239.
[8] V.I Yakerson, E.A. Fedorovskaya, A.L. Klyachko-Gurvich, A.M. Rubinshtein, Vapor Phase Catalytic Ketonation of CH3COOH over Oxides of Quadrivalent Metals and BeO, Kinetika i Kataliz, 2 (1961) 907-915.
[9] G.A.H. Mekhemer, S.A. Halawy, M.A. Mohamed, M.I. Zaki, Ketonization of acetic acid vapour over polycrystalline magnesia: in situ Fourier transform infrared spectroscopy and kinetic studies, Journal of Catalysis, 230 (2005) 109-122.
[10] M. Glinski, J. Kijenski, A. Jakubowski, Ketones from monocarboxylic acids: Catalytic ketonization over oxide systems, Applied Catalysis A: General, 128 (1995) 209-217.
[11] Y. Yamada, M. Segawa, F. Sato, T. Kojima, S. Sato, Catalytic performance of rare earth oxides in ketonization of acetic acid, Journal of Molecular Catalysis A: Chemical, 346 (2011) 79-86.
[12] M.A. Hasan, M.I. Zaki, L. Pasupulety, Oxide-catalyzed conversion of acetic acid into acetone: an FTIR spectroscopic investigation, Applied Catalysis A: General, 243 (2003) 81-92.
[13] K.M. Dooley, Catalysis of Acid/Aldehyde/Alcohol Condensations to Ketones, in: J.J.S.a.G.W. Roberts (Ed.) Catalysis, The Royal Society of Chemistry, Cambridge, 2004, pp. 293-319.
[14] C. Friedel, Ueber s. g. gemischte Acetone, Justus Liebigs Annalen der Chemie, 108 (1858) 122-125.
[15] A.M. Rubinshtein, A.A. Slinkin, V.I. Yakerson, E.A. Fedorovskaya, The reduction of CeO2 in the ketonization of ch3cooh, Russian Chemical Bulletin, 10 (1961) 2090-2092.
[16] A. Gangadharan, M. Shen, T. Sooknoi, D.E. Resasco, R.G. Mallinson, Condensation reactions of propanal over CexZr1-xO2 mixed oxide catalysts, Applied Catalysis A: General, 385 (2010) 80-91.
[17] C.A. Gaertner, J.C. Serrano-Ruiz, D.J. Braden, J.A. Dumesic, Catalytic coupling of carboxylic acids by ketonization as a processing step in biomass conversion, Journal of Catalysis, 266 (2009) 71-78.
[18] S. Rajadurai, J.C. Kuriacose, Catalytic activity of the 1:1:1 Zn, Cr and Fe mixed oxide: Mechanistic study of the ketonization of acetic acid, Materials Chemistry and Physics, 16 (1987) 17-29.
[19] R.C. Mehrotra, and R. Bohra, Metal Carboxylates, Academic Press, London, 1983.
[20] K. Nakamoto, J. Fujita, S. Tanaka, M. Kobayashi, Infrared Spectra of Metallic Complexes. IV. Comparison of the Infrared Spectra of Unidentate and Bidentate Metallic Complexes, Journal of the American Chemical Society, 79 (1957) 4904-4908.
[21] G.B. Deacon, R.J. Phillips, Relationships between the carbon-oxygen stretching frequencies of carboxylato complexes and the type of carboxylate coordination, Coordination Chemistry Reviews, 33 (1980) 227-250.
[22] D.A. Edwards, R.N. Hayward, Transition metal acetates, Canadian Journal of Chemistry, 46 (1968) 3443-3446.
[23] G.B. Deacon, F. Huber, R.J. Phillips, Diagnosis of the nature of carboxylate coordination from the direction of shifts of carbon□oxygen stretching frequencies, Inorganica Chimica Acta, 104 (1985) 41-45.
[24] J. Stubenrauch, E. Brosha, J.M. Vohs, Reaction of carboxylic acids on CeO2(111) and CeO2(100), Catalysis Today, 28 (1996) 431-441.
[25] M. Baudin, M. Wójcik, K. Hermansson, Dynamics, structure and energetics of the (111), (011) and (001) surfaces of ceria, Surface Science, 468 (2000) 51-61.

[26] M. S.C, Chapter 2 The Chemistry of the Pyrolytic Process, in: C.M. Serban (Ed.) Techniques and Instrumentation in Analytical Chemistry, Elsevier, 2010, pp. 7-48.
[27] D.R. Lide, CRC Handbook of Chemistry and Physics in, CRC Press LLC, Boca Raton, 2003-2004.

6.7 Tables and figures

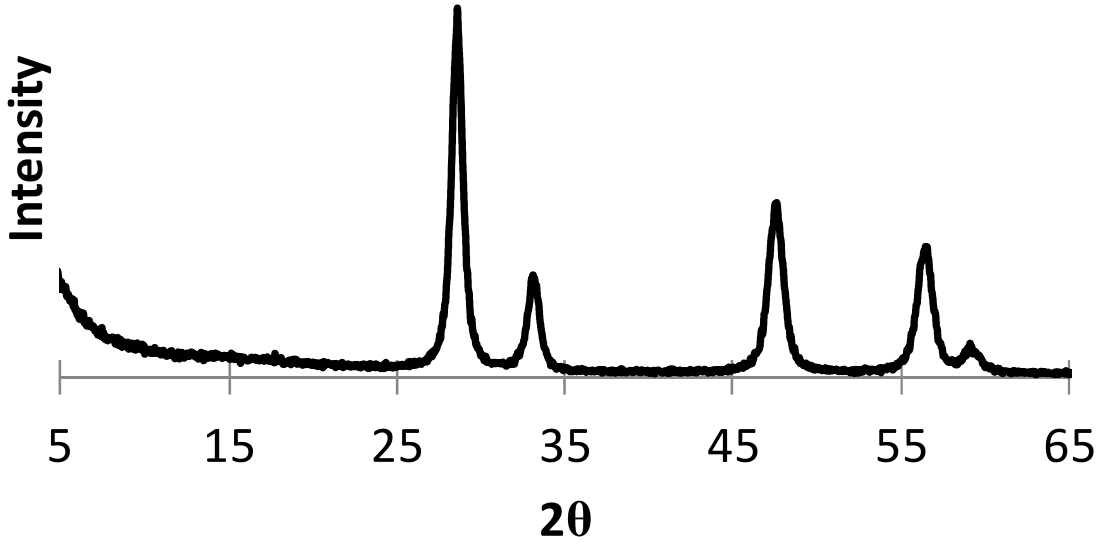

Figure 1. XRD profile of the ceria catalyst demonstrating cerianite structure.

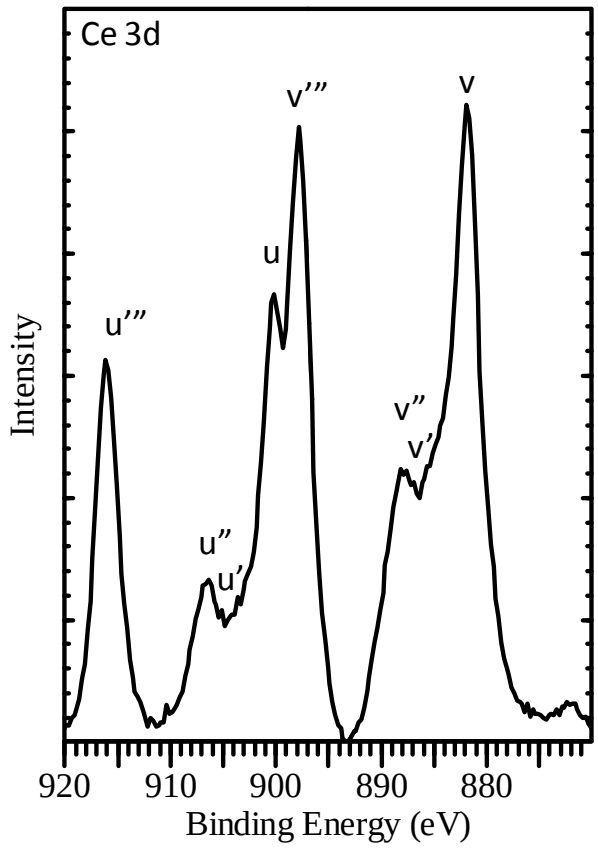

Figure 2. XPS of the ceria catalyst before reaction testing demonstrating the prevalence of the 4+ cerium oxidation state.

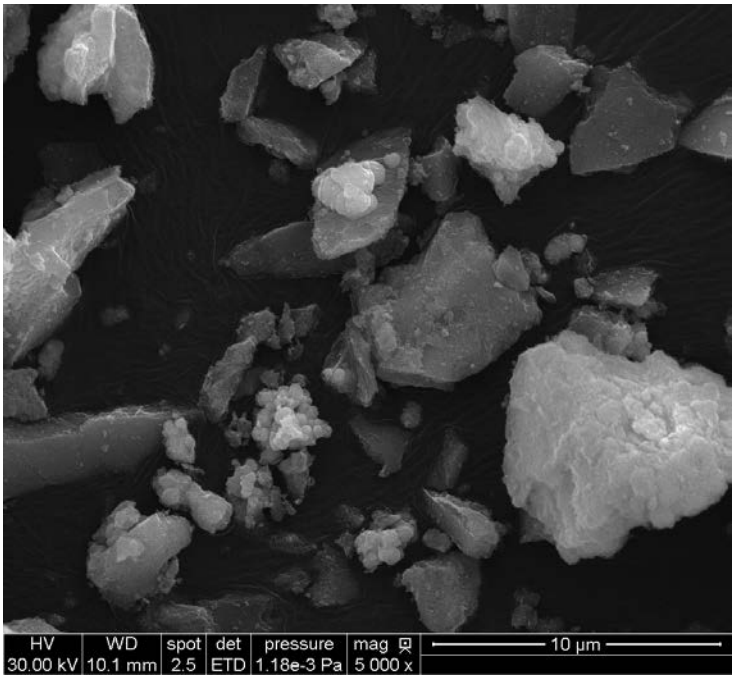

Figure 3. SEM image of ceria catalysts showing a non-uniform macro morphology.

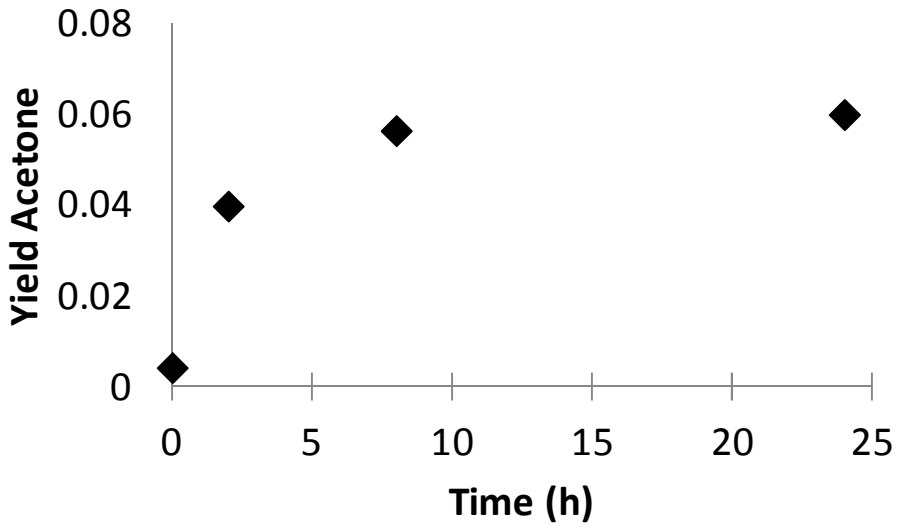

Figure 4. Ketonization of acetic acid indicating that the reaction can proceed at low temperatures and with toluene solvent(230 °C, 50 ml toluene, 1.0g acetic acid, 0.055 g ceria).

Table 1. Lattice energies of potential ketonization catalysts.[27]

Material	Lattice Energy (kJ/mol)
Al_2O_3	15916
Cr_2O_3	15276
MnO_2	12970
TiO_2	12150
ZrO_2	11188
CeO_2	9627
BeO	4514
ZnO	4142
MgO	3795
PbO	3520
$CaCO_3$	2804

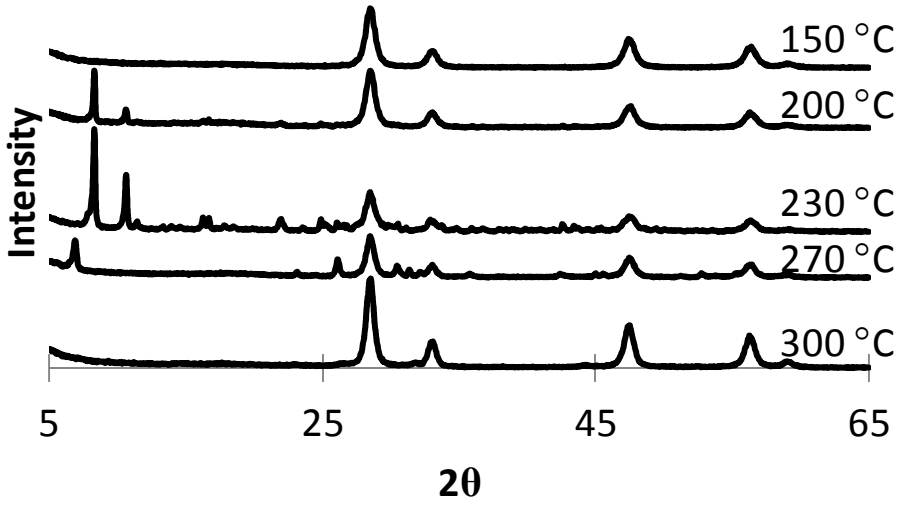

Figure 5. XRD figures of spent ceria catalysts at different temperatures in the ketonization of acetic acid (1.0 g acetic acid, 24 h, 0.20 g catalyst).

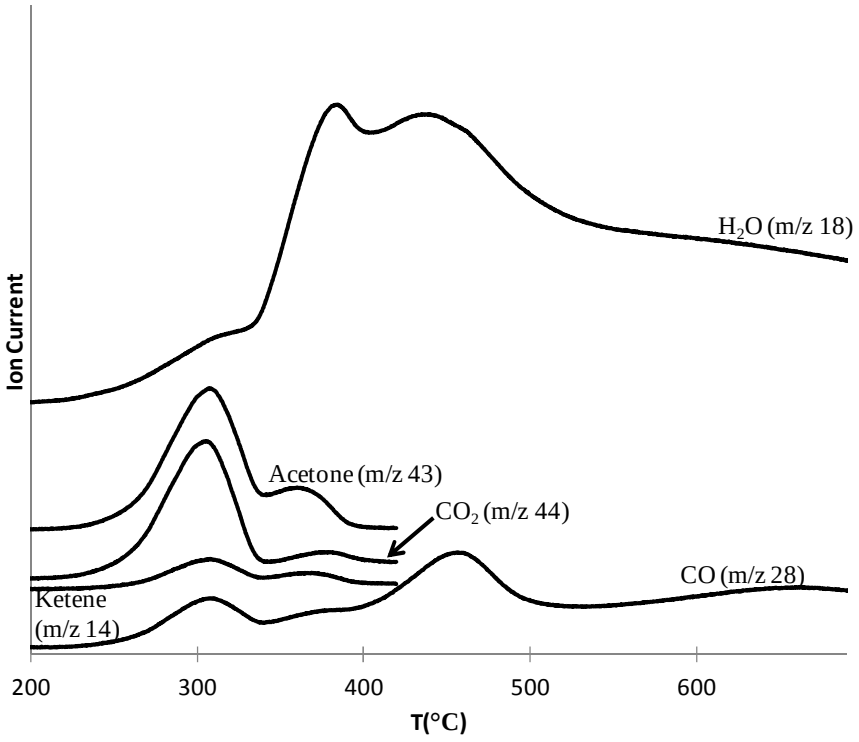

Figure 6. Temperature programmed decomposition of cerium oxide catalyst after use for 24 h in the ketonization of acetic acid at 230 °C.

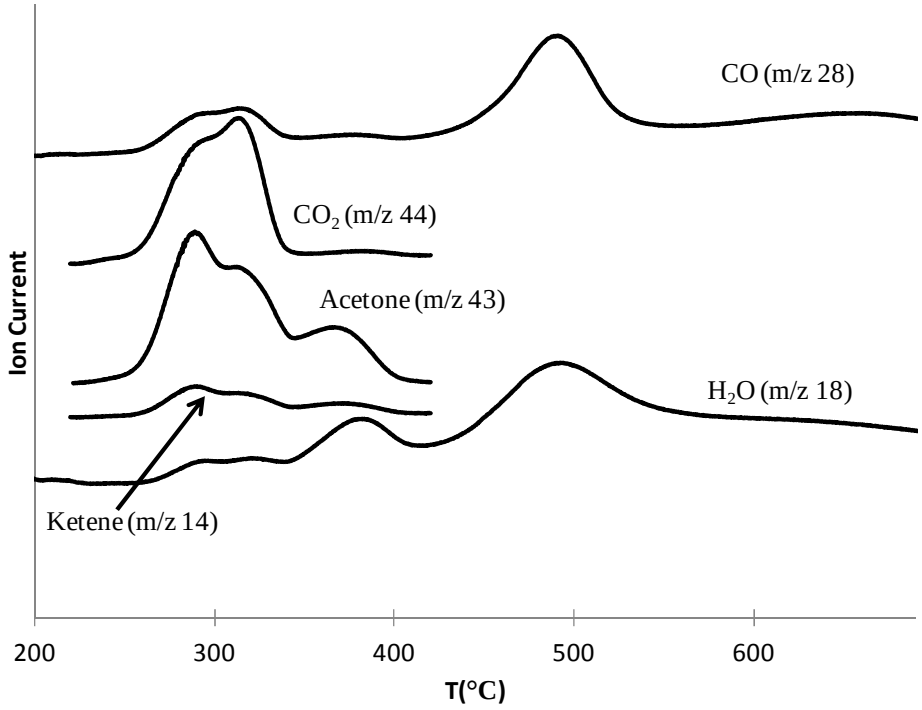

Figure 7. Temperature programmed decomposition of cerium acetate hydrate.

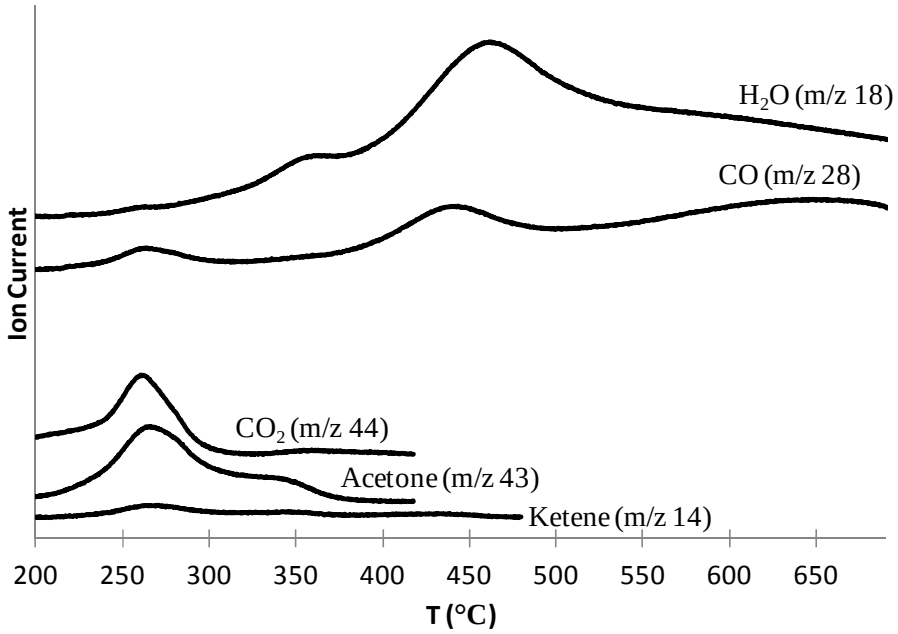

Figure 8. Ceria catalyst temperature programmed decomposition profile after being used in the ketonization of acetic acid at 300 °C for 30 min.

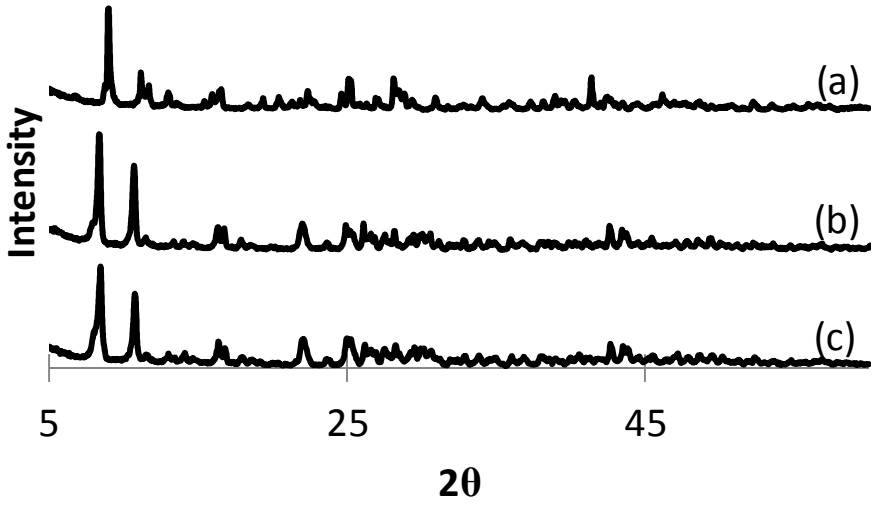

Figure 9. XRD figures of (a) fresh cerium acetate hydrate or (b) spent cerium acetate or (c) cerium carbonate hydrate used in the ketonization of acetic acid (0.85 g or 1.0 g acetic acid for acetate or carbonate, 2 h reaction, 230 °C, toluene solvent, 0.28g cerium acetate, 0.20g cerium carbonate) along with fresh cerium acetate hydrate.

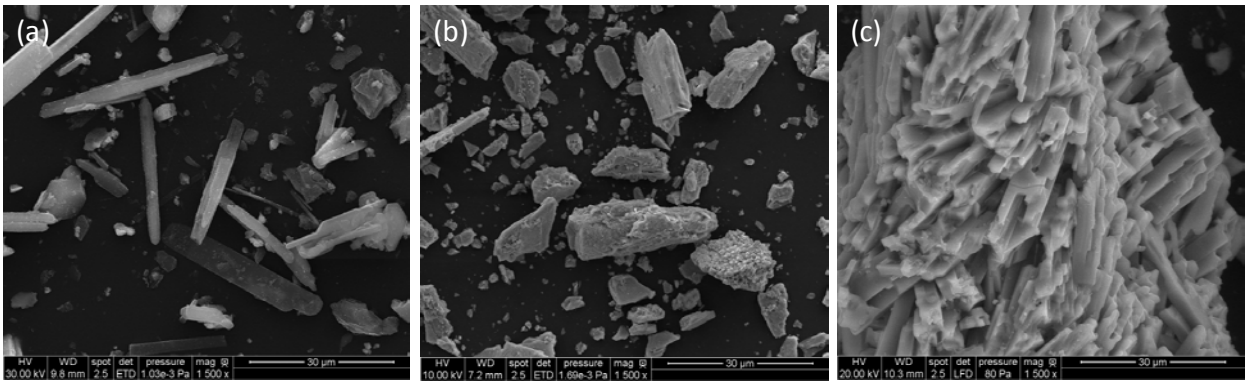

Figure 10. SEM images of ceria catalysts after use in (a) 24 h reaction with an acid/catalyst weight ratio of 18.1, 230 °C, 50 ml toluene (b) 24 h and 230 °C baking of ceria in solvent of toluene (c) cerium acetate hydrate after use in reaction with an acid/acetate weight ratio=3.1, 2 h reaction, 230 °C, 50 ml toluene.

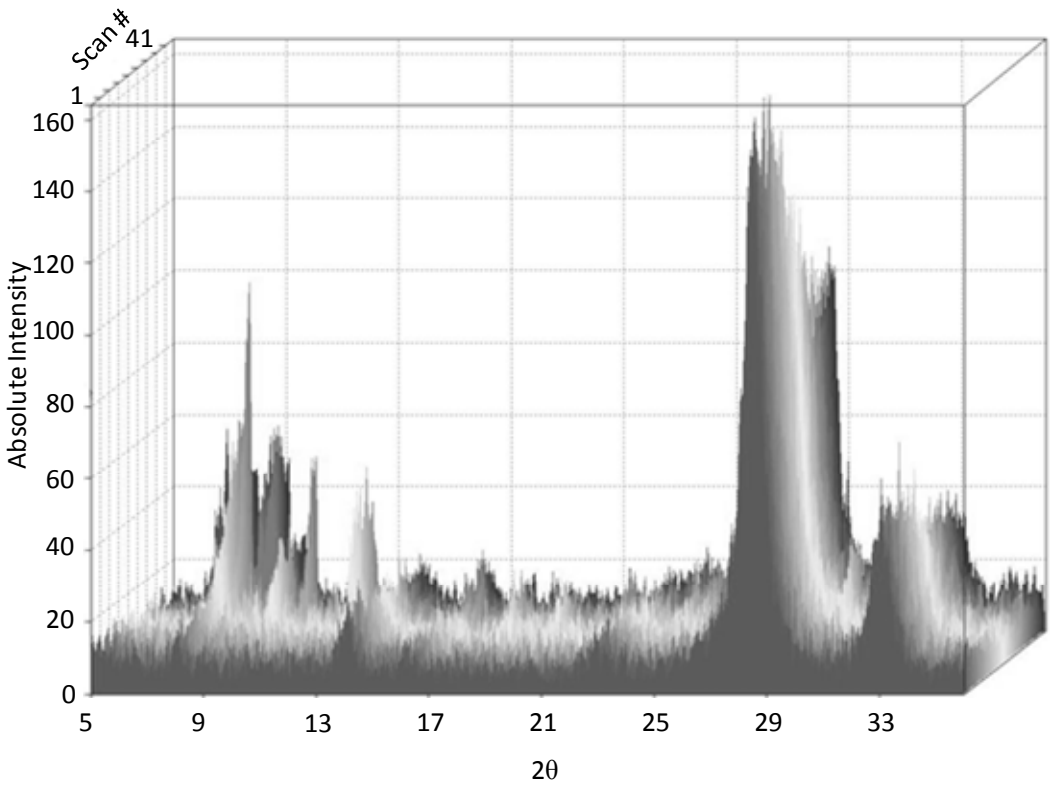

Figure 11. In-situ XRD characterization of ceria's behavior during the course of acetic acid vapor phase ketonization at various temperatures. Temperatures were increased after every 9 scans so that scans 1-9, 10-18, 19-27, 28-36, and 36-45 occurred at temperatures of 150, 200, 230, 270, and 300 °C respectively.

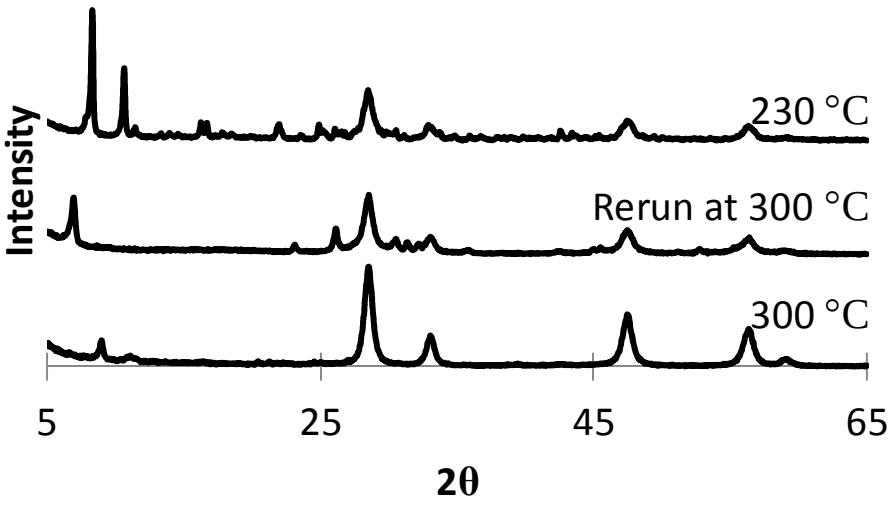

Figure 12. XRD profiles of ceria spent in 24 h reactions at 230 °C, after re-running the catalyst by baking it in toluene at 300 °C for 1 h, and ceria spent only in a 30 min reaction at 300 °C.

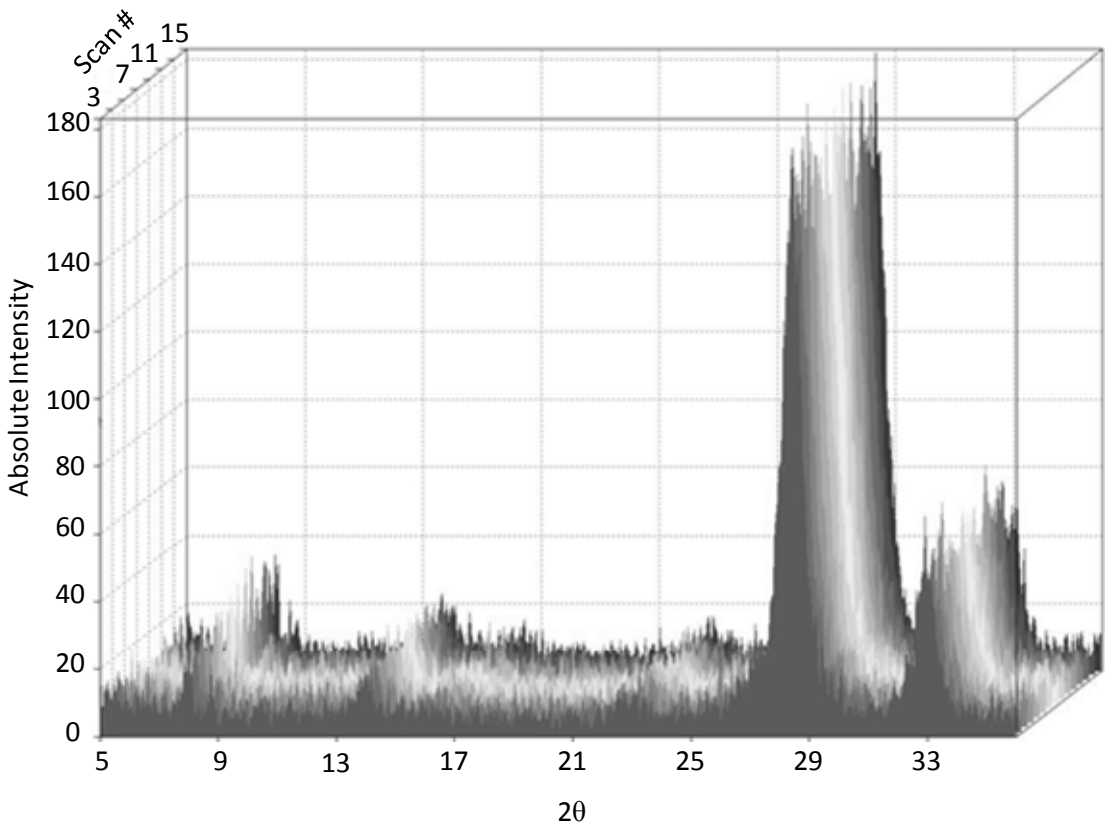

Figure 13. In-situ XRD of ceria exposed to acetic acid vapors at a constant temperature of 300 °C.

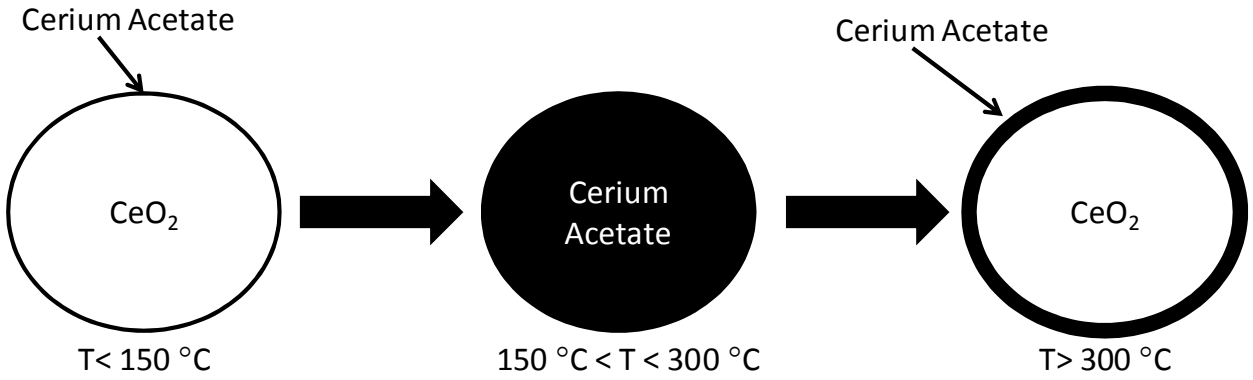

Figure 14. Different temperature regimes of ceria catalyzed ketonization. At low temperatures there is not enough energy for the acetic acid to break the Ce-O bonds, at intermediate temperatures acetates are able to form but are stable enough to form carboxylates in the bulk and at high temperatures, carboxylates can form but are rapidly decomposed to form acetone leaving the bulk structure maintained.

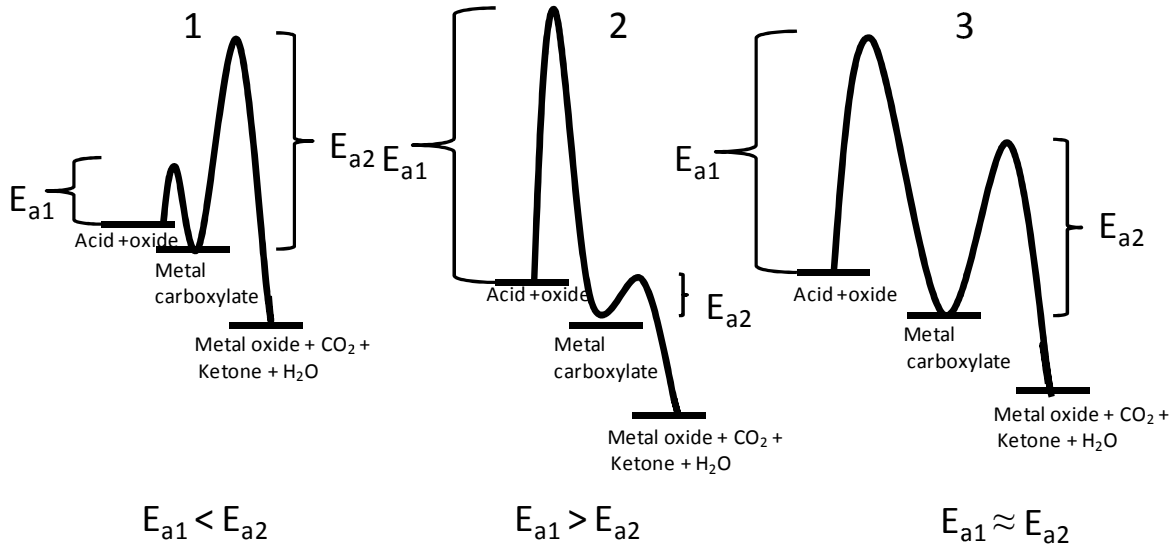

Figure 15. Representation of how the same pathway—where E_{a1} is the activation energy for metal carboxylate formation, and E_{a2} is the activation energy for the respective metal carboxylate decomposition—can lead to observation or lack thereof of metal carboxylate intermediates depending on the catalyst material properties. Scheme 1 would result in the formation of an observable metal carboxylate intermediate, scheme 2 would not, and scheme 3 would for a narrow temperature window.

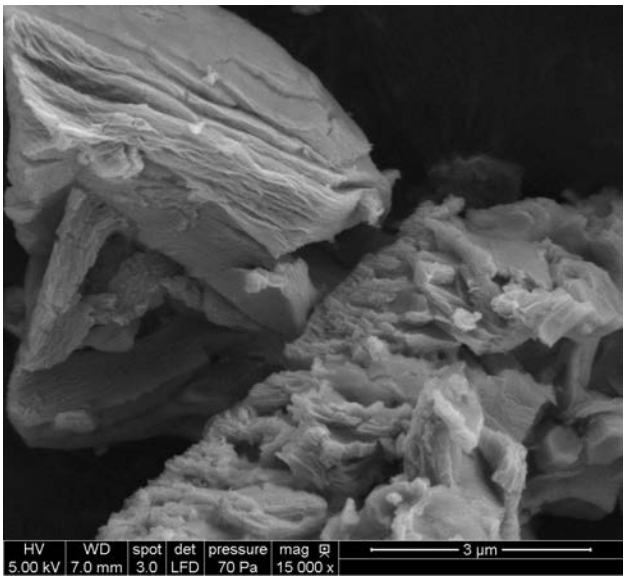

Figure 16. SEM image of ceria catalyst spent in a 24 h reaction at 315 °C with pivalic acid.

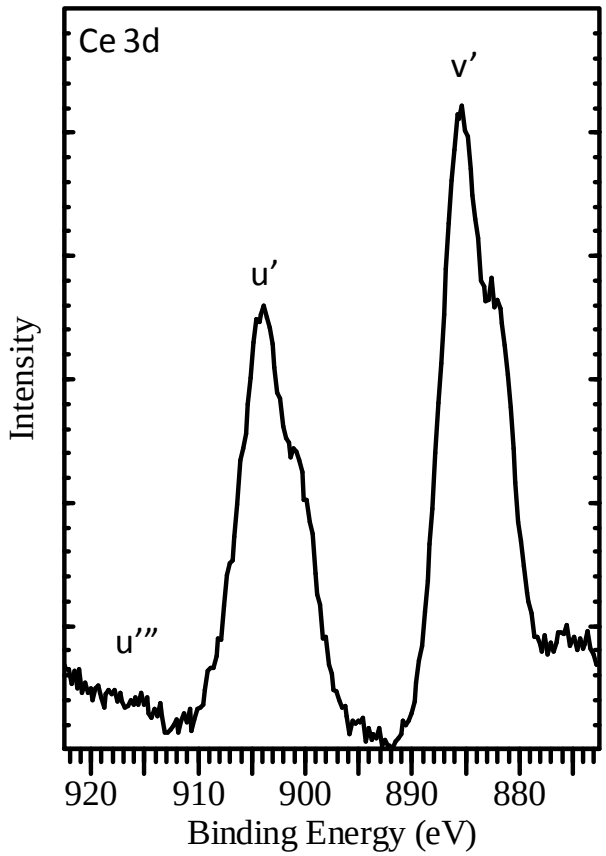

Figure 17. XPS spectra of ceria spent in a 24 h reaction with pivalic acid at 315 °C. The u'" peak ≈916 eV corresponding to Ce^{4+} has fully disappeared while the u' and v' associated with the Ce^{3+} state are prevalent.

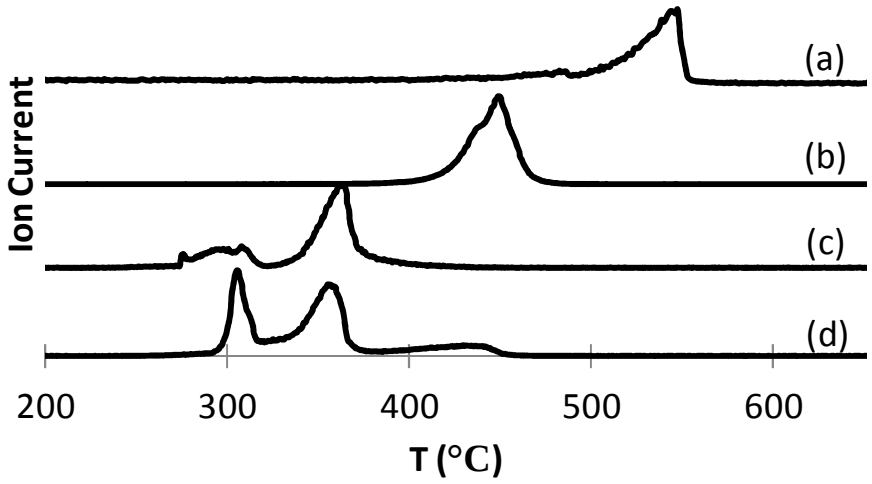

Figure 18. Normalized MS results obtained during the thermogravimetric analysis of cerium carboxylates with different degrees of branching (a) Cerium pivalate m/z=58, (b) Cerium isobutyrate m/z=71, (c) Cerium propionate m/z=86, (d) Cerium acetate m/z=58).

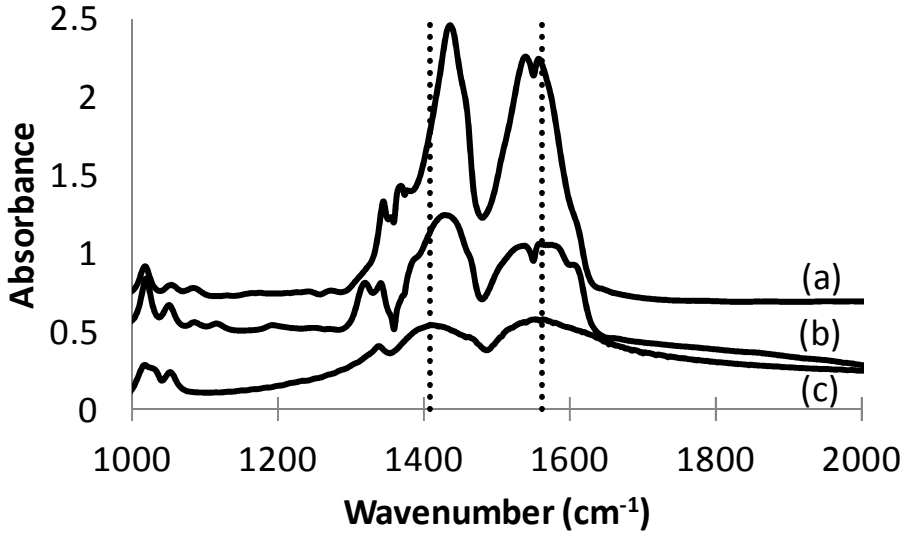

Figure 19. FTIR spectra of cerium acetate after (c) heat treatment at 230 °C, (b) ceria difference spectra after exposure to acetic acid at 230 °C, and (a) ceria difference spectra after exposure to acetic acid at 300 °C.

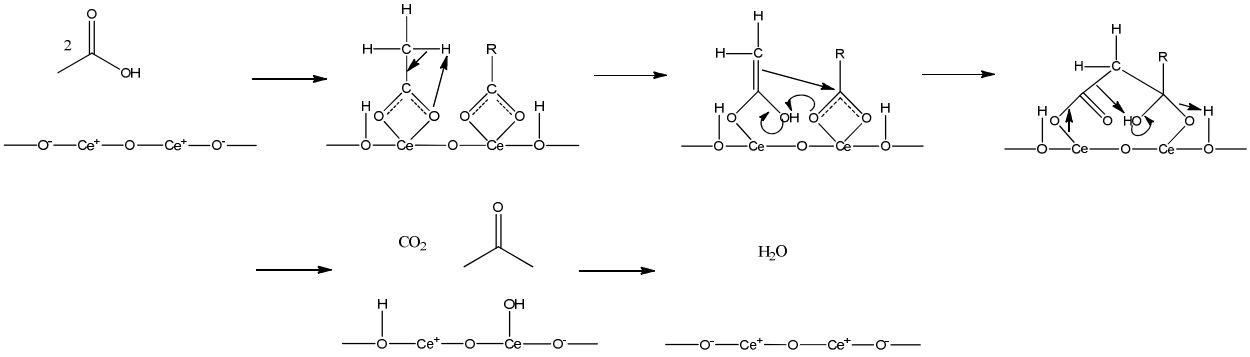

Figure 20. Proposed ketonization mechanism.

Chapter 7

$CeMO_x$ promoted condensed phase ketonization of biomass derived carboxylic acids

A paper to be submitted to Journal of Catalysis

Ryan W. Snell[1] and Brent H. Shanks[1]

[1]Department of Chemical and Biological Engineering, Iowa State University

Authorship roles:

Snell: Primary author

Shanks: Principal investigator

Abstract

Ketonization of the model bio-oil compound acetic acid was performed in the condensed phase using 5 different $CeMO_x$ catalysts. The catalysts were characterized using a number of different techniques both before and after reaction testing in the hope of gaining understanding of how material traits can lead to activity enhancements. A number of potentially important catalytic properties were found to be of little importance for the respective reaction. For instance, it was discovered that there was not a direct correlation between pre-reaction surface area with activity for ketonization at high or at low temperatures. Furthermore, better reducibility of the oxide did not appear to result in improvement of ketonization rates. XRD demonstrated that the temperature regime reaction testing occurred in influenced whether the crystal structure of the respective mixed oxide was destroyed. The temperatures of the various regimes were different, depending on composition of the catalytic material. It is proposed that the ease of formation of the resulting

metal carboxylate derived from the mixed oxide catalyst greatly influences the activity of the material. Moreover, this influence was found to be beneficial or detrimental varying on the ketonization reaction conditions.

Keywords: Mixed oxides; Ketonization; Bio-oil; Metal carboxylates; Temperature regimes

7.1 Introduction

With escalating costs of petroleum derived fuels and the increasing difficulty of obtaining these reserves, it is imperative that renewable alternatives be further developed. In 2010, the United States alone consumed 37.2 quadrillion BTUs of liquid fuels with the transportation sector accounting for 72 percent of this amount.[1] With a liquid fuel infrastructure in the trillions of dollar, it would be highly preferred to produce a drop-in renewable substitute.

Fast pyrolysis, involving the thermal breakdown of biomass in the absence of oxygen, has been examined as a potential starting point for the production of liquid fuels.[2-4] Unfortunately the resulting liquid product from fast pyrolysis, bio-oil, has a low energy density due to a large number of highly oxygenated compounds and a pH of 2-3 from many small organic acid making upgrading necessary.[2] Moreover, it would be preferred to perform this upgrading process in the condensed phase as many of the components of bio-oil are thermally unstable. Liquid phase reactions may also alleviate coking issues caused by lignin derived phenolic compounds through the process of condensing multiple fractions of the oil.

One reaction that would appear to be ideal for this upgrading application is ketonization, which involves coupling two carboxylic acids to form a ketone, CO_2, and H_2O. This reaction has already been probed in a number of manuscripts related to renewable fuel

applications.[5-8] Bio-related applications of ketonization are not new as the reaction was actually used to produce acetone industrially in the early 20th century from the decomposition of calcium acetate made through the mixing of lime and wood distillates.[9]

A large number of metal oxide catalysts have been explored and found to be active for ketonization.[10] However, ceria based catalysts are commonly believed to be among the best for the reaction.[11, 12] Recently, use of the ketonization reaction for catalytic upgrading of bio-fuels has tended to utilize mixed ceria-zirconia.[13-15] While clearly effective enough to be commonly used, there doesn't appear to be a firm reason why this catalyst is preferred to other potential mixed oxides in these reactions. It is known that a number of $CeMO_x$ catalysts can be active for ketonization. For instance, Nagashima et al. investigated many $CeMO_x$ oxides containing 10 mol% of the respective additional metal in the vapor phase ketonization of propanoic acid at 350 °C.[16] Catalysts containing M=Mn, Mg, or Cu were found to be more active than pure ceria—with $CeMnO_x$ being the best.[16] While further investigating the CeMnOx catalyst, Nagashima et al. found that increasing the Mn content to ~60% resulted in greater acid conversions.[16] Despite reports of mixed oxides being superior catalysts there does not appear to be an understanding of why this activity enhancement occurs.

The mixing of ceria with various oxides is known to significantly alter the material properties of the oxide. As an example, mixing of zirconia with ceria allows for the bulk oxide to undergo reduction at lower temperatures.[17] Ceria-alumina catalysts have also been discovered to allow for the bulk ceria to become more easily reduced similar to mixed ceria-zirconia catalysts.[18] Properties like these may potentially be of importance in ketonization

as it has been suggested catalyst redox characteristics may play a role in the reaction mechanism.[16, 19]

With the above considerations in mind it is apparent that there are a series of questions related to ketonization for bio-oil upgrading that need to be addressed. First, can condensed phase ketonization of small organic acids readily occur using mixed oxide catalysts? This question is important as due to the high temperatures necessary for ketonization to readily precede this reaction has been almost exclusively performed in the vapor phase. Secondly, which of the commonly used $CeMO_x$ catalysts are most active for this reaction? Thirdly, what characteristics of the catalyst are beneficial for ketonization? Attempting to answer these three questions in this work we synthesized and characterized 4 $CeMO_x$ catalysts and compared their traits with pure CeO_2. Next, condensed phase ketonization of the model bio-oil compound acetic acid was performed. Lastly, post reaction characterization of all 5 catalysts occurred and explanations for the differences in activity for the varying materials were proposed.

7.2 Experimental section

7.2.1 Material synthesis

Mixed oxide materials were made in a technique similar to that as by Serrano-Ruiz et al.[20] Batches were made to result in 40 g of the resulting oxide with a molar Ce:M ratio of 1. Initially the cerium precursor of cerium (III) nitrate hexahydrate (Roth >99.5%) was dissolved in water with the other nitrate—either manganese (II) nitrate tetrahydrate (Roth >98%), iron(III) nitrate nonahydrate (Merck >98%), zirconyl nitrate hydrate (Acros 99.5%), or aluminum nitrate nonahydrate (Riedel-de Haen ≥98.5%) for the respective mixed oxide. A pure ceria sample was also synthesized as a control. The nitrates were dissolved in water so

as to make a solution with a metal nitrate molarity of 0.7. On a Mettler-Toledo Labmax these solutions were then slowly added to 500 ml of water along with a 25% ammonia solution so as to keep a constant pH of 10. After this precipitation, the mixtures were aged for 72 h while stirring at pH 10. Next, the catalysts were vacuum filtered, washed with water and ethanol and dried at 110 °C overnight. Finally the materials were calcined at 450 °C for 2 h in air. The catalysts were then finely ground with a mortar and pestle.

7.2.2 Reaction testing

Reactions were performed on 75 ml Parr stainless steel 4598 batch reactors. Typically, the catalyst—0.1 g for the 300 °C 30 minute reactions or 0.2 g for the other reactions—1.0 g of acetic acid (Fisher 100%), 0.5 ml of the internal standard 1,4 dioxane (Fisher 100%), and 50 ml of the solvent toluene (Fisher 99.8%) were mixed and the reaction vessel pressurized with 30-40 bar nitrogen. After nitrogen pressurization, the reactions were heated either to 150 °C, 230 °C, or 300 °C while stirring at 400 rpm. Samples were taken into a liquid nitrogen cold trap and analyzed on an Agilent 7890 GC-FID.

7.2.3 Catalyst characterization

Catalysts were characterized using thermogravimetric analysis (TGA), Raman spectroscopy, N_2 physical adsorption, scanning electron microscopy (SEM), x-ray photoelectron spectroscopy (XPS), temperature programmed reduction (TPR), x-ray fluorescence spectroscopy (XRF), and x-ray diffraction (XRD).

TGA was done on a Perkin-Elmer STA 6000 under the flow of UHP nitrogen at 50 ml/min. Ramping occurred from 50 °C to the respective desired temperature at a rate of 3 °C/min. SEM imaging was done on a FEI Quanta-250 FE-SEM after first sputtering the samples with iridium. XPS was performed on a Physical Electronics 5500 Multi-technique

machine using an Al Kα source. A C1s peak location of 284.6 eV was used for standardizing peak locations. For surface area analysis, the BET method with N_2 adsorption was performed on a Quantachrome Autosorb machine. Degassing prior to analysis was done at 150 °C. A Siemens D-500 machine was utilized for XRD studies with a 0.15 detector slit while operated at 45kV and 30mA. For composition analysis, XRF was completed on a Bruker S4 Pioneer spectrometer. Raman spectroscopy was performed on a Renishaw Microscope with an Ar laser (488 nm). A laser power of 25 mW was used with a 20x magnification for all samples. A Micromeritics Autochem (II) Chemisorption Analyzer was utilized for TPR studies. For TPR experiments, multiple redox cycles were performed. First the sample was oxidized by heating to 400 °C under the flow of 10% O_2 in He. After cooling and purging with argon, the catalyst was exposed to 10% H_2 in Ar and heated to 450 °C at 5 °C/min while measuring results with a TCD detector. Next, the material was cooled under the flow of argon. This sequence was repeated again except that during the second reduction the temperature was ramped up to 990 °C.

7.3 Results

7.3.1 Catalyst pre-reaction characterization

Co-precipitation of the 4 different mixed oxides and pure ceria resulted in materials named CeO_2, $CeZrO_x$, $CeAlO_x$, $CeMnO_x$, and $CeFeO_x$. Examination of catalyst surface area using the BET technique demonstrated that the surface areas of $CeZrO_x$, $CeFeO_x$, and $CeAlO_x$ were significantly greater than found for pure CeO_2 (Table 1). Surface area of $CeZrO_x$ synthesized here (145 m^2/g) was greater than that (115 m^2/g) made by Serrano-Ruiz using the same technique.[20] XRF results showed that the materials all had roughly a Ce:M molar ratio of 1, similar to what was expected (Table 1).

XRD of the materials only showed peaks related to the cubic cerium oxide phase (Figure 1). As can be observed in Figure 1, the mixed oxide materials have smaller crystallite sizes than the pure ceria catalysts as evidenced by the broadening of the diffraction peaks. Incorporation of the additional smaller cation into the ceria cubic lattice is also observed through shifting of the peak location to higher 2θ values for the $CeMnO_x$ and $CeZrO_x$ catalysts. This phenomenon has been reported before.[20-23] SEM showed that the materials consisted of non-uniformly shaped particles (Figure 2).

TPR of the five catalysts showed significant differences in how easily the material was reduced and how well the redox properties were maintained. As demonstrated in Figure 3, CeO_2 had both low and high temperature reduction steps. This trait is commonly reported to be due to surface and bulk oxygen removal respectively.[24] Addition of other cations to CeO_2 clearly changed this reduction profile. Consistent with earlier reports, $CeZrO_x$ no longer showed this two step sequence but instead it appears the bulk and surface were reduced at the same time resulting in one large peak ~450 °C.[17] $CeAlO_x$, $CeZrO_x$, and CeO_2 all seemed to maintain their ability for redox cycling through at least two cycles while $CeFeO_x$ and $CeMnO_x$ did not consume as much H_2 during the second reduction step. $CeMnO_x$ reduction was similar to that found by Chen et al. in that two peaks ~250 °C and 350 °C occurred.[22] For both the manganese and the iron containing oxides it must be kept in mind that significant reduction of Mn and Fe is likely occurring along with the $Ce^{4+} \rightarrow Ce^{3+}$ transition. For instance the two peak reduction with the $CeMnO_x$ sample may be due to consecutive reductions from a high oxidation state of Mn to one more reduced .[25]

XPS is commonly used for determination of the surface cerium oxidation state.[26] Nomenclature for the Ce 3d spectra as used here was proposed by Burroughs et al. and is

now quite standard.[27] The u'" peak ~ a binding energy of 916.5 eV has been attributed to Ce^{4+} and is therefore frequently used for calculation of the cerium oxidation state.[15] Shyu et al. found that the area % of this peak in relation to the entire Ce 3d spectra area followed a linear correlation with the % Ce^{4+} in the sample.[28] Visual examination of the Ce 3d spectra for the five ketonization catalysts demonstrated different levels of cerium reduction in the fresh materials (Figure 4). It is clear that for the $CeZrO_x$ catalyst the u'" peak was decreased while the v' and u' values went up significantly. This may be expected as it is known that the addition of zirconia to ceria promotes vacancies charged balanced by the Ce^{3+} state.[29] Figure 5 shows the O1s spectra of the five catalysts. While many of the peaks have broad shoulders at higher binding energies, the $CeAlO_x$ spectra stands out in that clearly at least two large different peaks are evident. Despite the lack of evidence from XRD, this is likely due to the separation of ceria and alumina phases. The peak at the higher binding energy is attributed to alumina with the remaining peaks due to ceria-aluminate and/or pure ceria.[30]

As shown in Figure 6, Raman spectroscopy of the catalysts all showed peaks ~ 430-470 cm^{-1}. This is known to be due to the F_2g Raman active mode common for ceria.[20, 31, 32] From Figure 6, it can be seen that the CeO_2 and $CeAlO_x$ peaks have similar Raman shifts while $CeZrO_x$'s peak looks to be moved up a few cm^{-1}. This blue-shift for $CeZrO_x$ has been reported elsewhere [32, 33] The red-shift seen for $CeMnO_x$ and $CeFeO_x$ may be due to the heating of the sample.[31] However, it is also known that red-shifting can be related to longer M-O bonds.[34]

7.3.2 Ketonization reactions of acetic acid

Ketonization reactions of acetic acid resulting in the production of acetone, carbon dioxide, and water—as seen below—were performed in the condensed phase in stainless steel batch reactors.

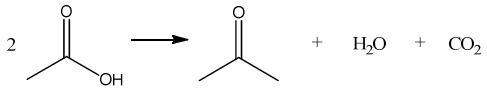

Initial testing occurred at 230 °C. Catalysts were found to be necessary for the reaction to proceed as a control run in their absence resulted in acetone yields under 0.1%. Catalyst runs were performed in duplicate and results are displayed in Figure 7. As can be observed, CeO_2 and $CeZrO_x$ were the most active catalysts and gave similar acetone yields after ~23 h of testing. $CeAlO_x$ gave intermediate acetone yields while $CeMnO_x$ and $CeFeO_x$ were the least active giving only ~4% yields at ~23 h.

Acetic acid ketonization was also performed at a higher temperature of 300 °C using a lower acid/catalyst ratio of 10. As shown in Figure 8 results were quite different from those found at 230 °C. At the higher temperature $CeMnO_x$ and $CeFeO_x$ were found to be the best catalysts. Reactions performed for the longer time of 45 minutes and a higher catalyst loading (acid/catalyst=5) were also completed. It was found that, agreeing with the results in Figure 8, the $CeMnO_x$ and $CeFeO_x$ materials were the best (Table 2). Ceria-manganese oxide catalysts were also discovered to be more active than other mixed oxides by Nagashima et al. when they performed vapor phase ketonization of propanoic acid at 350 °C.[16]

For low temperature testing, a condition of 150 °C was used. It was found that all materials were relatively inactive at this temperature with CeO_2 giving the greatest acetone yield of 1.2 % after 24 h. However, there were differences in the amount of acid that

disappeared during the reaction. $CeMnO_x$ and $CeFeO_x$ were found to have acid conversions of greater than 10 % while the other 3 materials all had acid disappearances at or below 6 %.

7.3.3 Post-reaction catalyst characterization

Characterization of the catalysts after reaction testing at 230 °C showed a number of interesting phenomena. For instance SEM demonstrated that during the course of reaction all the materials other than $CeMnO_x$ formed a large number of whisker or rod shaped materials (Figure 9). XPS of the 5 catalysts showed significant reduction of the surface cerium for all the catalysts (Figure 10). However, it was evident that CeO_2 was the least reduced with $CeFeO_x$ and $CeAlO_x$ having the most Ce^{3+} present. There have been reports of cerium reduction during the course of ketonization elsewhere.[15, 35]

XRD of the catalysts after reactions at 150 °C, 230 °C, and 300 °C showed that depending on the material and on the temperature of reaction various amounts of the catalyst crystal structure was disrupted. For example, as evidenced in Figure 11, after 24 h of exposure to acetic acid at 150 °C both $CeMnO_x$ and $CeFeO_x$ catalysts were significantly transformed from their original form. On the other hand, CeO_2, $CeZrO_x$, and $CeAlO_x$ all maintained their original fluorite structure. Figure 12 shows the XRD results after reaction testing at 230 °C. At this intermediate temperature, all 5 of the materials were significantly altered with very little of the original crystallinity maintained. Reaction testing at 300 °C again demonstrated differences between the catalysts (Figure 13). With this higher temperature reaction again only $CeMnO_x$ and CeFeOx were changed while the other oxides had similar XRD patterns as before ketonization.

7.4 Discussion

Amongst reasons described earlier, mixed oxides $CeAlO_x$, $CeMnO_x$, $CeFeO_x$, and $CeZrO_x$ were made as Al_2O_3[36], MnO_2[10], Fe_2O_3[37], and ZrO_x[38] have all been reported to be good ketonization catalysts by themselves. It was found that the addition of the respective metal into ceria altered a number of catalyst properties. However, after reaction testing we can effectively eliminate many of these material characteristics as being of importance in our ketonization reactions. As shown in Table 1, the BET surface area is significantly different for the 5 catalysts. However, as was found during reaction testing, a higher surface area clearly doesn't result in greater acetone yields. This implies that ketonization is either not taking place solely on the surface of the original materials or that significant surface area is being lost during the course of reaction.

TPR studies showed that addition of another cation into ceria created noteworthy alterations in the reduction profile of the catalyst. Again, coupling TPR results with reaction testing does not show an obvious trend between the ease of reduction and ketonization activity. Therefore it is not solely enhanced redox abilities that make mixed oxide catalysts more active than pure ceria. It also does not seem that the surface oxidation state of cerium in the fresh catalyst is of large influence in the reaction. As shown in Figure 4, initially the mixed oxides contained different ratios of Ce^{3+}/Ce^{4+}. $CeMnO_x$ and $CeAlO_x$ appeared to have more Ce^{4+} than did $CeZrO_x$ and while $CeZrO_x$ was more active than both at 230 °C, $CeMnO_x$ was better at 300 °C.

XRD results after acetic acid ketonization at 150 °C are quite interesting as they show $CeMnO_x$ and $CeFeO_x$ undergoing bulk restructuring while CeO_2, $CeAlO_x$, and $CeZrO_x$ did not. Likely what is occurring is attack by the acetic acid resulting in the formation of a mixed

metal oxyacetate. This carboxylate formation in the bulk phenomenon has been reported before with a number of different oxides [36, 39, 40].

After intermediate temperature reactions at 230 °C, a different type of interaction with the acetic acid reactant was found through XRD. Exposure to the acid at this temperature resulted in the formation of the acetate in the bulk for all five of the materials. Higher temperature reaction testing at 300 °C again showed that $CeFeO_x$ and $CeMnO_x$ preferred carboxylate creation while CeO_2 and $CeZrO_x$ remained in the original oxide phase.

To our knowledge this is the first finding of ceria mixed oxide ketonization where carboxylates are formed throughout the bulk. There may be a number of reasons for this. One is that a number of these materials have not been thoroughly examined in this particular reaction. Secondly, ketonization temperatures used here are lower than the 300-450 °C typically used for this reaction.[41] Lastly, it is possible that this is a condensed phase event and as ketonization—particularly of small organic acids—has almost been exclusively performed in the vapor phase, the phenomenon with regards to mixed metal oxides has not been discovered.

The formation of bulk carboxylates has been proposed to be of critical importance in ketonization.[36, 40, 42] Yakerson et al. examined vapor phase ketonization of acetic acid with TiO_2, CeO_2, SnO_2, ZrO_2 and BeO and determined that these materials did not undergo bulk carboxylate formation unlike group I and II carbonates or oxide catalysts.[42] It was then proposed that ketonization proceeded through different mechanisms depending on the strength of the metal-oxygen bonds.[42] Pestman et al. reached a similar conclusion in that they proposed oxides with weak M-O bonds promoted the reaction through a bulk decomposition mechanism while oxides with strong M-O bonds catalyzed ketonization

through a surface reaction.[36] They then proposed a mechanism for ketone formation proceeding via the surface catalytic route.[36] Mekhemer et al. recently performed vapor phase ketonization of acetic acid using MgO catalysts and determined that not only lattice energy, but also basicity may influence the formation of bulk acetates.[40] In their work it was proposed that temperature of reaction played a role in determining if the reaction proceeded via bulk decomposition or surface catalyzed mechanisms in that at >300 °C surface reactions begin to occur while at lower temperatures bulk decompositions resulted in the ketone.[40]

In our current work it appears that similar temperature regimes occur. However it seems as if there are low, middle, and high temperature regimes for $CeMO_x$ catalysts rather than just the 2 regimes found with MgO. The "M" additive to $CeMO_x$ apparently dictates when these various regimes change. One may look at it from a perspective where at low temperatures for CeO_2, $CeAlO_x$, and $CeZrO_x$ there is not enough energy to break the M-O bonds and form the carboxylate. At intermediate temperatures, there is sufficient amount of energy for carboxylate formation to overcome this barrier and the resulting metal acetate is stable so the oxide bulk is transformed. High temperatures are ~300 °C near where cerium acetate decomposes to form acetone.[43] These conditions, while having enough energy to form bulk acetates, cause the decomposition of the carboxylate. Thus the materials crystal structure remains intact. For $CeMnO_x$ and $CeFeO_x$ the carboxylate appears to be readily formed at lower temperatures and then seems to be stable to greater temperatures.

For all materials spent in 230 °C reactions for ~23 h, recalcination at 450 °C in air resulted in the formation of the oxide crystal lattice again as determined from XRD. However, for $CeFeO_x$ there was also an appearance of a peak near a 2θ value of 36. It is

likely that this was due to the formation of a second Fe_2O_3 phase. This demonstrates an important consideration unique to ketonization catalyzed by mixed oxides. Especially when operating in regimes where bulk transformation and decomposition of the catalyst occurs it is likely that oxide phase separation will eventually transpire. Severance of the two phases will significantly alter the properties of the catalyst and may result in decrease in activity at the desired conditions.

TGA of the spent catalysts was performed in order to understand the metal carboxylate formation and decomposition in greater detail (Figure 14). Decomposition of the 230 °C spent catalysts showed that $CeMnO_x$ and $CeFeO_x$ lost the largest wt% with $CeZrO_x$ and CeO_2 losing the least. This implies that the former two catalysts underwent acetate formation to a greater extent than did the latter two materials. Thus both TGA and XRD suggest that $CeMnO_x$ and $CeFeO_x$ form metal acetates more easily and in a stable fashion than do $CeZrO_x$ and CeO_2. Raman spectroscopy may help to explain why these materials act in this fashion. As shown in Figure 6, $CeZrO_x$ has the F_2g peak shifted to larger wavenumbers in comparison to CeO_2 while $CeMnO_x$ and $CeFeO_x$ have a smaller Raman shift. This may be the result of stronger M-O bonds in the $CeZrO_x$ catalyst with weaker M-O bonding for $CeMnO_x$ and $CeFeO_x$. These weaker M-O bonds open up the catalyst to attack by the organic acid and result in more facile formation of metal carboxylates.

SEM and XPS also showed changes in the catalysts occurring over the course of reaction testing in the intermediate temperature regime. For instance the formation of whiskers or rods, as evidenced in Figure 9, demonstrated that the macro-morphology of the catalyst changes along with the crystal structure during testing. As this occurred when testing at 230 °C, possibly the two findings are interrelated. Go and Jacobson recently found that

during formation of a mixed cerium gadolinium carboxylate—in their case formate—that the resulting product consisted of similar looking rod shaped materials.[44] The reduction of cerium as found with XPS is likely a result of metal acetate formation as well. As the catalyst was dried in air it is likely that much of the Ce^{3+} states would have been oxidized to Ce^{4+}, but in our case it appears that the Ce^{3+} state was stabilized, likely through the formation of Ce (III) acetate. While reduction occurred for all 5 catalysts, it was the most pronounced for $CeFeO_x$, $CeMnO_x$, and $CeAlO_x$. As these materials also had the most weight loss as determined by TGA is seems probable that cerium reduction and carboxylate formation are linked.

Catalyst activity also seems to be linked to these different regimes. During intermediate temperature testing, CeO_2 and $CeZrO_x$ were more active than $CeFeO_x$ and $CeMnO_x$ while at higher temperatures the reverse appeared to be true. As carboxylates in the bulk of the catalysts were formed at temperatures below where ketonization was found to occur only on the surface we may make the assumption that in our case the mechanism is the same for both temperature regimes. Therefore acetone is formed either through the thermal decomposition of the bulk carboxylate or through a similar thermal decomposition on the surface. Thus the two important steps in the reaction are the formation and decomposition of the metal acetate. At intermediate temperatures ketonization would be limited by the decomposition step so catalysts that do not form as stable a metal carboxylate and have stronger M-O bonds like $CeZrO_x$ and CeO_2 would be the most active. This correlation to the Raman results can be seen in Figure 15. At greater temperatures where decomposition readily occurs the reaction would be limited by formation of the carboxylate so materials with weaker M-O bonds and have easier acetate formation like $CeMnO_x$ and $CeFeO_x$ would be

preferred. $CeAlO_x$ likely acts a bit different as this catalyst was found to consist of two different phases—one being alumina—a catalyst less active than ceria.[10] Thus this material would promote the reaction more similarly to a mixture of ceria and alumina.

7.5 Conclusions

A number of different ceria based mixed metal oxide catalysts were synthesized and tested in the condensed phase ketonization reaction of acetic acid. This reaction and the corresponding conditions were chosen due to their relevance to bio-oil upgrading processes. It was found that a number of catalyst properties normally believed to be of benefit were not of large influence for the reaction such as BET surface area and redox abilities. Ketonization was found to proceed differently depending on which of 3 temperature regimes the reaction occurred at as well as which particular metal was introduced into the ceria framework. At intermediate temperatures catalysts—$CeZrO_x$ and CeO_2—that did not as readily form metal carboxylates were determined to be more active while at higher temperatures the ability to form this acetate were of benefit. Therefore when choosing a catalyst for a particular ketonization reaction system it is helpful to take into account the ease of formation for metal carboxylates as well as the temperature these materials thermally decompose.

7.6 References

[1] AEO2012 Early Release Overview, U.S. EIA, DOE/EIA-0383ER (2012).
[2] S. Czernik, A.V. Bridgwater, Overview of Applications of Biomass Fast Pyrolysis Oil, Energy & Fuels, 18 (2004) 590-598.
[3] A.V. Bridgwater, Review of fast pyrolysis of biomass and product upgrading, Biomass and Bioenergy, 38 (2012) 68-94.
[4] M.M. Wright, D.E. Daugaard, J.A. Satrio, R.C. Brown, Techno-economic analysis of biomass fast pyrolysis to transportation fuels, Fuel, 89 (2010) S2-S10.
[5] L. Deng, Y. Fu, Q.-X. Guo, Upgraded Acidic Components of Bio-oil through Catalytic Ketonic Condensation, Energy & Fuels, 23 (2008) 564-568.
[6] C.A. Gärtner, J.C. Serrano-Ruiz, D.J. Braden, J.A. Dumesic, Catalytic Upgrading of Bio-Oils by Ketonization, ChemSusChem, 2 (2009) 1121-1124.

[7] E.I. Gurbuz, E.L. Kunkes, J.A. Dumesic, Dual-bed catalyst system for C-C coupling of biomass-derived oxygenated hydrocarbons to fuel-grade compounds, Green Chemistry, 12 (2010) 223-227.
[8] E. Karimi, A. Gomez, S.W. Kycia, M. Schlaf, Thermal Decomposition of Acetic and Formic Acid Catalyzed by Red Mud—Implications for the Potential Use of Red Mud as a Pyrolysis Bio-Oil Upgrading Catalyst, Energy & Fuels, 24 (2010) 2747-2757.
[9] A To Alkanolamines, M. Grayson (Ed.) Kirk-Othmer Encyclopedia of Chemical Technology, John Wiley and Sons, New York, 1978.
[10] M. Glinski, J. Kijenski, A. Jakubowski, Ketones from monocarboxylic acids: Catalytic ketonization over oxide systems, Applied Catalysis A: General, 128 (1995) 209-217.
[11] S.D. Randery, J.S. Warren, K.M. Dooley, Cerium oxide-based catalysts for production of ketones by acid condensation, Applied Catalysis A: General, 226 (2002) 265-280.
[12] M. Renz, Ketonization of Carboxylic Acids by Decarboxylation: Mechanism and Scope, ChemInform, 36 (2005).
[13] E.L. Kunkes, D.A. Simonetti, R.M. West, J.C. Serrano-Ruiz, C.A. Gartner, J.A. Dumesic, Catalytic Conversion of Biomass to Monofunctional Hydrocarbons and Targeted Liquid-Fuel Classes, Science, 322 (2008) 417-421.
[14] C.A. Gaertner, J.C. Serrano-Ruiz, D.J. Braden, J.A. Dumesic, Ketonization Reactions of Carboxylic Acids and Esters over Ceria−Zirconia as Biomass-Upgrading Processes, Industrial & Engineering Chemistry Research, 49 (2010) 6027-6033.
[15] A. Gangadharan, M. Shen, T. Sooknoi, D.E. Resasco, R.G. Mallinson, Condensation reactions of propanal over CexZr1-xO2 mixed oxide catalysts, Applied Catalysis A: General, 385 (2010) 80-91.
[16] O. Nagashima, S. Sato, R. Takahashi, T. Sodesawa, Ketonization of carboxylic acids over CeO2-based composite oxides, Journal of Molecular Catalysis A: Chemical, 227 (2005) 231-239.
[17] F. Fally, V. Perrichon, H. Vidal, J. Kaspar, G. Blanco, J.M. Pintado, S. Bernal, G. Colon, M. Daturi, J.C. Lavalley, Modification of the oxygen storage capacity of CeO2-ZrO2 mixed oxides after redox cycling aging, Catalysis Today, 59 (2000) 373-386.
[18] L. Ilieva, G. Pantaleo, I. Ivanov, A.M. Venezia, D. Andreeva, Gold catalysts supported on CeO2 and CeO2-Al2O3 for NOx reduction by CO, Applied Catalysis B: Environmental, 65 (2006) 101-109.
[19] M.A. Hasan, M.I. Zaki, L. Pasupulety, Oxide-catalyzed conversion of acetic acid into acetone: an FTIR spectroscopic investigation, Applied Catalysis A: General, 243 (2003) 81-92.
[20] J.C. Serrano-Ruiz, J. Luettich, A. Sepúlveda-Escribano, F. Rodríguez-Reinoso, Effect of the support composition on the vapor-phase hydrogenation of crotonaldehyde over Pt/CexZr1-xO2 catalysts, Journal of Catalysis, 241 (2006) 45-55.
[21] M.H. Yao, R.J. Baird, F.W. Kunz, T.E. Hoost, An XRD and TEM Investigation of the Structure of Alumina-Supported Ceria–Zirconia, Journal of Catalysis, 166 (1997) 67-74.
[22] H. Chen, A. Sayari, A. Adnot, F.ç. Larachi, Composition–activity effects of Mn–Ce–O composites on phenol catalytic wet oxidation, Applied Catalysis B: Environmental, 32 (2001) 195-204.
[23] S. Abdollahzadeh-Ghom, C. Zamani, T. Andreu, M. Epifani, J.R. Morante, Improvement of oxygen storage capacity using mesoporous ceria–zirconia solid solutions, Applied Catalysis B: Environmental, 108-109 (2011) 32-38.
[24] H.C. Yao, Y.F.Y. Yao, Ceria in automotive exhaust catalysts : I. Oxygen storage, Journal of Catalysis, 86 (1984) 254-265.
[25] F. Kapteijn, L. Singoredjo, A. Andreini, J.A. Moulijn, Activity and selectivity of pure manganese oxides in the selective catalytic reduction of nitric oxide with ammonia, Applied Catalysis B: Environmental, 3 (1994) 173-189.
[26] A. Trovarelli, Catalysis by Ceria and Related Materials, in: G.J. Hutchings (Ed.) Catalytic Science Series, Imperial College Press, 2002.

[27] P. Burroughs, A. Hamnett, Anthony F. Orchard, Geoffrey Thornton, Satellite studies in the x-ray photoelectron spectra of some binary and mixed oxides of lanthanum and cerium, Journal of the Chemical Society, Dalton Transactions, 17 (1976) 1686-1698.
[28] J.Z. Shyu, K. Otto, W.L.H. Watkins, G.W. Graham, R.K. Belitz, H.S. Gandhi, Characterization of Pd/[gamma]-alumina catalysts containing ceria, Journal of Catalysis, 114 (1988) 23-33.
[29] E. Mamontov, T. Egami, R. Brezny, M. Koranne, S. Tyagi, Lattice Defects and Oxygen Storage Capacity of Nanocrystalline Ceria and Ceria-Zirconia, The Journal of Physical Chemistry B, 104 (2000) 11110-11116.
[30] R. Sohal, G. Lupina, O. Seifarth, P. Zaumseil, C. Walczyk, T. Schroeder, Improving the dielectric constant of Al2O3 by cerium substitution for high-k MIM applications, Surface Science, 604 (2010) 276-282.
[31] B. Fazio, L. Spadaro, G. Trunfio, J. Negro, F. Arena, Raman scattering of MnOx□CeOx composite catalysts: structural aspects and laser-heating effects, Journal of Raman Spectroscopy, 42 (2011) 1583-1588.
[32] B.M. Reddy, A. Khan, Y. Yamada, T. Kobayashi, S. Loridant, J.-C. Volta, Structural Characterization of CeO2−MO2 (M = Si4+, Ti4+, and Zr4+) Mixed Oxides by Raman Spectroscopy, X-ray Photoelectron Spectroscopy, and Other Techniques, The Journal of Physical Chemistry B, 107 (2003) 11475-11484.
[33] B. Reddy, P. Bharali, G. Thrimurthulu, P. Saikia, L. Katta, S.-E. Park, Catalytic Efficiency of Ceria–Zirconia and Ceria–Hafnia Nanocomposite Oxides for Soot Oxidation, Catalysis Letters, 123 (2008) 327-333.
[34] T. Masui, K. Koyabu, K. Minami, T. Egawa, N. Imanaka, Low-Temperature Redox Activity of Ce0.64Zr0.16Bi0.20O1.90/γ-Al2O3 and Ag/Ce0.64Zr0.16Bi0.20O1.90/γ-Al2O3 Catalysts, The Journal of Physical Chemistry C, 111 (2007) 13892-13897.
[35] A.M. Rubinshtein, A.A. Slinkin, V.I. Yakerson, E.A. Fedorovskaya, The reduction of CeO2 in the ketonization of ch3cooh, Russian Chemical Bulletin, 10 (1961) 2090-2092.
[36] R. Pestman, R.M. Koster, A. van Duijne, J.A.Z. Pieterse, V. Ponec, Reactions of Carboxylic Acids on Oxides: 2. Bimolecular Reaction of Aliphatic Acids to Ketones, Journal of Catalysis, 168 (1997) 265-272.
[37] J.C. Kuriacose, S.S. Jewur, Studies on the surface interaction of acetic acid on iron oxide, Journal of Catalysis, 50 (1977) 330-341.
[38] K. Okumura, Y. Iwasawa, Zirconium Oxides Dispersed on Silica Derived from Cp2ZrCl2, [(i-PrCp)2ZrH(μ-H)]2, and Zr(OEt)4Characterized by X-Ray Absorption Fine Structure and Catalytic Ketonization of Acetic Acid, Journal of Catalysis, 164 (1996) 440-448.
[39] Y. Yamada, M. Segawa, F. Sato, T. Kojima, S. Sato, Catalytic performance of rare earth oxides in ketonization of acetic acid, Journal of Molecular Catalysis A: Chemical, 346 (2011) 79-86.
[40] G.A.H. Mekhemer, S.A. Halawy, M.A. Mohamed, M.I. Zaki, Ketonization of acetic acid vapour over polycrystalline magnesia: in situ Fourier transform infrared spectroscopy and kinetic studies, Journal of Catalysis, 230 (2005) 109-122.
[41] L. Vivier, D. Duprez, Ceria-Based Solid Catalysts for Organic Chemistry, ChemSusChem, 3 (2010) 654-678.
[42] V.I. Yakerson, E.A. Fedorovskaya, A.L. Klyachko-Gurvich, A.M. Rubinshtein, Vapor Phase Catalytic Ketonation of CH3COOH over Oxides of Quadrivalent Metals and BeO, Kinetika i Kataliz, 2 (1961) 907-915.
[43] T. Arii, T. Taguchi, A. Kishi, M. Ogawa, Y. Sawada, Thermal decomposition of cerium(III) acetate studied with sample-controlled thermogravimetric-mass spectrometry (SCTG--MS), Journal of the European Ceramic Society, 22 (2002) 2283-2289.
[44] Y.B. Go, A.J. Jacobson, Solid Solution Precursors to Gadolinia-Doped Ceria Prepared via a Low-Temperature Solution Route, Chemistry of Materials, 19 (2007) 4702-4709.

7.7 Tables and figures

Table 1. Surface areas and compositions of synthesized catalysts.

Catalyst	SA_{BET} (m^2/g)	Ce:M mole ratio
CeO_2	70	
$CeZrO_x$	145	1:0.8
$CeAlO_x$	121	1:1.2
$CeMnO_x$	87	1:0.9
$CeFeO_x$	142	1:1

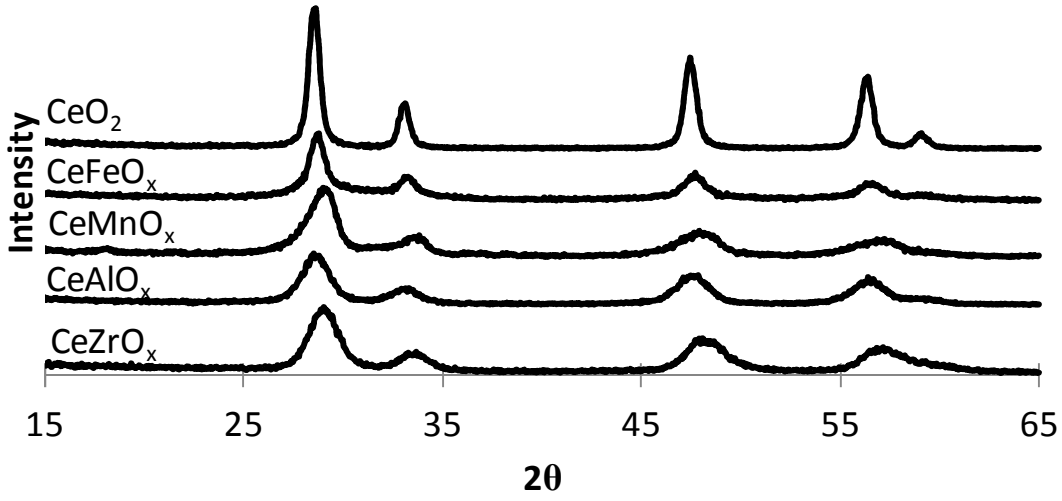

Figure 1. XRD profiles of the fresh mixed oxide catalysts.

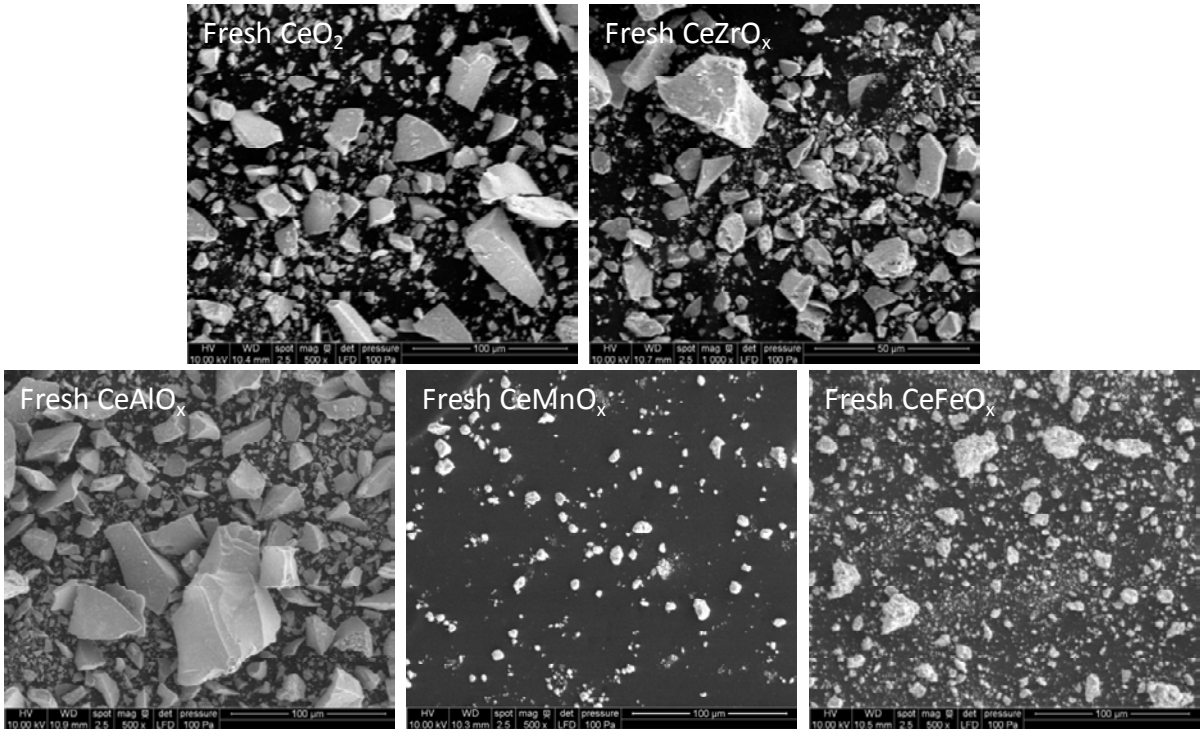

Figure 2. SEM images of the fresh mixed oxide catalysts.

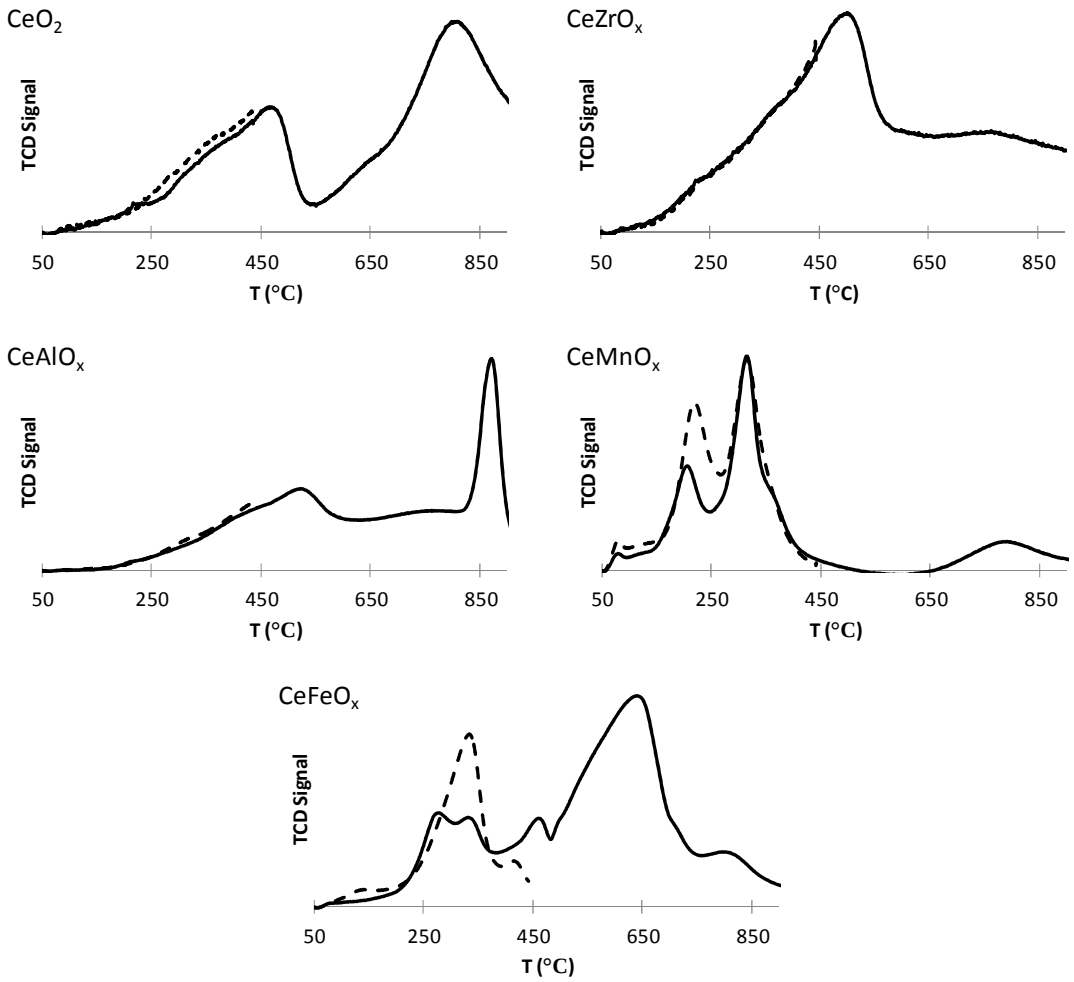

Figure 3. H_2 TPR of the $CeMO_x$ catalysts. The testing began with a reduction step up to 450 °C (- - -) followed by oxidation and a second reduction (—).

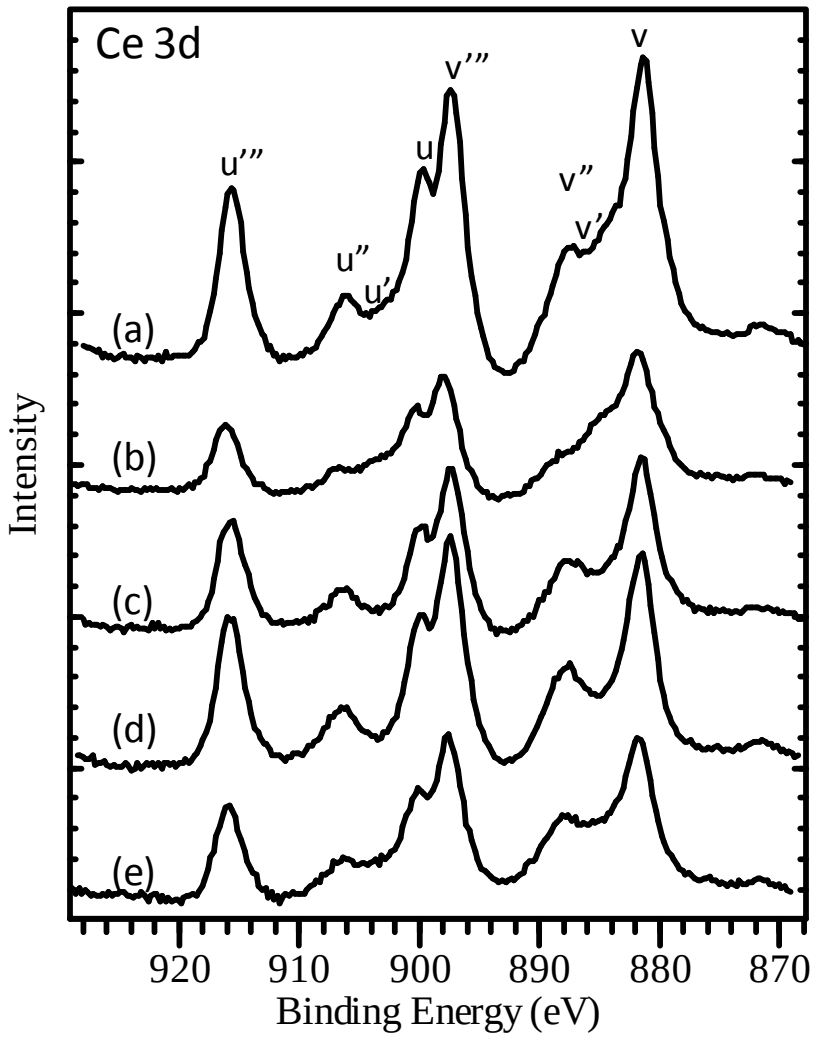

Figure 4. XPS spectra of the five (a) CeO_2, (b) $CeZrO_x$, (c) $CeAlO_x$, (d) $CeMnO_x$, and (e) $CeFeO_x$ fresh ketonization catalysts. Here, u'", v'", u", v", u, and v peaks are attributed to Ce^{4+} while the u' and v' peaks are related to Ce^{3+}.[15]

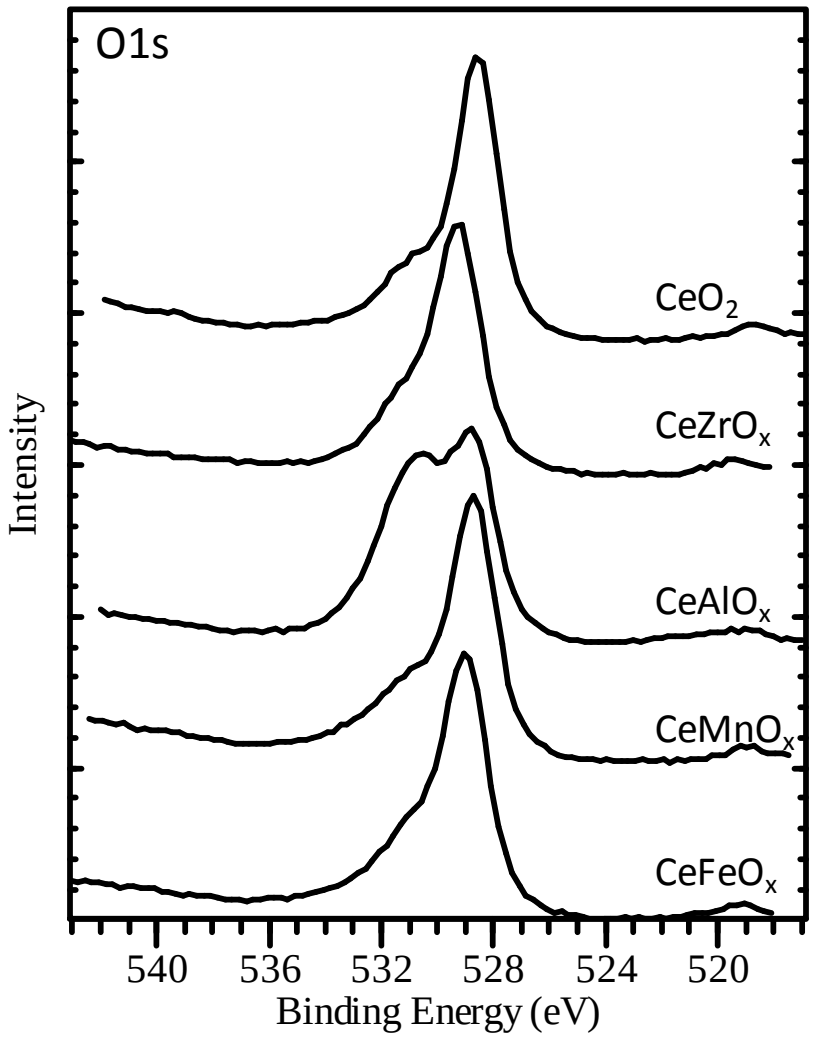

Figure 5. O1s XPS data for the five mixed oxide materials.

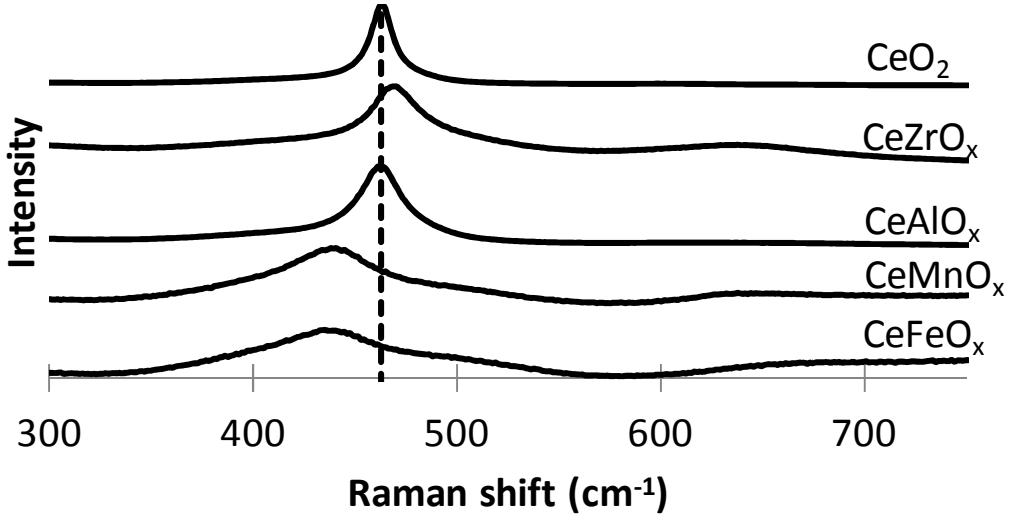

Figure 6. Raman spectra of the respective mixed oxide catalysts. Peak heights were normalized for clarity.

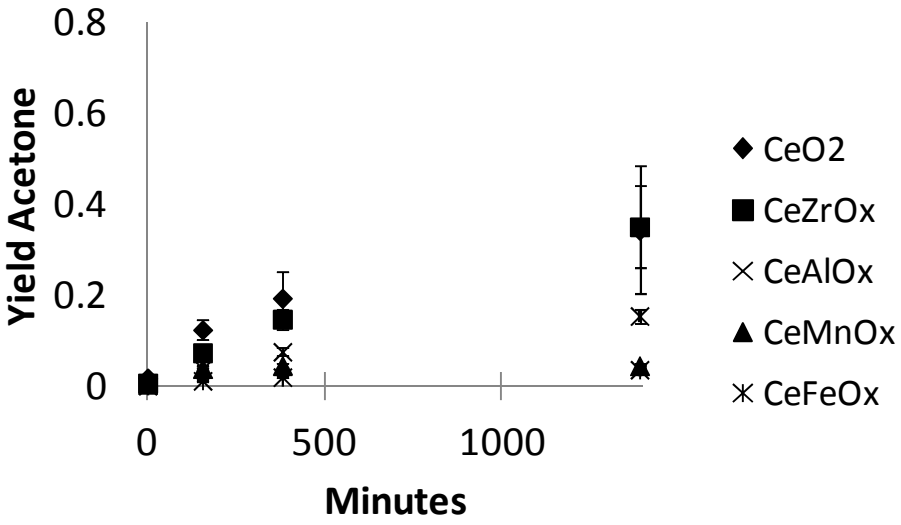

Figure 7. Ketonization of acetic acid at 230 °C promoted by the $CeMO_x$ catalysts (0.2 g catalyst and 1.0 g acetic acid). Error bars are related to the sample standard deviations from duplicate runs. It was found that CeO_2 and $CeZrO_x$ were the most active catalysts followed by $CeAlO_x$ and lastly $CeMnO_x$ and $CeFeO_x$.

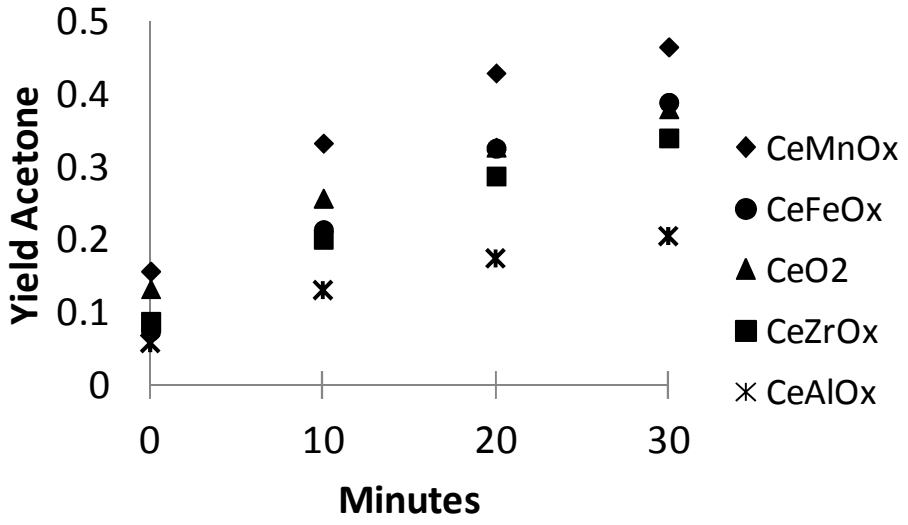

Figure 8. $CeMO_x$ promoted ketonization of acetic acid results at 300 ° (0.1 g catalyst, 1.0g acetic acid). At this temperature $CeMnO_x$ and $CeFeO_x$ were determined to be the best catalysts.

Table 2. Results from 300 °C ketonization reaction performed with an acid/catalyst ratio of 5.

Catalyst	Yield Acetone (45min)	Carbon balance
CeO_2	76	92
$CeZrO_x$	53 ±1	89
$CeAlO_x$	44	93
$CeMnO_x$	87±0	92
$CeFeO_x$	81	90

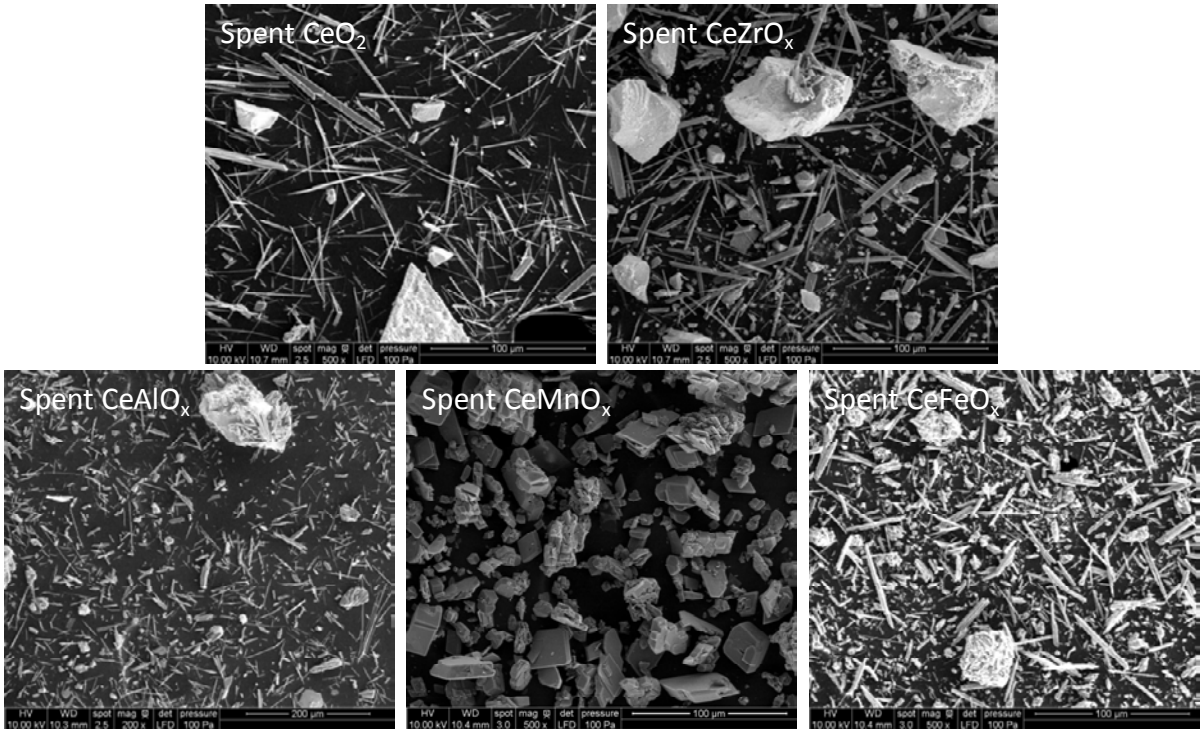

Figure 9. SEM images of catalysts after reaction testing at 230 °C for ~23 h.

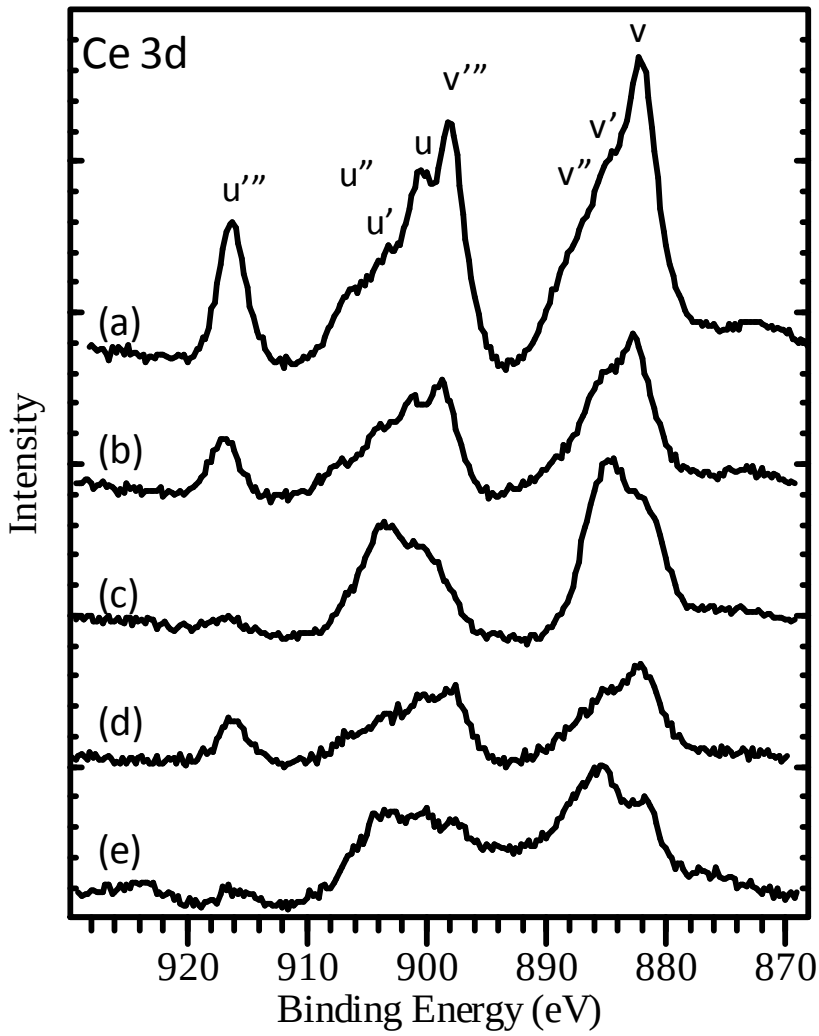

Figure 10. XPS of (a) CeO_2. (b) $CeZrO_x$, (c) $CeAlO_x$, (d) $CeMnO_x$ and (e) $CeFeO_x$ catalysts after acetic acid ketonization at 230 °C for ~23 h.

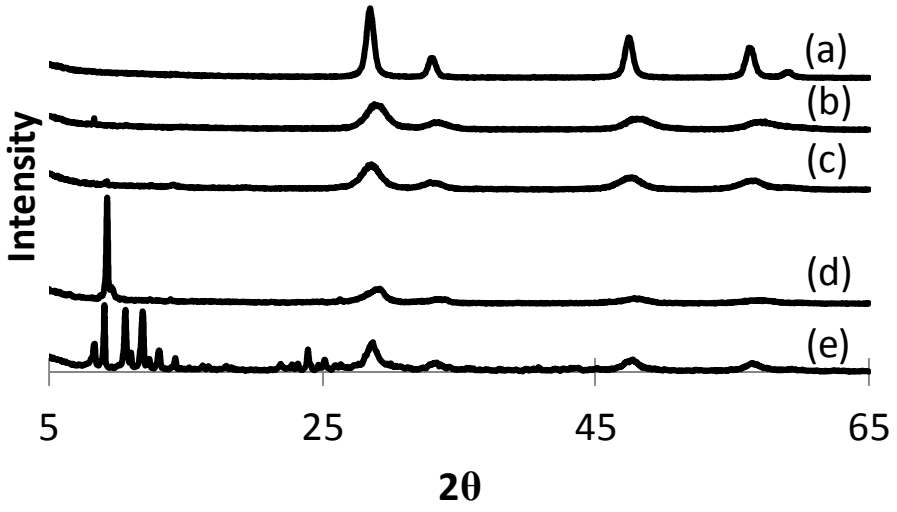

Figure 11. XRD results for (a) CeO_2, (b) $CeZrO_x$, (c) $CeAlO_x$, (d) $CeMnO_x$, (e) $CeFeO_x$ after reaction at 150 °C (24 h, 0.2 g catalyst, 1.0 g acetic acid).

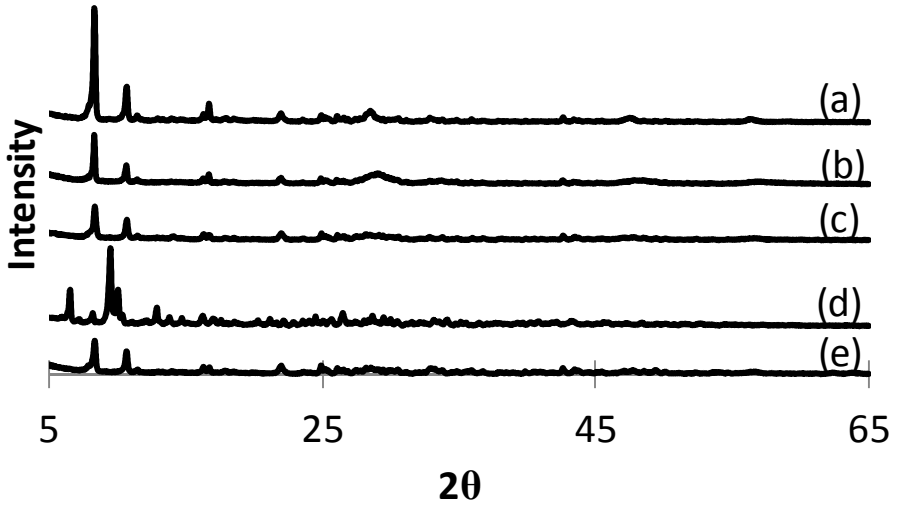

Figure 12. XRD results of spent (230 °C, 23 h, 0.2g catalyst, 1.0g acetic acid) (a) CeO_2, (b) $CeZrO_x$, (c) $CeAlO_x$, (d) $CeMnO_x$, (e) $CeFeO_x$.

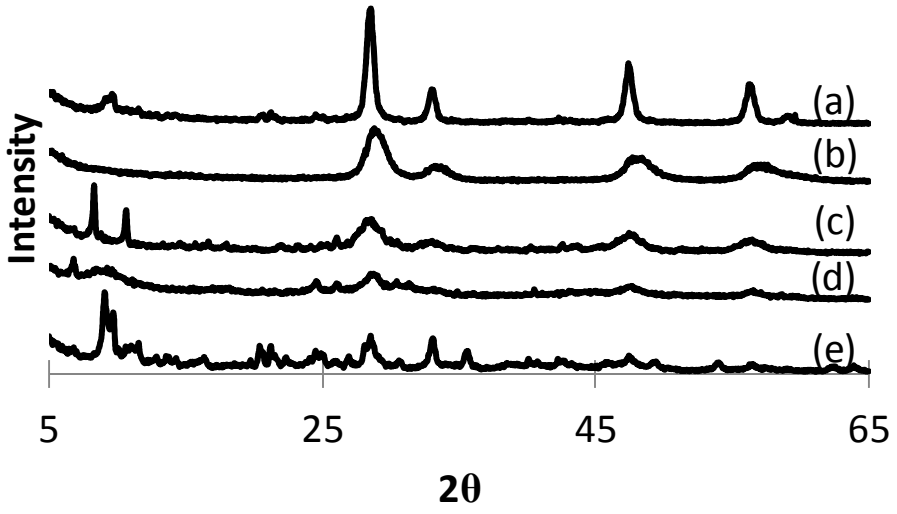

Figure 13. XRD patterns of (a) CeO_2, (b) $CeZrO_x$, (c) $CeAlO_x$, (d) $CeMnO_x$, (e) $CeFeO_x$ spent at 300 ° C. (30 min, 0.1 g catalyst, 1.0 g acetic acid).

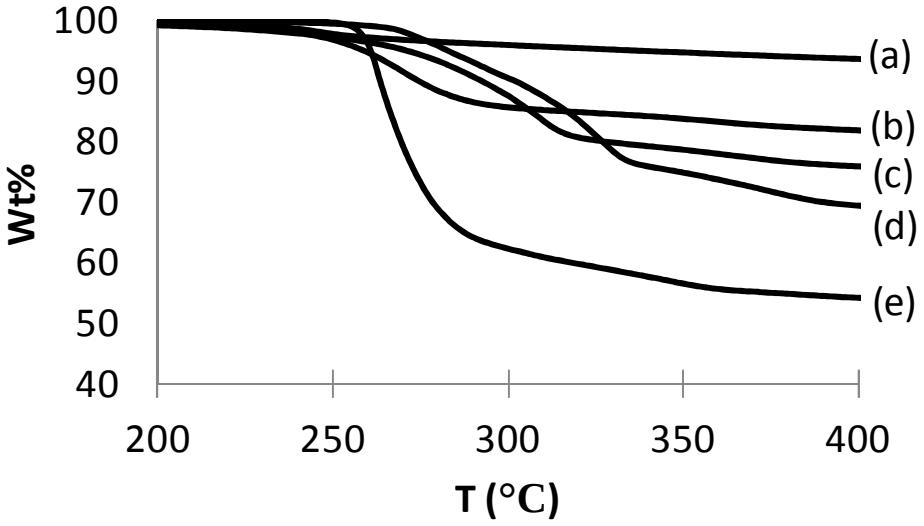

Figure 14. TGA results of catalysts (a) $CeZrO_x$, (b) CeO_2, (c) $CeAlO_x$, (d) $CeFeO_x$, (e) $CeMnO_x$ spent in reaction at 230 °C (~23 h, 0.2 g catalyst, 1.0 g acetic acid).

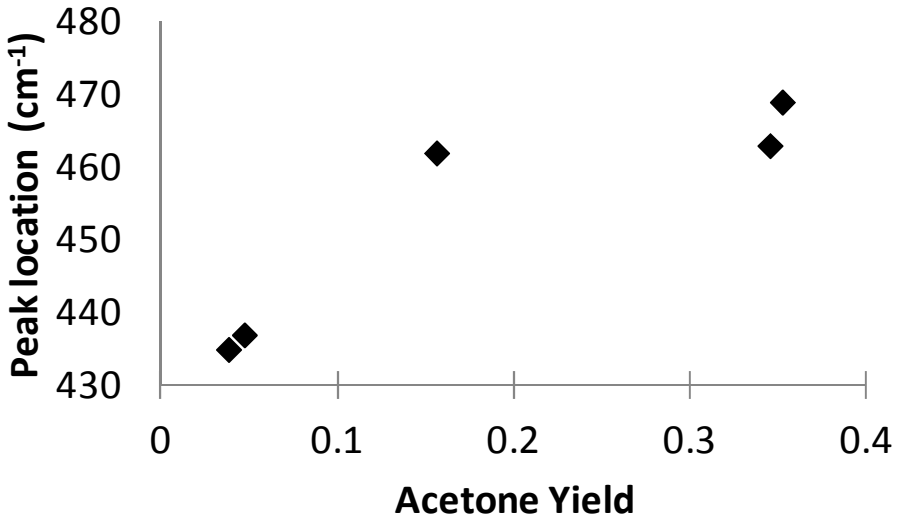

Figure 15. Raman peak location of fresh metal oxide catalysts plotted with acetone yields after 230 °C reaction (~23 h, 0.2 g catalyst, 1.0 g acetic acid).

Chapter 8

General conclusions

With the overarching theme of bio-oil upgrading to fungible transportation fuels, this work has focused primarily on the more fundamental chemistry of potentially relevant heterogeneously catalyzed C-C bond forming reactions. Instead of regurgitating all of the previously described results, here general conclusions will both briefly summarize findings and how they relate to the big picture of bio-oil upgrading.

The two reactions examined in this thesis were the aldol condensation, used to create C-C bonds between two aldehydes, ketones, or a mixture, and ketonization, involving the coupling of two carboxylic acids. Aldol condensations were examined as a way to save the numerous small aldehydes and ketones prevalent in bio-oil so that they are not lost as potential liquid fuels during hydrotreatment. Ketonization was researched as an efficient technique to remove acidity, increase the C-C chain length, and remove oxygen to increase the oil's energy density.

Aldol condensation work focused on examining the potential of using acid-base cooperative catalysts. This was researched as having weaker acid-base pairs instead of a strong acid or base would potentially cut down on undesirable side reactions in the bio-oil. It was found using aluminum phosphate catalysts that both acid and base sites were necessary to promote the desired cross condensation between model bio-oil ketones and aldehydes. Results demonstrating the cooperative catalysis between weak acids and bases also illustrate another advantage of using heterogeneous catalysts for bio-oil upgrading as it allows for the

coexistence of acids and bases while use of homogeneous catalysts would result in their neutralization.

Despite being an ideal reaction for bio-oil upgrading from a stoichiometric standpoint, ketonization has the distinct disadvantage for this application of the necessity of high temperatures. As it would be preferred to upgrade bio-oil in the condensed phase, more active catalysts are necessary so that this step would be practical from a processing standpoint. Unfortunately, very little was understood about the reaction including the mechanism and desirable catalyst properties. With this in mind the goal of our ketonization work was to gain a more fundamental understanding of the reaction to see if it is likely this type of catalyst engineering would be possible. Our initial work started with the simple system of using a pure cerium oxide catalyst to promote ketonization of the model bio-oil compound acetic acid.

It was found that the ketonization of acetic acid could indeed occur in the condensed phase using the ceria catalysts. As it had been previously reported that surface faceting of the catalyst could be of importance, investigations of the reaction using shape selective ceria nanocrystals were performed. Results showed that in more realistic reaction conditions, surface faceting was potentially not of great significance. Next, the variable of calcination temperature for the ceria catalysts and its influence on the ketonization of acetic acid was probed. Despite different material characteristics, there was no clear enhancement with calcination temperature. Moreover, it was found that severe surface area loss of the ceria catalysts occurred after only a short reaction time. Further studies demonstrated that ceria catalysts can promote the ketonization reaction through either the bulk or on the surface of the material depending on the calcination temperature and reaction conditions. Kinetic

experiments showed that both of these pathways are likely proceeding through the same mechanism. Therefore, coupled with the results obtained with the ceria nanocrystals, it can be stated that when using bulk ceria catalysts in condensed phase bio-oil upgrading, special synthesis resulting in specific surface faceting or surface areas is not likely to be necessary or useful.

Next, studies with a slightly more complex system using mixed $CeMO_x$ catalysts to promote acetic acid ketonization were done. It was discovered that the mixing of ceria with another oxide can drastically change its material properties as well as its ketonization activity. The ease of formation as well as temperatures necessary to form bulk carboxylates were found to be altered by the oxide mixed with ceria. At lower temperatures $CeMO_x$ catalysts that did not as readily form bulk carboxylates were more active while at higher temperatures the reverse was found to be true.

Along with the previously described ceria catalyzed ketonization results, these studies showed that temperatures high enough to result in the formation and subsequent decomposition of the respective metal carboxylate are likely necessary for the reaction to proceed. It is unlikely a catalyst could be developed where this formation and decomposition could occur at low enough temperatures to make condensed phase processing of small organic acids practical. Unfortunately this likely means that ketonization in the condensed phase as a bio-oil upgrading step may not be the best way to proceed. However, this does not mean that the ketonization reaction is not relevant for this application. Although not the most desirable option, vapor phase ketonization before condensation of the oil could still be explored as a potential option. Also, the use of selective absorbents able to be regenerated through ketonization as described in chapter 9 is another area worth exploring.

Chapter 9

Future directions

While much about the C-C bond forming aldol condensation and ketonization reactions and how they relate to the upgrading of bio-oil was learned in the course of this thesis, there remains many different directions that can be taken to further understanding. Here, keeping our previous results in mind, a couple different potential projects are briefly described.

Due to the inherent properties of biomass, it is likely that water will be involved with much of the processing for the production of biorenewable fuels and chemicals. Catalysis during bio-oil upgrading is no exception to these concerns as the oil contains a large fraction of water.[1] This is a major challenge to the heterogeneous catalysis community as many of the traditional catalysts used for petrochemical processes are of poor hydrothermal stability. Exposure to water is also troubling to the ketonization reaction as it has been claimed to be an inhibitor. For instance, Gaertner et al. found that with co-feeding 5 wt % water, hexanoic acid ketonization rates were decreased to roughly 1/3 of that with no additional water when using a $CeZrO_x$ catalyst.[2] It was claimed that this inhibition occurred due to water blockage of catalyst basic sites.[2] In light of our results, another potential explanation would be hydrolysis of the metal carboxylate bonds. Regardless, for ketonization reactions in which the active material is supported, not only the support hydrothermal stability but also exposure of the active sites to water must be of concern.

A similar challenge was addressed recently in the esterification reaction.[3] In that particular work, it was found that modifying the local catalytic environment by the addition

of hydrophobic groups to the surface of an acid functionalized mesoporous silica based catalyst, that water tolerance could be significantly enhanced. Unfortunately with the high temperatures necessary for ketonization this type of functionalized mesoporous silica catalyst is not likely to be stable in the presence of water. Therefore alternatives must be examined. Carbon supported catalysts would likely be a good place to look for a hydrothermally stable support. Of carbon based supports, carbon nanotubes (CNT) provide a particularly attractive possibility for a number of experimental reasons. For instance, along with good hydrothermal stability, CNT have a relatively high surface area and tunable pore size. Another advantage would be the ability to potentially create a locally hydrophobic environment in the hope of excluding water from the metal oxide active site. This could potentially be achieved through the selective dispersion of the metal oxide inside of the hydrophobic CNT. Locating the oxide particles inside the CNT could also have other effects related to confinement or electronics.[4] Thus a project is envisioned in which cerium oxide is put either outside or inside CNT and its activity tested in the ketonization of carboxylic acids with and without water present. These results could then be compared to a catalyst in which cerium oxide is supported on a non-hydrothermally stable non-hydrophobic material such as SBA-15.

Our research into the ketonization reaction appears to demonstrate that temperatures necessary to form and decompose metal carboxylates are necessary. Thus it seems unlikely that condensed phase ketonization of small organic acids for bio-oil upgrading purposes will become practical from a processing standpoint. However, this does not mean that the reaction is of no value for upgrading. It may be possible for one to use the metal carboxylate formation and decomposition properties explored in this thesis to advantage in fast pyrolysis applications. For example, as metal carboxylates are thermodynamically favored [5], if an

oxide or carbonate that selectively forms a high temperature decomposition metal carboxylate can be found, the material may be able to act as an absorbent. Thus before condensation of the oil, this absorbent would selectively remove the acids. Then after the oil was condensed the sorbent would be regenerated through heating, decomposing to form the respective ketone. Therefore, in practical terms, the acidity of the oil would be removed, oxygen content reduced, and the carbon from the acids saved. A project is envisioned in which various potential absorbents are examined to see if they could selectively absorb carboxylic acids while not absorbing other bio-oil compounds. If such a material is found, the decomposition of the resulting metal carboxylate could then be researched to understand the temperature of ketone formation. Finally, location of the absorbent in the fast pyrolysis process would need to be determined. It may be that certain compounds would need to be condensed out before exposure of the oil to the absorbent to prevent coking, side reactions, or undesirable absorption.

References

[1] S. Czernik, A.V. Bridgwater, Overview of Applications of Biomass Fast Pyrolysis Oil, Energy & Fuels, 18 (2004) 590-598.
[2] C.A. Gaertner, J.C. Serrano-Ruiz, D.J. Braden, J.A. Dumesic, Catalytic coupling of carboxylic acids by ketonization as a processing step in biomass conversion, Journal of Catalysis, 266 (2009) 71-78.
[3] S. Miao, B.H. Shanks, Esterification of biomass pyrolysis model acids over sulfonic acid-functionalized mesoporous silicas, Applied Catalysis A: General, 359 (2009) 113-120.
[4] X. Pan, Z. Fan, W. Chen, Y. Ding, H. Luo, X. Bao, Enhanced ethanol production inside carbon-nanotube reactors containing catalytic particles, Nat Mater, 6 (2007) 507-511.
[5] R. Pestman, R.M. Koster, A. vanDuijne, J.A.Z. Pieterse, V. Ponec, Reactions of carboxylic acids on oxides .2. Bimolecular reaction of aliphatic acids to ketones, Journal of Catalysis, 168 (1997) 265-272.